Summer 2021

# Novel Quantification and Localization of Water and Solute Transporters in the Tissues of the Spiney Dogfish (Squalus acanthias)

Tolulope B. Ojo

NOVEL QUANTIFICATION AND LOCALIZATION OF WATER AND SOLUTE TRANSPORTERS IN THE TISSUES OF THE SPINEY DOGFISH (*Squalus acanthias*)

by

TOLULOPE OJO

(Under the Direction of Christopher Cutler)

ABSTRACT

The dogfish, *Squalus acanthias* is a marine cartilaginous elasmobranch found in the North Atlantic and Pacific oceans. Dogfish synthesize and excrete urea as a product of nitrogen metabolism. They also convert ammonia into urea and retain this urea, such that their plasma is isosmotic or slightly hyperosmotic to the surrounding seawater. To facilitate the regulation of body fluid and to maintain ionic concentrations and osmotic pressure, Dogfish use ion and solute transporters (e.g., NCC, UT-1) and aquaporin water channel proteins. Studies have identified some of the aquaporin genes in the elasmobranch genome, but their functions are mostly uncharacterized. Recent transcriptomic studies deposited sequence data for duplicate copies of AQP3 (AQP3-2) and its splice variant as well as 'long' and 'short' splice variants of UT-1 and a second novel UT (Brain UT) expressed in Dogfish. To investigate changes in expression of AQP3-2, UT-1, Brain-UT and NCC in the kidney as salinity changes, the fish were acclimated to 75%, 100% and 120% seawater for 7 days. Cloning and sequencing experiments were used to generate primers and antibodies for further studies. Through this, the sequence of a novel gene splice variant of the Brain UT was identified in the brain. The tissue PCRs and western blots confirmed the presence of these genes. Proteins with expected molecular weights were identified for these genes except for NCC. Western blots for AQP3-2 and UT-1 had additional bands which implies the potential presence of other splice variants. The quantitative PCR (qPCR) quantification of mRNA/cDNA expression of these genes showed that only the AQP3-2 spliceoform and UT-1 long splice variant had statistically significant differences and only AQP3 expression increased with increasing salinity as expected. Imunohistochemical localization experiments showed that AQP3-2 is located in the basolateral membranes of the EDT and LDT. UT-1 was localized to most of the nephron, suggesting that urea reabsorption occurs along most of its length. NCC staining was suggested to be localized to the PIb and LDT. These results (especially the qPCR), suggest that adjustments, outside of those to renal transporter expression changes, are used by the fish to acclimate to different salinity environments.

INDEX WORDS: *Squalus acanthias*, Elasmobranch, Aquaporin, Urea transporter, Osmoregulation, AQP3, AQP3-2, UT-1 long and short, NCC, Brain UT, Spliceoform, Western blotting, Immunohistochemistry, qPCR, Tissue PCR, Kidney.

# NOVEL QUANTIFICATION AND LOCALIZATION OF WATER AND SOLUTE TRANSPORTERS IN THE TISSUES OF THE SPINEY DOGFISH (*Squalus acanthias*)

by

TOLULOPE OJO

B.S., University of Lagos, Nigeria 2015

A Thesis Submitted to the Graduate Faculty of Georgia Southern University

in Partial Fulfillment of the Requirements for the Degree

MASTER OF SCIENCE

COLLEGE OF SCIENCE AND MATHEMATICS

# NOVEL QUANTIFICATION AND LOCALIZATION OF WATER AND SOLUTE TRANSPORTERS IN THE TISSUES OF THE SPINEY DOGFISH (*Squalus acanthias*)

by

TOLULOPE OJO

| | |
|---|---|
| Major Professor: | Christopher Cutler |
| Committee: | Vinoth Sittaramane |
| | Tiehang Wu |

Electronic Version Approved:
July 2021

# DEDICATION

To the glory of God and in loving memory of my dad Michael Olukayode Ojo.

# ACKNOWLEDGMENTS

My life is like a book and this chapter of my life could not have been written without the contributions of many people. I am immensely grateful to my family for their sacrifices, for always supporting me in my aspirations and for encouraging me to keep going when the journey seemed impossible. I am here today because they believe in me. I love you Timi, Eni, and Ire for giving me joy and reasons to laugh.

I would also like to thank my supervisor Dr. Christopher Cutler for his advice, mentorship, encouragements, and investment thorough out my period of study and in this career path that I have chosen. I also appreciate you and Ms Karin watching out for my well-being. I am grateful to my committee for their patience and contributions in making this study worthwhile. Next, I'd like to thank Keith Kurt and the undergraduate students in Dr Cutler's lab that provided moral and intellectual resources for this study. A big thank you to all the graduate students who helped me succeed directly and indirectly. Particularly, I'd like to thank Erin Arneson and Shawna Defreitas for their camaraderie. I am grateful to the faculty at the biology department for opening their doors to me, especially to those who gave me opportunities to work in their labs and broaden my knowledge of molecular biology.

To my Statesboro New Covenant Church family, I would mention you all by names, but I fear I would need more than a paragraph to do so. Thank you for being my family away from home. I will always remember the rivers we crossed together, the waves we walked, the walls we scaled and the mountains we climbed. Thank you for surrounding me with love and warmth in my coldest hours, for standing up for me when I needed people in my corner and lifting me up when I didn't have the strength to do so myself. To the people I have met and volunteered with at various community events/activities, thank you all for introducing me to southern hospitality and a world different from what I know.

This project was funded in part by grants from the College of Graduate Studies and Graduate Students Organization.

TABLE OF CONTENTS

Page

ACKNOWLEDGMENTS.....3
LIST OF TABLES.....5
LIST OF FIGURES.....6
CHAPTER
1 INTRODUCTION……...7
Osmoregulation…….7
Ornithine Urea Cycle…….9
Spiney Dogfish...……...10
Aquaporins……...…14
Urea Transporters…….....23
NaCl Cotransporter……...…27
Objectives of the Study…….30
2 MATERIALS AND METHODS……31
Fish and Tissue Sampling…….....31
Total Cellular RNA Extraction…….....33
Amplification of the Complete Brain UT cDNA Sequence …….35
Cloning and Sequencing…….....39
Antibody Production and Western Blotting…….....43
Immunohistochemistry…….....46
cDNA Production and qPCR…….....49
3 RESULTS……..……57
RT-PCR of samples from different tissue.....57
Western Blots result.....59
Immunohistochemistry.....67
qPCR.....85
4 DISCUSSION…….....101

REFERENCES .....110

APPENDIX Sequencing and Cloning Information and Results…….....123

# LIST OF TABLES

Page

Table 1: Mammalian Aquaporin, their Transport Characteristics and Their Tissue distribution.....16
Table 2: Comparison of the Percentage Identity of Partial Derived-Amino Acid Sequences of Four Aquaporin Gene Homologues……..……..19
Table 3: Prevalence of Aquaporins Identified in Deuterostome Animals …….....21

LIST OF FIGURES

Page

Figure 1: Schematic Drawing of the Course of a Single Nephron. …….....13
Figure 2: Schematic Presentation Showing the Timelines of Fish Sampling ……...……...32
Figure 3: Agarose Gel Electrophoresis of *Squalus acanthias* Kidney Expt.1 Samples.....….....53
Figure 4: Agarose Gel Electrophoresis of the PCR Amplification Products of Study Genes……...58
Figure 5: Western Blot for AQP3-2 Antibody (A1) using Crude Membrane Protein Extracts.....60
Figure 6: Western Blot for AQP3-2 Antibody (A1) using Purified Plasma Membrane Protein Extracts…….…….62
Figure 7: Western Blot for UT-1 Antibodies using Crude Membrane Protein Extracts…….....64
Figure 8: Western Blot for NCC/2 (A2) Antibody using a Crude Kidney Membrane Protein Extract……...66
Figure 9: Initial Kidney Section Immunohistochemical Images Labeled with the AQP3-2 A1 (A and A2 Antibodies and no-Primary-Antibody Control....…….....68
Figure 10: Immunohistochemistry Images of Sinus Zone AQP3 Antibody and AQP4/2 Antibody....…….....70
Figure 11: Immunohistochemistry Images of AQP3-2 (A1) Antibody Staining on Serial Sections of the Sinus Zone LDT and Convoluted Bundle Zone....…….....72
Figure 12: AQP3-2 Antibody Staining in the Sinus Zone, the Straight Bundle Zone, and the Convoluted Bundle Zone....…….....74
Figure 13: Immunohistochemistry Image of Initial Kidney Sections Labeled with the UT-1 A1 and A2 Antibodies....…….....76
Figure 14: Immunohistochemistry Image of the Sinus Zone showing UT-1 Staining and is also labeled with either AQP3 or AQP4/2 Antibodies.....78
Figure 15: Immunohistochemistry Image of UT-1 Staining in the Bundle Zone.....80
Figure 16: Immunohistochemistry Image of UT-1 Staining (A1 antibody) in the Sinus Zone and Convoluted Bundle Zone....…….....82
Figure 17: Immunohistochemistry Image of NCC/2 Antibody Staining....…….....84
Figure 18: Graph comparing the number of AQP3 mRNA/cDNA Molecules of *Squalus acanthias* Kidney....…….....86
Figure 19: Graph comparing the number of AQP3-2 mRNA/cDNA Molecules of *Squalus acanthias* Kidney....…….....88
Figure 20: Graph comparing the number of AQP3-2 Spliceoform mRNA/cDNA Molecules from of *Squalus acanthias* Kidney....…….....90
Figure 21: Graph comparing the number of Brain UT mRNA/cDNA Molecules of *Squalus acanthias* Kidney....…….....92
Figure 22: Graph comparing the number of UT-1 Long Spliceoform mRNA/cDNA Molecules of *Squalus acanthias* Kidney....…….....94
Figure 23: Graph comparing the number of UT-1 Short Spliceoform mRNA/cDNA Molecules of *Squalus acanthias* Kidney….....96
Figure 24: Graph comparing the number of NCC/2 mRNA/cDNA Molecules of *Squalus acanthias* Kidney....…….....98
Figure 25: Graph comparing the number of RP-LP0 mRNA/cDNA Molecules of *Squalus acanthias* Kidney.…….....100

# CHAPTER 1

# INTRODUCTION

## Osmoregulation

Osmoregulation depends on the relationship between the solute-to-solvent concentrations of the internal body fluids (extracellular and intracellular) and the outside medium that surrounds an animal. Unless the internal body fluids and the outside medium have the same osmotic/solute concentration, water will enter the body when its fluids contain a higher concentration of solute and leave the body when the surrounding medium contains a higher concentration. Electrolytes will similarly diffuse through the body down electrochemical gradients. These considerations hold true at both the extracellular and intracellular level. Body fluid regulation is essential for all organisms to survive in their respective habitats, including freshwater (FW), seawater (SW), and terrestrial environments. Thus, potentially, marine animals face problems of dehydration and the elimination of excess salts, while freshwater animals must conserve their salts and eliminate excess water (organisms that keep their internal fluids iso-osmotic don't have such problems). (Hammerschlag 2006).

It is known that teleost fish regulate their plasma Na and Cl concentrations and osmolality at levels about one-third of SW. Meanwhile, cartilaginous fishes (sharks, skates, rays, and chimaeras) have adopted a unique osmoregulatory strategy for adaptation to the high-salinity marine environment. Cartilaginous fishes control plasma ions to levels approximately one-half of surrounding SW while they retain high concentrations of the nitrogenous compound urea as an osmolyte (known as the "ureosmotic strategy"). As a result, their body fluids are slightly hyperosmotic to surrounding SW.

Marine and euryhaline elasmobranchs in seawater reabsorb and retain urea and other body fluid solutes, such that osmolarity remains slightly hyper-osmotic to their surrounding seawater; consequently, they experience little or no osmotic loss of water (Smith 1931, Thorson 1962). Any water that is gained by osmosis across the gills is quickly balanced by renal, rectal gland or gastrointestinal tract excretion.

Marine elasmobranchs also drink a relatively small amount, with the level of SW ingestion

generally varying with the environmental salinity and being greater at higher environmental salinities (Anderson *et al*. 2007, Evans *et al.* 1979, Hazon *et al.* 2003). The continuous inward diffusion of Na and Cl (salt) across the intestine from the environment is compensated for by salt excretory mechanisms in the rectal gland and kidney (Burger 1965, Burger and Hess 1960, Haywood 1973, Robertson 1975).

**Osmoregulation in Elasmobranchs**

Elasmobranch species are predominantly marine, although some 10% are estuarine, 2% are euryhaline and 1% are obligate in fresh water (Morgan *et al.* 2003). Marine elasmobranchs retain large amount of urea, thereby raising the osmolality of their body fluids slightly above that of their ambient seawater and facilitating the uptake of free water by osmosis via their gills. At present, general theory holds that urea is produced in the liver and retained in the blood, this is due to the very low permeability of the gills and, reabsorption mechanisms of the kidney (Perlman and Goldstein 1988). Despite the low urea permeability of the gills, due to their relatively large surface area, the gills represent the major site of urea loss (93.3%) that does occur, in comparison to losses (via urine) from the kidney (6.7%) (Wood *et al* 1995). Recent studies have shown that urea can also be produced in the muscle and the intestine (intestine has some smooth muscle which might be the source) (Kajimura *et al.* 2006).

As environmental salinity increases or decreases, many marine elasmobranchs will raise or lower their plasma osmolality accordingly so that the iso-, hyper-osmoregulatory strategy is maintained. Intrinsic to this strategy is the independent regulation of sodium-chloride and urea; therefore, the raising and lowering of plasma osmolality is largely dependent on the elasmobranchs' ability to retain or excrete the principal solutes and this ability influences individual species' tolerance limits to changes in environmental salinity. However, species regarded as predominantly marine such as the European dogfish, *Scyliorhinus canicula*, Japanese dogfish, *Triakis scyllia*, spiny dogfish, *Squalus acanthias*, and the little skate, *Raja erinacea*, all demonstrate the capacity to survive and osmoregulate in varying environmental salinities to either a greater or a lesser extent (Martin 2005). Of course, bullsharks

(*Carcharhinus leucas)* are euryhaline and so can do it to a much greater extent than stenohaline marine sharks.

All elasmobranchs examined to date, except the freshwater potamytrygonid rays, are ureotelic; that is, they synthesize and excrete urea as an end product of nitrogen metabolism (Wood *et al.* 2002). In marine elasmobranchs, plasma osmolarity is high, largely because body fluid concentrations of organic nitrogenous compounds, such as urea and trimethylamine oxide (TMAO), are high. Plasma urea levels generally comprise over 30% of total plasma osmolarity (Madsen *et al.* 2015).

**Ornithine–urea cycle (OUC)**

The OUC is the dominant pathway of urea production in elasmobranchs. This anabolic pathway allows ammonia to be detoxified into urea through a series of mitochondrial and cytosolic enzymes. Urea accounts for one-third to one-quarter of total osmolytes in plasma and muscle, with trimethylamine oxide (TMAO) and amino acids also contributing significantly to the elevation of plasma osmolality (Robertson 1975). Generating urea in the OUC allows for the detoxification of noxious ammonia produced by amino acid catabolism. This mechanism is of particular importance in animals that do not have the luxury of directly excreting ammonia into their immediate environment. Particularly, aquatic animals, that cannot simply excrete ammonia into the water because of physical or chemical limitations, rely heavily on the OUC and urea production to avoid hyperammonaemia.

While urea is of great importance as an osmolyte to marine elasmobranchs, it is also energetically expensive to produce. To synthesize 1 mole of urea via the O-UC, 5 moles of ATP need to be hydrolyzed to ADP (Anderson *et al.* 2012). As a result, the excretory organs of elasmobranchs (kidney and gills) are specialized to reduce urea permeability and to actively retain urea (Morgan *et al.* 2003). Elasmobranchs are ureosmotic; converting ammonia into urea and retaining this urea such that their plasma is isosmotic or slightly hyperosmotic to the ambient seawater (Hazon *et al.* 2003). This strategy results in a slight influx of water and thus reduces the need to gain water via drinking, which, in turn, reduces the intake of

salts. Unfortunately, urea can destabilize proteins at these high concentrations and thus must be counteracted; a feat elasmobranchs accomplish by maintaining relatively high plasma levels of the protein stabilizing chemical, trimethylamine oxide (TMAO).

**Spiney Dogfish**

A significant part of the current knowledge about osmoregulation comes from studies in spiney dogfish, confirming this shark species as a valuable animal model for osmoregulation in cartilaginous fishes (Anderson *et al.* 2007, Chana-Munoz *et al.* 2017, Itaru *et al.* 2007, Lacy and Reale 1985, Schmidt-Nielsen *et al.* 1972). Additionally, spiney dogfish have been used in other scientific fields for example in the study of choroid plexus transport (Villalobos and Renfro 2007) and drug discovery. Marine cartilaginous fishes such as *Squalus acanthias* (spiney dogfish) are ureotelic organisms. This means that they synthetize and excrete urea as the final product of the nitrogen metabolism. Besides that, they are also ureosmotic organisms with urea being the main osmolite. Consequently, they retain large amounts of urea in their plasma in order to increase the osmolarity and maintain their body fluids at isosmotic or slightly hyperosmotic levels with respect to sea water. To achieve such a high concentration of urea in their body, efficient pathways of urea synthesis and retention are crucial, with liver, muscle, kidneys, intestine, and gills being the primary tissues involved in this process. As a marine organism, they are adapted to high salinity environments due to the adoption of this unique urea-based osmoregulation strategy.

Although spiny dogfish are used as a model in a variety of biological research studies, only limited sequence resources providing transcriptome data are publicly available. No complete genome of an elasmobranch species currently exists, and this is a cause of severe limitation to molecular-based research studies.

**Kidney as an osmoregulatory organ in Spiney Dogfish**

The kidney is one of the most critical organs used in cartilaginous fishes, where urea, as well as water and other small molecules are freely filtered by the glomerulus renal corpuscle. Additionally, to minimize urea loss to the environment, cartilaginous fishes have developed a specialized renal system with an extra nephron loop (compared to human or teleost fish renal tubules) and this correlates with an efficient urea reabsorption system that cartilaginous fish have. Possibly due to the extra nephron loop, cartilaginous fish nephron can reabsorb more than 90% of filtered urea from the glomerular filtrate (Anderson *et al.* 2007, Kempton 1953). The kidney consists of two zones; the bundle zone (with enclosed counter- current nephron loops) and the sinus zone, with open blood sinuses between nephrons (where the blood system can take up any water and solutes reabsorbed from the nephron) (Hentschel *et al.* 1998, Lacy and Reale 1985, Lacy *et al.* 1985, Lacy and Reale 1986). The renal tubule in the kidney also has five major segments (see figure 1 below): neck, proximal, intermediate, distal, and collecting ducts with each segment further subdivided. Due to the complex architecture of the kidney, it has been difficult to apply classical physiological methods to understand the various processes of urea absorption that are active in the kidney of cartilaginous fishes (Hyodo *et al.* 2014).

Friedman and Hebert (1990) described a passive model of renal urea reabsorption in *S. acanthias*. The model is based on the presence of the countercurrent arrangement of nephron segments in the kidney bundle zone. The countercurrent arrangement is composed of four segments from a single nephron grouped to form two loops, which together with a fifth segment are all enclosed by a continuous peritubular sheath (Friedman and Herbert 1990, Lacy and Reale 1985, Lacy *et al.* 1985, Lacy and Reale 1986). The model requires: (1) a proximal nephron segment highly permeable to water; (2) a relatively distal segment with a high rate of active salt transport but impermeable to water and urea; (3) a loop through a sinus zone segment with high hydraulic (water permeability) but low urea permeability, thus allowing osmotic equilibration of water that also increases tubular urea concentrations; and (4) a relatively terminal nephron segment within a bundle zone that is theorized to be highly permeable to urea

but not water, resulting in passive diffusion of urea from tubular fluid into the interstitial fluid within the bundle zone. Friedman and Hebert identified in the kidney of *S. acanthias* a countercurrent arrangement and a diluting nephron segment (early distal tubule (EDT)) in the dorsal bundle of the peritubular sheath that has a high rate of active salt absorption and low water and urea permeability (satisfying the second requirement listed above in their model (Friedman and Herbert 1990); see also Figure 1). Despite this observation and their model, a system of passive renal urea reabsorption remains to be experimentally validated. However, morphological studies have revealed that the renal tubules of marine cartilaginous fishes are highly elaborate and show unique features compared with those of other vertebrates. Friedman and Herbert also suggested that the second sinus zone loop i.e., the late distal tubule (LDT) would have high water permeability. The unique anatomical and morphological features have thus been considered to be important for urea reabsorption (Hyodo *et al.* 2003, Hyodo *et al.* 2014).

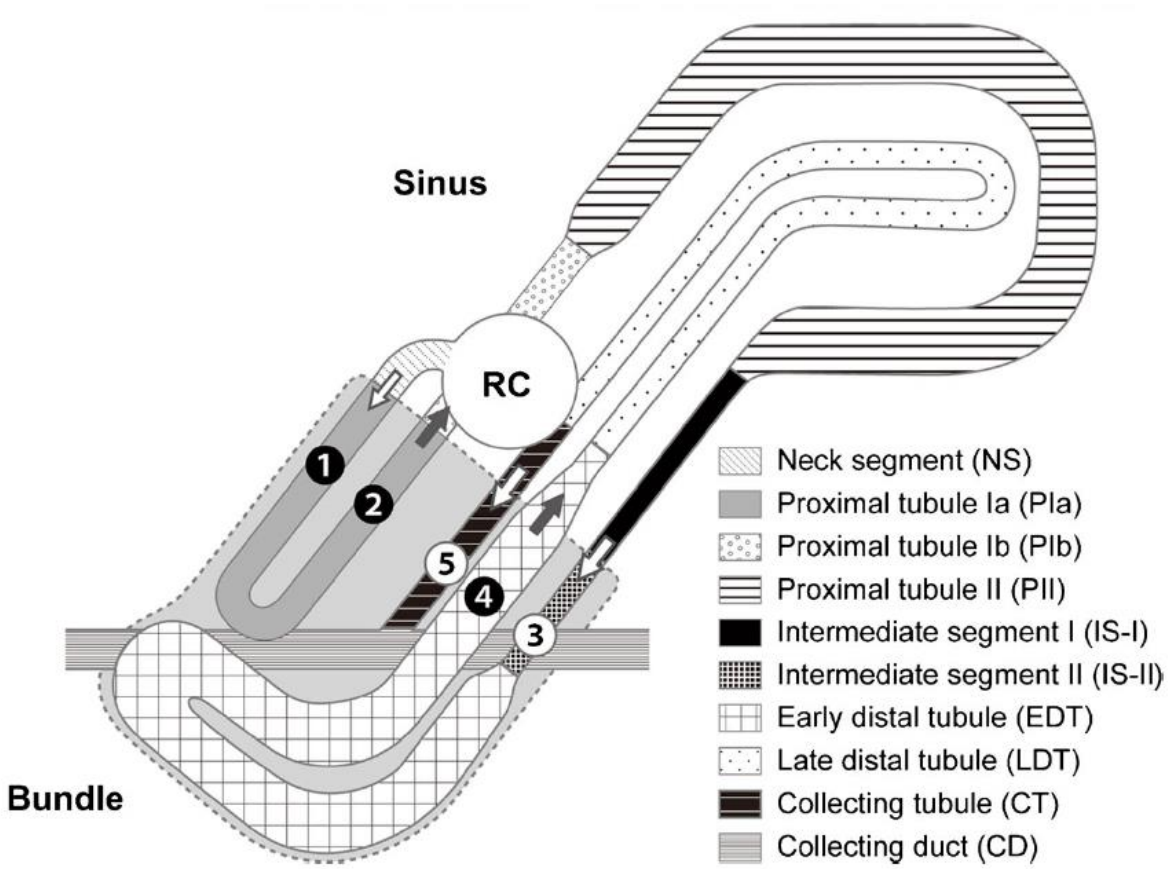


**Figure 1**: Schematic drawing of the course of a single nephron. (Kakamura *et al.* 2015). RC = renal corpuscle/glomerulus.

**AQUAPORINS (AQPs)**

Water is a major component of all living cells as well as the surrounding extracellular spaces. Transport of water into and out of cells occurs during digestion, respiration, circulation, regulation of body temperature, elimination of toxins, neural homeostasis, and during many other essential body functions. Water crosses cellular plasma membranes mainly by two fundamentally distinct pathways: 1) simple diffusion through the lipid bilayer; and 2) channel-mediated water transport. Although other transporters may carry water with whatever solute they are transporting, the main category of water transporters that have been characterized to date are members of the major intrinsic protein (MIP) /aquaporin (AQP) water channel gene family.

Aquaporins (AQPs) are a family of small, primarily hydrophobic proteins. They are ancient and hence, are found in most organisms including microbial organisms, plants, invertebrate, and vertebrate animals. AQPs were originally identified as channels facilitating water transport across the plasma membrane. Although their discovery was preceded by the discovery of the Major Intrinsic Protein of the lens of the eye (MIP), which was a previously unidentified family member (Gorin *et al* 1984). The importance of AQPs is not only limited to the cellular level such as cell volume regulation but also extends to transepithelial water and solute (i.e., fluid) transport and to whole-body water and small solute homeostasis (Hammerschlag 2006).

Structurally, AQPs have six transmembrane domains with the NH2- and COOH-termini in the cytoplasm. The pore is made of two highly conserved short stretches of amino acid residues named asparagine-proline-alanine (NPA) boxes that form a pore for water and/or small molecules such as glycerol and urea. With the progress of the genome projects in many species, more and more AQP-like sequences have been identified on the basis of amino acid sequence similarities, especially around NPA boxes.

AQPs have a diversity of functions: some related to water transport such as fluid secretion, fluid absorption, and cell volume regulation, and the others not directly related to water transport such as cell adhesion, cell migration, cell proliferation, and cell differentiation. Accordingly, AQPs play an important role in physiology and pathophysiology of organisms such as osmoregulation, lipid metabolism, organogenesis and regeneration and cancer.

In mammals, the AQPs are a large gene family of 13 members, which have been grouped into 3 broad sub-families. These include the 'water-selective' AQPs which comprise AQP0, 1, 2, 4, 5, and 6; (Hasler *et al.* 2007), the aquaglyceroporin group which contains AQPs 3, 7, 9 and 10 that are permeable to water and/or glycerol and/or urea, and finally AQP8, and the superaquaporins, AQPs 11 and 12 which are an anomalous group of channels with lower amino acid homology. Recently it has been determined that four more aquaporin genes have been shown to exist in some non-mammalian animals (termed AQP13-16) (Finn *et al.* 2014).

Table 1: Mammalian aquaporin, their transport characteristics, and their tissue distributions. (Wood *et al.* 2002).

| | Transport | Distributions |
|---|---|---|
| **Aquaporins** | | |
| AQP0 | Water | Eye |
| AQP1 | Water | Brain, eye, kidney, heart, lung, gastrointestinal tract, salivary gland, liver, ovary, testis, muscle, erythrocytes, spleen |
| AQP2 | Water | Kidney, ear, ductus deferens |
| AQP4 | Water | Brain, kidney, salivary gland, heart, gastrointestinal tract, muscle |
| AQP5 | Water | Salivary gland, lung, gastrointestinal tract, ovary, eye, kidney |
| AQP6 | Water, urea (+/−), anion | Brain, kidney |
| AQP8 | Water, urea (+/−), ammonia | Testis, liver, pancreas, ovary, lung, kidney |
| **Aquaglyceroporins** | | |
| AQP3 | Water, urea, glycerol, ammonia | Kidney, heart, ovary, eye, salivary gland, gastrointestinal tract, Respiratory tract, brain, erythrocyte, fat |
| AQP7 | Water, urea, glycerol, ammonia | Testis, heart, kidney, ovary, fat |
| AQP9 | Water, urea, glycerol | Liver, spleen, testis, ovary, leukocyte |
| AQP10 | Water, urea, glycerol | Gastrointestinal tract |
| **Superaquaporins** | | |
| AQP11 | Water? | Testis, heart, kidney, ovary, muscle, gastrointestinal tract, leukocytes, liver, brain |
| AQP12 | Unknown | Pancreas |

**AQP3 and its paralog/isoform**

AQP 3 is part of a subclass of aquaporin water channels, termed aquaglyceroporins, which are also usually able to transport water, glycerol and perhaps urea and other small solutes. The signature sequence for aquaglyceroporins will be an aspartic acid residue in the AQP3's second NPA box, which expands the pore to accept larger molecules such as glycerol (Cutler *et al.* 2007).

Mammalian AQP3 is expressed in several locations including the basolateral membrane of epithelial cells in the kidney collecting duct, the airways, and the intestine, as well as in the epidermis, the urinary bladder, the conjunctiva, and the cornea (Chana-Munoz *et al.* 2017, Wang and Li 2017). AQP3 expression is known to be regulated by vasopressin, cAMP, and hypertonicity and may be regulated by corticosteroids. Its transport can be blocked by nickel, copper, and an acidic pH environment (MacIver *et al.* 2009).

Aquaporin-3 (AQP3, originally called glycerol intrinsic protein, GLIP, based on its glycerol-transport function) was cloned initially from rat kidney (Cutler *et al.* 2005, Cutler *et al.* 2007 Echevarrı́a *et al.* 1996, Madsen *et al.* 2015), these original cloning studies and follow-up data from multiple labs have demonstrated AQP3-facilitated water and glycerol transport. (Rojek *et al.* 2008). Initial phenotype analysis of AQP3 null mice, generated by targeted gene disruption, showed a urinary concentrating defect resulting from reduced water permeability in the collecting duct (Rojek *et al.* 2008). Although the aquaporin family includes two sub-groups of proteins: the aquaporins, which constitute cell membrane channels selective for water, and a group of homologs; the aquaglyceroporins (of which AQP3 is a member) differ from the other two groups of AQPs because, in addition to being a water channel, it transports glycerol and to some extent urea (Kempton 1953, Madsen *et al.* 2015).

**Aquaporin expression in Elasmobranchs**

The first homologue of the aquaporin water and small solute channel gene family isolated from an elasmobranch (aquaporin 1e; AQP1e), was identified in the bullshark (*Carcharhinus leucas*) (Cutler *et al.* 2012). A previous study carried out by Dr Cutler (Cutler *et al.* 2007) identified the orthologues of AQP1e in the dogfish shark (*Squalus acanthias*) and cloned and sequenced genes encoding other aquaporin isoforms present in dogfish shark osmoregulatory tissues (such as gill, intestine, esophagus, kidney, and rectal gland). This study showed genes that had higher levels of homology to human AQP 1 and represented the orthologue of this gene (see Table 2.)

Table 2. Comparison of the percentage identity of partial derived-amino acid sequences of four aquaporin gene homologues isolated from the dogfish shark (*Squalus acanthias*) in relation to the sequences of human aquaporin genes. (Cutler *et al.* 2007).

| | Human AQP1 | Human AQP2 | Human AQP3 | Human AQP4 | Human AQP5 |
|---|---|---|---|---|---|
| *Squalus* AQP1 (1e) | 64.6 | 54.0 | 18.8 | 50.4 | 57.5 |
| *Squalus* AQP1e (1e2) | 47.7 | 46.0 | 18.8 | 43.4 | 49.6 |
| *Squalus* AQP3 | 19.5 | 21.8 | 69.9 | 24.8 | 22.6 |
| *Squalus* AQP4 | 44.2 | 45.1 | 25.6 | 78.8 | 46.9 |

Recent studies have also identified some of the aquaporin genes in the elasmobranch genome (Madsen *et al.* 2015), but their functions are mostly uncharacterized (Madsen *et al.* 2015). A comprehensive gene survey (Finn *et al* 2014) revealed that the Elasmobranch, Little Skate has copies of AQP0, 1, 4, 9, 10, 11 and 12, but also 2 copies of AQP3 (see Table 3). Additionally, there are two aquaporin genes not found in mammals, AQP14 and 15 (formerly AQP1e). (Cutler *et al.* 2005, Cutler *et al.* 2007). Also, the laboratory of Dr Cutler has identified and cloned a copy of AQP8 from *Squalus acanthias* (unpublished) illustrating that all the genomic/transcriptomic studies up to today are likely incomplete. AQP4 has previously been characterized in *Squalus acanthias* (Cutler *et al.* 2012). Additionally, it is clear from Cutler 2007 (Cutler 2007), and Madsen et al., 2015 (Madsen *et al.* 2015) that *Squalus acanthias* also expresses AQP 0, 1, 3, 4, 9 and 15. Subsequently, a transcriptomics study (Chana-Munoz *et al.* 2017) deposited sequence data for *S. acanthias* for AQP 0, 1, 4, 9, 15 as well as duplicate copies of AQP3 (in this thesis termed AQP3 and AQP3-2), as well as a splice variant of AQP3-2. (Finn *et al.* 2014, Chana-Munoz *et al.* 2017).

Table 3: Prevalence of aquaporins identified in deuterostome animals. (Finn *et al.* 2014).

| | | AQP | | | | | | | | | | | | | | | | ∑ | ∑ |
|---|---|---|---|---|---|---|---|---|---|---|---|---|---|---|---|---|---|---|---|
| | **Animal** | **0** | **1** | **2** | **3**[a] | **4** | **5** | **6** | **7** | **8** | **9** | **10** | **11** | **12** | **13** | **14** | **15** | **16** | **classes** | **paralogues** |
| Eutheria | Human | 1 | 1 | 1 | 1 | 1 | 1 | 1 | 5[b] | 1 | 1[c] | 1 | 1 | 2 | | | | | 13 | 18 |
| Metatheria | Tasmanian devil | 1 | 1 | 1 | 1 | 1 | 1 | 1 | 1 | 1 | 1 | 1 | 1 | 1 | | 1 | | | 14 | 14 |
| Prototheria | Platypus | 1 | 1 | 1 | 1 | 1 | 1 | 1 | 1 | 1 | 1 | 1 | 1 | 1 | 1 | 1 | | | 15 | 15 |
| Aves | Zebra finch | 1 | 1 | 1 | 1 | 1 | 1 | | 1 | 1 | 1 | 1 | 1 | 1 | | 1 | | | 13 | 13 |
| Crocodylia | American alligator | 1 | 1 | 1 | 1 | 1 | 1 | | 1 | 1 | 1 | 1 | 1 | 1 | | 1 | 1 | 1 | 15 | 15 |
| Testudines | Chinese softshell turtle | 1 | 1 | 1 | 1 | 1 | 1 | 1 | 1 | 1 | 1 | | 1 | 1 | | 1 | 1 | 1 | 15 | 15 |
| Serpentes | Burmese python | 1 | 1 | 1 | 1 | 1 | 2 | 1 | 1 | 1 | 1 | 1 | 1 | 1 | | 1 | | | 14 | 15 |
| Iguania | Green anole | 1 | 1 | 1 | 1 | 1 | 2 | 1 | 2 | 1 | 1 | 1 | 1 | 1 | | 1 | | | 14 | 16 |
| Amphibia | Western clawed frog | 1 | 1 | | 1 | 3 | 2 | 2 | 1 | 1 | 1 | 1 | 1 | 1 | 1 | 1 | | 1 | 15 | 19 |
| Actinistia | Coelacanth | 1 | 1 | 3 | 1 | 1 | | | 1 | 1 | 1 | 1 | 1 | 1 | | 1 | 1 | | 13 | 15 |
| Acanthopterygii | Nile tilapia | 2 | 3 | | 2 | 2 | | | 1 | 2 | 2 | 2 | 2 | 1 | | 1 | 1 | | 12 | 21 |
| Paracanthopterygii | Atlantic cod | 2 | 2 | | 2 | 2 | | | 1 | 3 | 2 | 2 | 2 | 1 | | 1 | | | 11 | 20 |
| Protacanthopterygii | Atlantic salmon | 4 | 4 | | 4 | 4 | | | 1 | 8 | 4 | 4 | 4 | 2 | | 1 | 2 | | 12 | 42 |
| Ostariophysi | Zebrafish | 2 | 2 | | 2 | 1 | | | 1 | 4 | 2 | 2 | 1 | 1 | | 1 | 1 | | 12 | 20 |
| Elopomorpha | Japanese eel | 2 | 2 | | 2 | 4 | | | 1 | 5 | 2 | 3 | 2 | 1 | | 1 | 1 | | 12 | 26 |
| Holostei | Spotted gar | 1 | 1 | | 1 | 1 | | | | 1 | 1 | 2 | 2 | 1 | | 1 | 1 | | 11 | 13 |
| Chondrichthyes | Little skate | 1 | 1 | | 2 | 1 | | | | | 1 | 1 | 1 | 1 | | 1 | 1 | | 10 | 11 |
| Hyperoartia | Sea lamprey | 1[d] | | | 2 | 1 | | | | 1 | | 2 | | 1[e] | | 1 | | | 7 | 9 |
| Tunicata | Vase tunicate | | | | 1 | 1 | | | | 1 | | | | | | | | | 3 | 3 |
| Cephalochordata | Amphioxus | | | | 2 | 2 | | | | 5 | | | | 2 | | | | | 4 | 11 |
| Hemichordata | Acorn worm | | | | 1 | 5 | | | | 1 | | | | 2 | | | | | 4 | 9 |
| Echinozoa | Purple sea urchin | | | | 3 | 5 | | | | 3 | | | | 2 | | | | | 4 | 13 |
| Asterozoa | Bat star | | | | 2 | 4 | | | | 2 | | | | 2 | | | | | 4 | 10 |
| Number of | exons | 4 | 4 | 4 | 6 | 4 | 4 | 4 | 6 | 5-6 | 6 | 6 | 2–3 | 3–4 | 6 | 5–6 | 4–5 | 4–5 | | |
| Number of orthologs | examined | 173 | 223 | 111 | 183 | 212 | 106 | 88 | 114 | 214 | 144 | 141 | 147 | 139 | 8 | 69 | 22 | 7 | | |

[a] Basal deuterostome glps are listed under AQP3.
[b] In addition to a functional *AQP7*, humans encode four pseudogenes (*AQP7p1*, *-7p2*, *-7p3*, and *-7p4*).
[c] Amongst eutherian genomes, chiropteran bats are an exception with at least 3 copies of *AQP9* encoded by 1, 5 or 6 exons.
[d] The *aqp01* gene in Arctic lamprey is encoded with 5 exons.
[e] This ortholog is not found in the current version of the sea lamprey genome (Pmar7), but fragments are present in the Arctic lamprey genome (LetJap1.0).

doi:10.1371/journal.pone.0113686.t003

The order of evolutionary appearance of water selective AQPs due to gene/genome duplication is as follow: AQP4 gave rise to AQP1 (and at some point AQP14 in some animals). AQP1 gave rise to AQP15 in some animals and AQP0. AQP0 gave rise to AQP2, 5 and 6 but only in land animals or those evolving to move onto land. (AQP2 is known to be critical for urine concentration (above iso-osmotic levels) and water conservation in land animals). For aquaglyceroporins. AQP3 (GLIP) was duplicated and that gave rise to what becomes AQP7 and 10 after another duplication. AQP3 was also duplicated again to give rise to AQP9. We now know that there is a further duplication of AQP3 in some animals, as in sharks. Many of the above duplications come from genome wide duplication events, of which there are 2 between tunicates (invertebrates) and humans (so potentially 4 of any gene). There was an extra genome wide duplication at the beginning of teleost fish followed by many duplicate losses (probably around 50% in eel and 75% in zebrafish).

Chondrichthyians are one of the few taxonomic groups of animals for which there is still a paucity of genomic information. The closest genomes to those of elasmobranch sharks are those of a member of the chimaera elephant shark (*Chondrichthyian holocephali)*, or ghost shark (*Callorhinchus milii*). The sequence data from the *C. milii* is a good reference, as it provides genomic intron and exon information for a variety of genes, which is useful for quantitative PCR primer design. A transcriptomic survey of transcripts being expressed in the kidney (Chana-Munoz *et al.* 2017) reported that a second (duplicate) copy of the AQP3 (AQP3-2) gene and a splice variant (spliceoform) version were expressed in dogfish *Squalus acanthias* kidney. AQP3-2 and its splice variant gene were hypothesized to play a role in water and urea absorption (Chana-Munoz *et al.* 2017). As a consequence of the limited genomic information available on elasmobranch species, very few studies of the role of aquaporins in water balance have been made and the expression of AQP 3-2 and its spliceoform has not otherwise been identified in shark tissues.

**UREA TRANSPORTERS (UT-1)**

The ability of animals to translocate urea across internal membranes as well as across epithelia in contact with the environment has been known for decades. For many years, urea had been thought to cross the cell plasma membrane relatively freely by simple diffusion. However, in vitro studies revealed that urea permeability across artificial lipid bilayers was considerably lower than previously thought (Gallucci *et al.* 1971). This is particularly true for cartilaginous fishes where much higher levels of plasma urea exist. A specific transport is required for urea movement across the plasma membrane. Among several proteins reported, facilitative urea transporters (UTs) transport urea most efficiently and play a crucial role in the urinary concentration mechanism.

The UT proteins belong to the solute carrier family of transporters (SLC), a large family of proteins that transports substances such as carbohydrates, nucleotides, amino acids, ions and various chemicals across cell membranes. Urea transporters of the UT type are members of the SLC14 solute carrier family (Shayakul *et al.* 2013). The first UT was identified from the rat kidney by Hediger and colleagues (Shayakul *et al.* 1996). This protein is now known as UT-A2 and is encoded by the SLC14A2 gene. Subsequently, Olives *et al*. (Olives *et al*. 1994) isolated a cDNA encoding a different UT now known as the UT-B. The UT-A (SLC14A2) gene and the UT-B (SLC14A1) gene occur in tandem on chromosome 18 in the mouse, rat, and human and most probably represent the result of tandem duplication from the ancestral UT gene (Fenton *et al.* 2000).

In particular, the UTs (SLC14A) allow the facilitated diffusion of urea across biological membranes. In mammals, UT-A and UT-B each give rise to multiple alternatively spliced isoforms, at least six for UT-A and two for UT-B (Shayakul *et al.* 1996). The transcripts for urea transporters have been detected in several tissues; however, for most of the isoforms, the highest expression was found in the kidney (Bagnasco 2005, Klein *et al.* 2011). The major UT-A isoforms expressed in the kidney are UT-A1, UT-A2, and UT-A3. In the mammalian kidney, both UT-A1 and UT-A3 are highly expressed in the inner medullary collecting duct (IMCD), whereas UT-A2 is expressed in the thin descending limb of the

loop of Henle. In the IMCD, urea is reabsorbed by UT-A1 and UT-A3 from the forming urine, in which urea is concentrated after the reabsorption of water, NaCl, and other useful substances.

The urea reabsorption by UT-A1 and UT-A3 is regulated by vasopressin and other factors via PKA and PKC-mediated pathways. Type-A UT proteins (UT-1) are responsible for the high urea permeability of the collecting duct.

With respect to marine elasmobranchs, Smith, and Wright (1999) cloned and characterized a cDNA encoding a UT-1 type urea transporter (known as ShUT) from the spiny dogfish (*Squalus acanthias*) kidney (Smith and Wright 1999). Kakumura *et al* reported that the Chimaera; Elephant fish/Ghost fish have UTs, and Chimaera's are closely related to elasmobranchs (Kakumura *et al.* 2009). In the study, three cDNAs encoding UTs were isolated from the kidney of elephant fish, *Callorhinchus milii*, and these were termed efUT-1, efUT-2 and efUT-3. EfUT-1 is orthologous to other known elasmobranch UTs including that from *Squalus acanthias* (Kakumura *et al.* 2009, Takabe *et al.* 2016). The efUT-1 and efUT-2 were shown to be widely expressed in a number of tissues including the kidney, efUT-3 was only found in the kidney and interrenal gland. Two 5' end splice variants of the efUT-1 and efUT-2 genes were also shown to be expressed. In the kidney of marine elasmobranchs, urea reabsorption from filtered urine is essential for maintaining high levels of urea in the body. For example, in the kidney of the houndshark, (*Triakis scyllium)*, Yamaguchi *et al*. found that a facilitative urea transporter (UT) is localized to a specific nephron segment, the collecting tubule (CT), suggesting that the collecting tubule has an important role in the urea reabsorption process (Yamaguchi *et al.* 2009). However, a recent study (Imaseki *et al.* 2019) showed that the mRNA expression of UT-1 in Bullshark (*Carcharinhus leucas*) and Houndshark kidney was not significantly changed by an acclimation of the fish to low salinity environments (FW and 30% SW respectively), although interestingly the trends in mRNA levels in the two species were in opposite directions. Messenger RNA expression was also localized to the collecting tubule of the bullshark.

Finally, the transcriptomics study (Chana-Munoz *et al.* 2017) showed that there are 'long' and 'short' 3' splice variants of UT-1 expressed in *S. acanthias* and these were compared to similar variants in Elephant fish (*C. milii*) and Atlantic Stingray (*D.sabina*). A partial transcript of a second UT gene (in this thesis termed 'Brain UT') was also identified in the *S. acanthias* brain.

**Brain UT**

In mammals, there are two types of urea transporters: urea transporter (UT)-A and UT-B. The UT-A transporters are mainly expressed in kidney epithelial cells while UT-B demonstrates a broader distribution in kidney, heart, brain, erythrocytes, testis, urinary tract, and other tissues. UT-A1, -A2, -A3, and -A4 are encoded by a same gene while UT-B is encoded by a different gene (Trinh-Trang- Tan *et al.* 2003). Urea transporter-B has a wide tissue distribution. In the kidney, it is located in the endothelial cells of the descending vasa recta (DVR; (Pallone 2000, Tsukaguchi *et al.* 1997, Xu *et al.* 1997). In the brain UT-B is mainly expresses in the astrocytes, the ependymal cells, as well as subgroups of neurons in the dorsal root ganglia and the inferior colliculus, and cells in the anterior pituitary gland (Berger *et al.* 1998, Chou and Knepper 1989). The erythrocyte membrane contains abundant UT-B (Olives *et al.* 1995) which not only mediates rapid movement of urea across red blood cells, but also serves as a Kidd (JK) antigen (Olives *et al.* 1995, Timmer *et al.* 2001). In addition, UT-B is found in the colon (Inuoe *et al.* 2004), sertoli cells in the testis (Fenton *et al.* 2007, Fenton and Knepper 2007), the heart, liver, spleen, and lung, stomach (Lucien *et al.* 2005), and epithelial cells in the urinary tract including the bladder, ureter, and pelvis lumens. The wide distribution of UT-B suggests that UT-B has broad physiological functions in humans.

The two UT subfamilies of UT-A and UT-B are encoded by Slc14a2 and Slc14a1 gene, respectively. Urea transporter-B is the only transcription product of Slc14A1 gene in humans, mice, and rats. The SLC14a1 for human UT-B was first cloned from human erythrocytes and is located at the single-gene locus of chromosome 18q12.1-q21.2. It is homologous to the mouse (Yu *et al.* 2019). There

are two SLC14a1 mRNA transcripts due to variable polyadenylation, and they are expressed for a 45-kDa protein (Lucien *et al.* 1998).

The UT-B-mediated urea transportation is inhibited by urea analogues and other compounds, including phloretin, dimethylurea, acrylamide, methylurea, thiourea, methylformamide, and PCMBS (Perlman and Goldstein 1988). UT-B is also down-regulated by dDAVP, an agonist of the type II vasopressin receptor (Trinh-Trang-Tan *et al.* 2003). In 2009, the crystal structure of UT-B was determined (Levin *et al.* 2009). The membrane-spanning pore consisting of two halves of the protein has a filter to select proper molecules to pass.

UT-B is responsible for the maintenance of urea concentration, male reproductive function, blood pressure, bone metabolism, and brain astrocyte and cardiac functions. In UT-B null mice, the urea clearance rate is reduced by 25% while the urea concentration increases by 30% and urea concentration in urine decreases by 35%. The UT-B null mice demonstrate higher urine output than wild-type mice (Bankir *et al.* 2004, Lei *et al.* 2011, Yang and Bankir 2005).

Smith and Wright 1991 show that the kidney of *S. acanthias* contains at least one protein capable of urea transport and indicate the existence of other homologues. One of the homologues discovered is a 380-amino acid hydrophobic protein (ShUT). The homology of ShUT to similar-length mammalian UT-A2 and UT-B2 urea transporter proteins is about 60% amino acid identity and the identity with UT-A2 is slightly higher than with UT-B2. ShUT also lacks residues that, to date, have been found only in UT-B2 family members. The functional mechanisms of UT-B currently remain elusive. This study for the first time characterized the tissue distribution of a widely expressed UT paralog, here called ‘Brain UT,’ whose expression was also investigated in the kidney of *S. acanthias*.

**Na-Cl COTRANSPORTERS (NCC)**

The chloride-cation cotransporters (CCC) are a family of genes responsible for electroneutral cotransport of Na+ and/or K+ and Cl- ions across the plasma membrane (Gamba 2005). Three major classes of CCC exist: those transporting Na+, K+, 2Cl- (NKCC), those transporting NaCl (NCC) and those transporting KCl (KCC).

NCC was first cloned and identified in 1993 from the urinary bladder of the winter flounder teleost fish (flNCC) by means of a functional expression strategy in Xenopus laevis oocytes (Gamba *et al.* 1994). NCC belongs to the SLC12 (SLC12A3) cation-chloride cotransporters' family (Human Genome Organization). This family receives its name because all members transport one or two chloride ions coupled with a cation (Na+ and/or K+). Up to date, there are nine known genes of the SLC12A family known as SLC12A1-SLC12A9; and they encode for NKCC2, NKCC1, NCC, KCC1, KCC2, KCC3, KCC4, CCC9 and CIP, respectively, localized in different chromosomes in humans. While NKCC1 and NKCC2 have been identified in *Squalus acanthias*, NCC was only recently identified (Moreno *et al.* 2019) and there is no evidence yet of what KCC or other CCC gene paralogs exist in sharks (Gangnon *et al.* 2002, Xu *et al.* 1994).

The NCC is an apically located cotransporter protein that uses the Na+ ion inward gradient to perform secondary active transport of NaCl into the cell. In the elasmobranch kidney, tubular urea reabsorption was reported to be correlated with sodium reabsorption at a ratio of 1.6:1 (Schmidt-Nielsen *et al.* 1972). This observation led the researchers to expect that cotransporters such as NCC (and NKCC2) contributes importantly to the urea reabsorption process by reabsorbing the salt and hence diluting the urine, allowing subsequent water reabsorption and concentration of the urea to facilitate its reabsorption (Friedman and Herbert 1990, Galluci *et al.* 1971).

Despite NCC importance in renal physiology, pathology, and pharmacology, little is known about specific amino acid residues or structural domains where transported ions bind to the cotransporter. To

date, only a limited number of membrane transporters have been identified in the spiney dogfish. However, there has been a recent localization of NCC to late distal tubule of bullshark and a localization of NCC to houndshark gill (Imaseki *et al.* 2019, Takabe *et al.* 2016, Yamaguchi *et al.* 2009).

**Hypothesis**

If the reaction of the homeostatic system of the sharks to changes in environmental salinity was simply to make adjustments by making changes to the rate of renal salt and urea reabsorption, then it could be hypothesized that in higher salinity environments higher reabsorption of urea and salts would potentially occur. Therefore, a higher level of expression of renal urea and salt transporters would be expected in the kidney and of course the opposite would be true in lower salinity environments. However, there are many factors that at the very least complicate the situation and could lead to a different outcome in terms of renal transporter expression. Firstly, it is assumed that plasma osmolality and consequently plasma NaCl and urea concentrations would rise in higher salinities and would be lower in lower salinities. This has been shown in experiments in the Euryhaline Bullshark (*Carcharhinus leucas*; (Imaseki *et al*. 2019)) and the Houndshark (*Triakis scyllium*; (Yamaguchi *et al.* 2009)) acclimated to different environmental salinities, where both NaCl and urea plasma levels rose in higher salinities and fell in lower ones. Additionally, there has been a suggestion that Elasmobranchs preferentially may lose more urea than NaCl when they are in lower salinity environments (Anderson *et al*. 2007, Yamaguchi *et al.* 2009). Also with changes to the environmental salinity, there could be changes to :- 1) the gill water and urea permeability (although unlikely in the long term, changes in branchial water flow can occur during the transition to a new salinity environment (Anderson *et al*. 2007)); 2) the drinking rate of the animals (known to be increased in elevated salinity environments (Anderson *et al*. 2007, Evans 1979, Hazon *et al.* 1997); 3) to the rectal gland fluid secretion rate (which is known to be increased in lower salinity environments; (Anderson *et al*. 2007)) and also 4) to the glomerular filtration rate (GFR) of the kidney nephrons due to changes in blood perfusion of glomeruli or due to other mechanisms that can shut off the filtration of certain nephrons (Brown and Green 1987) as well as 5) changes to the rates of

osmolyte and fluid reabsorption from the nephron and fluid secretion into the nephron (Beyenbach *et al.* 1985, Brown and Green 1987, Sawyer and Bayenbach 1985, Schmidt-Nielsen *et al.* 1972). All these factors could impact and potentially lessen the need for changes to transporter gene expression in the kidney. Overall though, it seems the biggest factor in the acclimation of the fish to different environmental salinities is the adjustment of total body fluid volume. Yamaguchi et al., (2009) show that (in *Triakis scyllium*) there are significant changes in body mass following acclimation to different environmental salinities, implying an uptake of water in lower salinities (increase in weight, accounting for around 32% of the osmotic adjustment occurring) and a loss of water (decrease in weight, in higher salinities accounting for around 60% of the osmotic adjustment occurring), this effect on body fluid volume has also been seen in other Elasmobranchs (Anderson *et al*. 2007). Of course, increases or decreases in the levels of body water (fluid) volume produce changes both to the concentration of urea and NaCl, and the overall plasma osmolality as also demonstrated in the Euryhaline Bullshark (*Carcharhinus leucas*; (Imaseki *et al*. 2019)) and the Houndshark (*Triakis scyllium*; (Yamaguchi *et al.* 2009)) acclimated to different environmental salinities. So, whether further adjustments to the expression of water and osmolyte transporter genes in the kidney would be required is unclear.

For aquaporin water channels in general, Friedman and Hebert (1990) produced a model suggesting that the LDT would have high levels of osmotic water permeability to re-equilibrate the concentrations of remaining osmolytes in the renal filtrate following the absorption of NaCl in the previous EDT segment (Friedman and Herbert 1990), and therefore it could be predicted that the LDT would probably express water channel genes. However other authors have suggested that a large amount of the fluid reabsorption processes occur in the proximal tubule (Brown and Green 1987) and therefore this might be a site for the expression for aquaporins also. Aquaporins can be used for cellular fluid homeostasis (to maintain cell volume) and therefore potentially any cell could express aquaporins for that purpose.

Regarding urea transport, Friedman, and Hebert's (1990) model of renal reabsorption mechanisms also suggested that urea uptake could occur in the nephron's collecting tubule (CT) and indeed Imaseki *et al*., (2019) and Yamaguchi *et al*., (2009) have shown expression of UT transporter mRNAs and/or protein in the CT. However, Schmidt-Neilsen and Bankir, (2003) have suggested that there is a significant reabsorption of urea in the proximal tubule and Brown and Green, 1987 showed that the vast amount of fluid and osmolyte reabsorption occurs in the proximal part of the nephron (although it wasn't clear how far along the nephron this includes). Therefore, it could be predicted that there could be significant expression of urea transporters (UT-1, Brain UT but also AQP3-2 and/or AQP3) in the proximal parts of the nephron.

Regarding the NCC, NaCl cotransporter, both Imaseki *et al*., (2019) and Yamaguchi et al., (2009) have shown expression of NCC in the LDT and therefore this would have to be seen as the most likely location of NCC in *Squalus acanthias* kidney also. Summarily, the hypothesis is that increasing or decreasing the salinity of the seawater environment of *Squalus acanthias* will lead to an increase or decrease in urea/salt reabsorption which will concomitantly lead to increase or decrease in the expression of the genes involved in the reabsorption process.

**Objectives of this research**

To contribute to answering the important but yet unsolved question of how elasmobranchs maintain elevated level of urea in their body fluids, this thesis focuses on the identification and cellular localization of various pumps, channels, and transporters in the nephron segments of the kidney of *S.acanthias*. These molecules include the urea transporters (UT-1) and a second recently identified urea transporter protein isoform/gene, Brain UT, the Na-Cl cotransporter (NCC), and the aquaporin, AQP3-2 and its splicesoform. This study also investigated the effects of gradual acclimation to higher and lower environmental salinities of elasmobranchs and how this resulted in changes to the mRNA expression of the various transporters.

# CHAPTER 2

# MATERIALS AND METHODS

## Fish and tissue sampling

To determine the Aquaporins and transporters directly involved in any kind of osmoregulatory or body fluid volume regulation processes in the shark, an attempt was made to disturb the shark regulatory system to try to cause changes in the expression of effector protein components. In other words, the external environmental salinity of the fish was manipulated to try to modulate the expression of aquaporin (and others) genes, such as UTs and NCCs. At the Mount Desert Island Biological Laboratory (MDIBL) at Salisbury Cove, in Maine, small (800–1500 g) adult mixed sex dogfish were (otherwise) randomly selected from a stock tank and were unfed during the experiment. All experimental animal protocols used were in compliance with IACUC regulations and had both GSU and MDIBL IACUC approval. The fish were placed in pairs in four-foot experimental tanks (approximately 1000 l). The acclimation of dogfish to dilute seawater (SW) in stages over 7 days was a protocol modified from Pannabecker and Danzler (2005). A similar protocol to acclimate fish to 120% SW was then also devised. Two groups of sharks (Experiment 1 and Experiment 2 with six fishes per group) were held in SW adjusted to either 75% salinity or 120% salinity in stages. The stages were 85% 3 days, 80% 2 days, and 75% 2 days or 100% 3 days, 115% 2 days, 120% 2 days (See Figure 2). Differing salinities were produced by the addition of de-chlorinated tap water, or sea salt (Instant Ocean) using a re-circulating system including a cooler to maintain temperature and biofilters. Control animals were kept in 100% salinity (normal) SW (around 31–32 ppt at MDIBL) for the same period. Salinity was controlled using a model 85 dissolved oxygen, conductivity, salinity, and temperature meter (YSI). At the end of the 7-day experiment, fish were sacrificed and various tissues including the kidneys (per salinity acclimation samples) were removed by dissection. Kidneys were homogenized using a polytron homogenizer (Kinematica). All tissues were homogenized in solution D for RNA extraction (Cutler and Cramb 2008, Dantzler 2005).

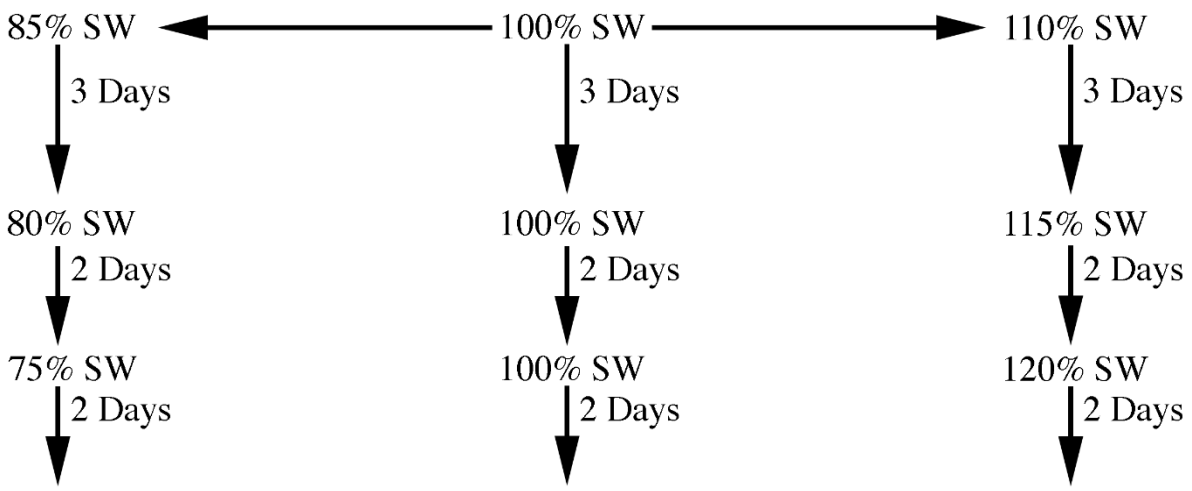


**Figure 2:** Schematic presentation showing the timelines of fish sampling.

**Total Cellular RNA Extraction**

Total RNA was extracted from the tissues and prepared by scraping off the epithelium from tissue using a glass slide or razor blade. Experiment 1 samples were already extracted prior to the start of the project (and the method used for those is described below) but experiment 2 samples (100% and 120% SW only) were extracted as part of this project.

Scrapings were homogenized in ice cold Solution D (4 M guanidinium isothiocyanate, 25 mM tri sodium citrate, 0.5% v/v sarkosyl, 0.1 M 2-mercaptoethanol) (Chomczynski and Sacchi, 1987) using a syringe and 16-gauge needle. Total RNA was otherwise prepared from whole tissues homogenized in ice cold Solution D, using either a syringe and 16-gauge needle or a polytron blender (Kinematica) running at approximately 25,000 rpm. In all experiments, tissues were homogenized in 10 mL of Solution D per gram of tissue. Crude membrane homogenates were stored at -20 or -80℃. (Chomczynski and Sacchi 1987, Cutler 2007, Cutler and Cramb 2008).

Since this project was part of an extension of research begun many years before in my supervisor's lab. RNA (experiment 1) samples used had been extracted by previous students. Various tissues were dissected from euthanized dogfish sharks (*Squalus acanthias*) and homogenized in Solution D using 10ml per gram of tissue. The homogenates were then stored at -80˚C for further extraction. Soft tissues (brain, and epithelial scrapes from the gill [using a razor blade] and gastro-intestinal tract [using a glass slide]) were homogenized using a syringe and 16-gauge needle, whereas hard tissues (liver, kidney, rectal gland, skeletal muscle, heart etc.) were homogenized using a Kinematica polytron homogenizer. Tissue homogenates were defrosted and then 0.9ml was placed in a 1.5ml microfuge tube and used for RNA extraction. 90$\mu l$ of 2M Sodium acetate pH 4.0 was added to the tube containing the solution and mixed briefly by vortexing. 0.45ml of water saturated phenol was then added and vortexed briefly. Afterwards, 144$\mu l$ of 1-Bromo-2-Chloro Propane (BCP) was added to the tube. This was mixed thoroughly by vortexing until a white emission was formed.

The solution was then spun at a high-speed centrifuge at 14000rpm and 20,817g for 15 minutes at 0℃. After spinning, three layers were seen in the tube containing the solution. The upper aqueous phase (containing RNA) was removed. This was done carefully without taking the interface layer (containing whitish protein precipitates) or the organic phase (containing Phenol, BCP and DNA). The volume of the aqueous solution obtained was measured with a pipette and was transferred into a new microcentrifuge tube. 0.1 volumes of BCP (relative to the amount of aqueous phase obtained) was added and mixed thoroughly by vortexing. This was then spun at high-speed centrifuge of 14000rpm and 20,817g for 15 minutes at 0℃. As before, after centrifugation an aqueous phase was formed at the top of the sample, and this was transferred to a new tube and measured and 0.2 volumes (relative to this new aqueous phase) of isopropanol was added to the tube and vortexed. Then 0.2 volumes of a high salt buffer ((1.2M tri-sodium citrate and 0.8M NaCl) were added and mixed by vortexing.

The solution was kept at room temperature for 10 minutes to allow for RNA precipitation. Afterwards, the tube was collected for spinning in the microcentrifuge at a full speed of about 14000rpm and 20,817g for 10minutes. The liquid (isopropanol+ high salt buffer) was collected after centrifuging by pipetting. 0.5ml of 70% ethanol was then added to the pellet and spun at 14000rpm and 20,817g for 5minutes. The liquid (ethanol) was taken off while making sure that the pellet was not disturbed at the bottom of the tube. To get rid of unwanted salts, another 0.5ml of 70% ethanol was added to the pellet and spun in the microcentrifuge at full speed of about 14000rpm and 20,817g for 5 minutes. The liquid (ethanol) was taken off by pipetting carefully as previously stated. The ethanol was removed as much as possible without losing the pellet and the tube was left with cap open to allow the pellet dry. Finally, to re-suspend the RNA a volume of distilled water proportionate to the size of the RNA pellet obtained (between 20µl and 250µl depending on the tissue) was added to the dried pellet.

Total RNA was then quantified using a UV-Vis spectrophotometer set to 260nm wavelength. Agarose gel electrophoresis was performed to quantify and normalize the RNA based on the fluorescent intensity of the 18S and/or 28S rRNA bands. Experiment 2 tissue homogenates were prepared, stored at -

80˚C and then extracted as above except an additional round of BCP organic extraction was performed on the samples.

**Amplification of the complete Brain UT cDNA sequence using PCR and Smarter 3' RACE PCR**

The RACE cDNA Amplification procedure provides a method for performing both 5'- and 3'-rapid amplification of cDNA ends (RACE). The aforementioned transcriptomics paper (Chana-Munoz *et al.* 2017) had the 5' end sequence of Brain UT (as well as a version probably including some introns) but the sequence was not complete as it was missing its 3'end (i.e., the end of the coding sequence). Therefore, a 3'RACE procedure was carried out to clone and sequence the 3' end of the Brain UT gene sequence to confirm which of the two sequence versions from the transcriptomics paper was the correct transcript (as opposed to a genomic) sequence. The two 3' RACE brain cDNAs that were used for this study had been previously made by Dr. Cutler's lab from a Smarter RACE kit (Takara).

The 5' end segment of the gene was amplified (from before the start codon to the middle of the coding region and was designed to overlap with the 3' RACE fragment produced). For the Brain UT 5'end amplification, a regular PCR master mix containing d $H_2O$, buffer, 10mMDNTPs and phusion enzyme was put together.

For the amplification of the 5' end segment of Brain UT the following primers were used.

Sense, Phusion polymerase Tm =70˚C

CTCGGGCAAA CATTCCGGCA TTAACTACAG TTTG

Antisense, Phusion polymerase Tm =70˚C

TGCGGCCATA TACACCGACA GAGCA

**Note**: For primers of 20+ nucleotides, Phusion reactions can be performed with a PCR annealing temperature at Tm+3˚C, so for Tm's of 69˚C or above, 72˚C would be used.

The smarter 3' RACE PCR experiment was done in two rounds to improve specificity of the PCR (i.e., nested PCR was used). For the first round of 3’ RACE PCR, a technique called ‘touchdown’ PCR was used. The 'touchdown' PCR was as suggested in the kit protocol (5 cycles with annealing primer at 72˚C for 3 minutes, 5 cycles at 70˚C for 30 seconds and 25 cycles at 68˚C for 30 seconds). The kits Universal primer (UPM) mix and a sense Brain UT gene specific primer (Squal brain UT 3R 1) was used for this first round of PCR. The UPM primer mix contained both a short primer and a longer one. The longer primer can bind to the Smarter IIA oligo sequence that is part of the 3’ RACE cDNA synthesis oligo dT primer (CDS) on the end of each cDNA. The shorter primer can bind to products made by the longer primer but at lower temperatures. For the experimental setup, 1µl Brain UT gene specific primer, 2µl of UPM primer mix and 1µl of dogfish brain 3’ RACE cDNA was added to a PCR tube. This was repeated for the second lot of dogfish brain 3’ RACE cDNA. Finally, just before addition to the thermocycler, 16µl of the master mix was added. The mastermix contained 4ul 5X phusion polymerase buffer, 0.4ul 10mM dNTPs, 0.2ul of phusion DNA polymerase (NEB) and 11.4ul d $H_2O$.

3’ RACE

Universal primer mix (UPM) and Squal Brain UT 3’ RACE 1 (gsp)

Touchdown PCR Cycling parameters: -

- 5 cycles: 94°C 30 sec, 72°C 3 min
- 5 cycles: 94°C 30 sec, 70°C 30 sec, 72°C 3 min
- 3 cycles: 94°C 30 sec, 68°C 30 sec, 72°C 3 min

The product of the ‘touchdown’ PCR was then used as a template in the second round of PCR with a second internal (nested) Brain UT gene specific primer. The second round of PCR reactions is known as nested PCR because the gsp sequence used is expected to be part of the products made in the first round of reactions. This means that only the correct products made during the first round of reactions

will have that gsp (Squal brain UT 3R 2) sequence in them (and amplify in the second round of PCR) anything else that's (incorrect) made in the first round won't amplify in the second.

The first reaction was put together by adding 1µl of primer (Smarter Nested Xl primer) to two tubes and 1µl Squal brain UT 3R 2 primer in each. 0.5µl of touch down PCR products from the two dogfish brain cDNAs was added into the corresponding tubes followed by 17.5µl of the master mix. The reactions were then run in the PCR machine. An agarose gel was run and the DNA bands with expected fragment sizes were cut out for purification and cloning experiments. Second round of PCR reactions involved regular PCR. Both rounds of reactions were carried out with Phusion polymerase.

Older kits had in them a Smarter nested XL primer which was basically the other half of the long universal primer compared to the short universal primer (back half; UPS) i.e., the front half. However, this was not included in the kit bought so an extended short primer version was made (Eton Bio).

Smarter nested XL primer, Phusion polymerase Tm =69˚C

GGCAAGCAGT GGTATCAACG CAGAGT

Squal brain UT 3R 1 Phusion polymerase Tm =69˚C

gtacaatggcatcttggttggccttcaact

Squal brain UT 3R 2 Phusion polymerase Tm =69˚C

ggagattggtattggtggctactactgcct

The nested second round of reactions used…

Smarter Nested XL primer and Squal Brain UT 3' RACE 2 (ngsp)

Cycling parameters: - initial denaturation 98˚C for 30 seconds

Cycles 1-35, 98˚C 10sec, 72˚C 3 min

The complete coding sequence of AQP3-2 and its spliceoform were also cloned and sequenced. A piece of RPL-P0 was also cloned and sequenced. However, cloning and sequencing experiments were not done for UT-1 long and short as the sequence was already in the gene bank and in the transcriptomics paper (Chana-Munoz *et al.* 2017). Dr Cutler's lab had also already cloned and sequenced the NCC gene's cDNA beforehand.

Primers were designed as follows

Squalus AQP3-2 Sense Phusion Tm = 71˚C Product = 934bp

ACCAGCATCG GCTTCTCACA GAA

Squalus AQP3-2 Anti Phusion Tm = 69˚C

CTTCAGAGAA TCATAATCCA TGCACTGTCT

Elasmobranch RPL-P0 cloning primers product = 775bp

Elas RPLP0 sense Phusion Tm 69.8 ˚C

Agggaagaca gagctacgtg gaagtcca

Elas RPLP0 anti Phusion Tm 68.6˚C

Aatgggaagg agtagtctgt ctccacagc

**TA- cloning of DNA fragments**

Several cDNA fragments (AQP3-2 spliceoforms, Brain UT, NCC, UT-1 and RPL-P0) were amplified using PCR and then cloned into bacteria to verify their identity. The PCR used cDNA previously generated from brain, kidney, and stomach total RNA of *Squalus acanthias*. Pre-existing general cDNA samples were used to initially amplify (using PCR) Brain UT cDNA fragments for cloning and sequencing and for confirmation of the locations of its expression, but all the qPCR was on kidney cDNAs.

DNA fragments for cloning were made using Phusion polymerase and a proprietary buffer made by the manufacturer, adenine overhangs were subsequently added separately using taq polymerase with 1x taq buffer and 0.1mM dATP. Fragments were run on an agarose gel, cut out using a scalpel under a UV light and purified using the NEB Monarch purification kit (as previously described).

The vector used for cloning was pCR4-TOPO vector with attached topoisomerase enzymes (Life technologies). The vector was mixed with either AQP3-2 spliceoforms, UT-1, RPLP0, Brain UT or NCC cDNA fragments and left for 30 minutes for the vector and the DNA to combine before being added to chemically competent E. coli bacteria.

To insert the plasmid into the bacteria, the tube containing the bacteria and the plasmid was heat shocked at 42℃ in a dry block heater for exactly 30 seconds and returned to ice. Each lot of 12.5µl of bacteria had 62.5µl of SOC medium added to them before being placed on a rotating wheel in an incubator set to 37℃ for an hour to allow the bacteria to recover from the heat shock. After recovery, 37.5µl of the bacteria was pipetted onto an LB agar plate containing kanamycin and spread. Plates were incubated overnight at 37℃. Once the bacteria were sufficiently grown, individual colonies were picked using sterilized toothpicks and the bacteria on the toothpick were used to inoculate 1 ml of terrific broth containing kanamycin at a concentration of 50µg/ml. The tubes were then grown in an incubator at 37℃ overnight.

**PCR Colony amplification of bacterial colonies from TA- cloning of cDNA fragments**

The bacteria culture tubes were collected and re-suspended by vortexing until a cloudy solution was seen. 1.5ml microfuge tubes were labeled and 50µl of each bacterial culture was pipetted into corresponding tubes. The new tubes were spun for 30 seconds at 14000 rpm. The medium was quickly taken out of from the opposite side of where the pellet was in each tube and discarded. The bacterial pellet in the tubes were suspended by vortexing them in 500µl of d $H_2O$ to make the colony template solution. After vortexing, the tubes were placed on ice. To amplify the DNA inserted into the plasmid vector, 1µl of M13 forward and 1µl of M13 reverse bacteriophage primers at a concentration of 4µM were added to each 200µl PCR tubes. 0.5µl of each colony lysate solution was then added to each tube. The needed amount of reactions worth of the master mix was then prepared by multiplying the volume with the standard; 2µl 10x taq polymerase buffer, 0.4µl of 10mM dNTP, and 15µl of distilled water and thoroughly mixed by pipetting. 0.1µl of taq polymerase was added 17.5µl of the master mix was added to each tube containing the primers and colony DNA to give a total reaction volume of 20µl. The tubes were placed into a PCR thermocycler paused at 92℃. After all the tubes were placed in the thermocycler, the thermocycler was then released from pause so that the PCR program could be completed. The cycling parameters used were: $96^0$C for 1 sec to denature; $60^0$C for 15 sec to anneal the primers; and $72^0$C for 40 sec to extend DNA products. This was programmed for 25 cycles. The PCR amplification products were then run on a 1.5% agarose gel and evaluated for the presence of inserts (bands of 180bp of plasmid DNA plus the size of the inserted DNA). 3 colonies that gave signals that looked clean (no second bands) and had approximately the correct length, as determined by primers used, were selected. The DNA from the 3 selected colonies was then reamplified and purified using EdgeBio QuickStep 2 PCR Purification kit (as per manufacturer's instructions).

**Purification of DNA from agarose gel slices**

DNA Gel extraction and purification was performed using New England Biolabs® Monarch DNA gel extraction kit. DNA fragments were run on an agarose gel and relevant bands were excised from the gel using a scalpel. This gel was dissolved using the kit's included Gel Dissolving Buffer (400$\mu l$ per 100mg of gel) and was incubated between 37°C to 55°C and periodically vortexed for 10 minutes. The DNA sample was loaded into a filter column and centrifuged for 1 minute (all centrifugation was done at 16000 g). The DNA in the column was washed using 200$\mu l$ DNA wash buffer and spun again for 1 minute, this step was repeated. The column was then transferred to a clean 1.5ml tube and 20µl of Elution Buffer was added. After incubating for a minute, the column was centrifuged for 1 minute.

**Quantification of gel using logic DNA marker and calculation of the concentration of the insert DNA**

The purified DNA was quantified using agarose gel electrophoresis employing Logic DNA marker. Concentration was determined by measuring the fluorescence of the bands and comparing those values to that of the known DNA marker bands. Concerning the production of standards for qPCR, the molecular weight of each fragment was calculated from its sequence and then Avogadro's number was used to calculate the number of molecules/µl.

The numbers obtained for each band's stain intensity above was used to calculate the concentration of plasmid insert DNA relative to the known amounts of DNA in the standard/ marker DNA. The standard/marker used were from bands with 10, 20, 30 or 40ng and the amount of plasmid insert DNA in each of unknown concentration samples was 2µl. Two markers that were closest in intensity to the intensity of the DNA samples were picked (one more, one less), and the differences in the amount of DNA between the 2 marker bands were calculated. The differences between the 2 marker bands were also calculated. The numbers obtained from these calculations were used to calculate how much intensity there was per ng DNA i.e., between the 2 DNA marker standards that was used. The intensity of the 2 marker bands were taken off the intensity of the samples. Using the number obtained from the intensity per ng DNA, the amount of DNA that the intensity equal to was determined. This

number was added to the amount of DNA that was in the lower (intensity/DNA amount) of the two markers. This gave the amount of DNA in the sample bands. The numbers obtained were then used to calculate the amount of DNA per µl that is in the sample. Once the concentrations of the samples were calculated, the average was used to calculate the volume needed for sequencing.

**Calculation of the volume needed for sequencing**

The size of base pair of the DNA was added to the size of insert (180bp) and divided by 1000. The value obtained was then multiplied by 20. The answer obtained in ng was finally divided by the concentrations determined above (ng/µl). The amount calculated was added to 1µl of T3 primer and dried in the centrifugal evaporator for 15minutes and sent for sequencing.

**RT-PCR of samples from different tissue**

The cDNAs generated from the gill, rectal gland, kidney, esophagus, stomach, intestine, brain, muscle, eye, and liver of dogfish sharks were used to determine the presence or absence of mRNA expression in different tissues and confirm the expression of AQP3-2 and its spliceoform, UT-1 long and short splice variants, Brain UT, NCC and the RPL- P0 (housekeeping control gene) in the kidney. Primers that amplified the complete coding regions were used for AQP3-2 and its spliceoform, UT-1 long and short splice variants. A different sense primers was used for the tissue PCR for Brain UT, this was different from the primers used for the 5' end piece amplification (the antisense primer was common to both). The PCR for these was run at an annealing temperature of 72˚C for 50secs. Otherwise, the primers designed for qPCR were used for NCC and RPL-P0 at an annealing temperature of 68˚C for 15 secs and 35 cycles. A regular PCR master mix containing d $H_2O$, buffer, 10mMdTPs and phusion flex hot start enzyme was put together and used for the PCR experiment. The PCR product was run on a 1.8% agarose gel and the image taken using the gel doc camera (syngene).

**Antibody production**

Polyclonal antibodies for AQP3-2, UT-1 and NCC were made using manufactured polypeptide sequences. Antibodies were made by Genosphere Biotechnologies (Paris, France) sequences (see information below)

AQP3/2: - CQNVKLMSQKPKGRR 10ml A1 0.77 mg/ml A2 0.91 mg/ml

AQP3 antibody peptide: - CGGIGEENVKLANVKLRESS

UT-1: - CKNRRIYQEMKKMEQ 10ml A1 0.549 mg/ml A2 0.40 mg/ml

NCC: - CEGEVRLSSNKLPEE 4ml 0.494 mg/ml (2015 Genscript Antibody)

NCC/2: - NDGFKDEAIVNELRKDC 5ml A1 0.41 mg/ml A2 0.44 mg/ml

To conjugate the peptide, terminal cysteines and sometimes glycines were sometimes added to the peptide to extend it without affecting its immunogenicity. Glycines are preferred because they have no side chain (H only) and are hence not very immunogenic. Also, although cysteines are not part of the gene sequence, they were added to attach the peptide to the carrier protein (KLH) and the affinity purification column.

**Western blotting detection and quantification of proteins**

AQP3-2, UT-1 and NCC have yet to be studied in the tissues of *Squalus acanthias*. Western blotting was used to investigate the presence of these proteins and to enable quantification of their amounts. The protein samples used were Crude membrane extracts that had been made previously. The homogenized tissue samples had been prepared using Protease Inhibitor Cocktail V (RPI) and pelleted by centrifugation at 5000g. The supernatant was removed, and the pellet was re-suspended in buffer containing protease inhibitors and stored frozen at -80℃. A cocktail of chemicals was prepared to denature the proteins. 4x denaturing buffer was added that contained the following: 250mM tris pH 6.8, 8% 2-mercaptoethanol, 8% SDS, 40% Glycerol, 0.02 % Bromophenol Blue (dye). The samples were then

heated in a PCR machine to 99℃ for three minutes. The protein crude membrane extract samples used were obtained from Squalus kidney and brain.

The SDS-polyacrylamide gel electrophoresis followed the procedures of Laemmli (Laemmli 1970). Two gels were used for each experiment, each has an acrylamide resolving gel and stacking gel. A 40% stock of acrylamide with a ratio of 29:1 acrylamide:bis-acrylamide was used to make them. The resolving gel required 10% acrylamide with a ratio of 29:1 acrylamide:bis-acrylamide except for NCC where a 6% gel was used. A lower percentage (5%) acrylamide was prepared for the stacking gel. For two gels, 70ml of resolving gel was prepared using: 33.3 ml $H_2O$, 17.5ml 40% acrylamide stock, 17.5 ml 1.5M tris pH 8.8, and 0.35 ml 20% SDS. These were mixed and then had 0.7 ml 10% ammonium persulfate and 0.056ml TEMED setting agents added. The liquid gel was added to the apparatus using a 30ml syringe with a 16-gauge needle attached and left to set for 30 minutes. A small amount of Isobutanol was added to smooth out the top surface. After setting, the surface was then washed with distilled water. The stacking gel was made right before the 30 minutes expired. The gel was made with 10.276ml $H_2O$, 1.750ml 40% Acrylamide stock, 1.750ml 1M Tris pH 6.8, 0.070ml 20% SDS. These were mixed and then had 0.140ml 10% ammonium persulfate, 0.014ml TEMED polymerization agents added. The gel was poured, and the comb was added and left for 30 minutes to set. After setting, the comb was removed, and the wells were rinsed using distilled water. The gel running buffer (25mM tris, 250mM glycine, and 0.1% SDS) was then added to the tank after the apparatus was prepared and the gel was attached to the electrophoresis apparatus. The samples were loaded into the wells. Additionally, kaleidoscope protein markers (Biorad) was added to the gel on each sides of the samples (10 µl). The gels ran overnight for around 16 hours at around 45 volts.

Following the completion of electrophoresis, the gels were removed, and the gels proteins were electroblotted on to a polyvinylidene fluoride (PVDF) membrane filter (Biorad's Sequi-Blot). For electroblotting, fiber pads and blotting paper were prepared. The blotting paper (48mM tris and 39mM Glycine) was wet in blotting buffer and a PVDF filter (used to bind the proteins) was wet using 100%

methanol. The cassette was prepared by placing the wet filter paper on the clear side of the cassette (positive electrode side). The gel was removed from the electrophoresis tank and the casting clamps were removed. The gel was placed on top of the PVDF filter and massaged to remove any air bubbles. Wet blotting paper was put on top of the gel and a fiber pad was added above that. The cassette was closed and inserted into the blotting tank. The tank was then filled with buffer and was left to run overnight at 15 volts. A large stock of 1X TNT buffer at pH 8 was prepared using 10mM tris, 150mM NaCl and 0.05% Tween 20. 5% nonfat dry milk powder (Blotto blocking agent) was added to 10 ml of 1x TNT buffer in separate glass trays labeled for AQP3-2, UT-1 and NCC antibodies respectively.

The western blot strips were removed from the apparatus and placed into glass trays containing the TNT buffer and the blocking agent. The dishes were put onto a rocking platform and incubated for 30 minutes. The blots were washed three times using 10 ml of 1x TNT buffer. After the washing, 25µl of the antibodies (AQP3-2, UT-1 and NCC respectively) at a 1 in 400 dilution was added to the appropriate dish and was incubated on the platform for 1 hour.

The samples were then washed 4 times followed by the addition of 5µl of the secondary Donkey Anti-rabbit antibody with attached alkaline phosphatase enzyme (1/4000 dilution) and this was allowed to incubate for 1 hour. All blots were washed 4 times with the 1x TNT buffer and then 5ml of 1 step NBT/BCIP reagent (with 1mM levamisole endogenous alkaline phosphatase suppressor; Peirce/Thermofisher) was added to the dish and 1-10 minutes of swirling was performed to allow the color to develop. Finally, the strips were washed with distilled water and dried and photographed.

**Immunohistochemistry**

Tissues were dissected out of euthanized dogfish sharks, cut into <4mm pieces as necessary, placed into histological cassettes and placed in fixative (fresh 4% paraformaldehyde made up in phosphate buffered saline) for >2hour. After fixation, cassettes were processed through increasing alcohols (1 hour in each of 50%, 70%, 85%, 95% 2 x 100%). Cassettes were then transferred to 2 lots of histochoice clearing agent, followed by 3 lots of molten paraffin wax held at around 58-60˚C, for 1 hour in each lot. Finally, tissues were removed from cassettes and placed in a stainless-steel mold and manipulated into the correct orientation. The mold was then filed with molten wax and the body of the cassette (minus its lid) was placed on top of the mold, with more wax poured into the cassette body. The molds were then transferred to a cold plate around 0˚C to set. After setting the wax blocks attached to the cassette body were snapped out of the molds. Organ samples preserved in paraffin embedded blocks prepared from previous experiments (as described above) were available to use for immunohistochemistry. Blocks were cooled on ice to harden the wax and then placed in the chuck of a Leica microtome, where 5 µm thick tissue sections were then cut. Sections were transferred to a float bath of distilled water heated to 35-37˚C, to smooth out wrinkles in the sections. Slides were brought up underneath the wax sections until the edge of the section attached to the slide surface. Slides were then pulled out of the water to attach the whole section to the slide. Slides were place almost vertical to allow water to drain out from between the slide and the section. The slides were heated on a slide drier overnight at around 50-55˚C.

When immunohistochemistry was to be performed on the slide, wax was removed by putting the slides into a slide rack and then placing the slide rack into two lots of histochoice clearing agents for 5 minutes, followed by a series of increasingly dilute ethanol solutions from 100%, 95%, 85%, 70%, and 50% (5 minutes in every alcohol solution). Slides were then rinsed with phosphate buffered saline (PBS) for 5 minutes. Slides were then incubated in 400ml of a solution containing 50% PBS buffer, 3.5g NaCl and 0.05% Tween 20 detergent for 10 minutes to permeabilize the tissue. This was followed by 5 minutes

in 400ml of a solution of PBS buffer containing 1.07g of ammonium chloride which reacts with and neutralizes any remaining paraformaldehyde fixative. The tissue on sections was then ringed with a hydrophobic Aqua hold PAP pen (Scientific Devices Lab.) and they were then placed horizontally in a slide box, and sections were then blocked first using a proprietary "Background Buster" blocking solution for 30 minutes. This was dropped onto the slides from a poly bottle. Afterwards, the slides were washed 3 times with PBS. Slides were then further blocked using a solution of PBS buffer containing 1% BSA protein and 0.1% gelatin. For some slides where necessary (due to low signal levels) to enhance the staining, extra steps were carried out using a tyramide superboost amplification kit (Life Technologies). This was done by adding 50µl of hydrogen peroxide to slides for 1hour, the slides were washed 3 times with PBS. This was followed by 50µl of blocking buffer (10% goat serum) which was added for 1hour. The primary antibodies were prepared (99µl PBS, 1µl antibodies) and 100µl was added to the slides for 1hour incubation period. To detect the primary antibodies, for non-amplified slides, 100 µl of a secondary antibody, donkey anti-rabbit IgG with a fluorescent tag attached (Alexa fluor plus 488; Life Technologies) was added for another 1hour incubation period. For tyramide amplified slides, a goat anti-rabbit secondary antibody (with poly-horse radish peroxidase (HRP) enzymes attached) was used. Also, for slide incubated with a mouse anti-acetylated tubulin monoclonal antibody, and a goat anti-rabbit IgG (labeled with Dylight 550 fluorescent dye; Thermofisher) secondary antibody was used. The slides were washed with PBS 4 times between each incubation periods. For the tyramide amplified slides only, 100 µl of the tyramide (linked to Alexa 488 fluorescent dye) solution was then added to the slides for 10mins followed by the tyramide kit's stop solution. The tyramide kit's secondary antibody HRP enzymes cause a reaction between the tyramide and nearby tyrosine amino acids of proteins, depositing multiple Alexa 488 dye molecules close to the primary antibody's location. Slides were washed again 3 times with PBS. On some non-amplified or tyramide-amplified slides, further steps were included to deploy a further rabbit antibody. These slides were incubated in 10% normal rabbit serum for 30 minutes to block the initial secondary antibodies used that can bind rabbit IgG. The slides were then washed in PBS 3 times and then incubated with rabbit anti-dogfish AQP3 or AQP4/2 polyclonal antibodies labeled with a CF633

fluorescent dye (labeled using Biotium's antibody CF633 dye labeling kit) for 1 hour, and they were then washed a further 4 times with PBS buffer. All slides were further treated with Biotium "True Black autofluorescence quencher" for 30seconds. Slides were washed a further 3 times with PBS buffer and mounted with Prolong diamond coverslip mounting medium (Thermofisher), which contained DAPI as a counter stain that stains the nucleus. Finally, the slides were visualized using a Zeiss LSM 710 confocal laser-scanning microscope and images taken. The microscope was set up to collect light only from the non-overlapping parts of the various dye emission spectra.

For immunohistochemistry experiments used to localize proteins to different parts of the shark nephron, various tools were used to identify different segments. Previous studies had shown that cells with cilia/flagella (also known as multi-cillary cells) were present in the neck and proximal tubule nephron segments and these diminished in the intermediate nephron segments and were absent from the distal tubule segments and collecting duct (Lacy and Reale 1985a, Hentschel 1987, Hentschel 1991, Lacy and Reale 1995). Therefore, an acetylated tubulin antibody (Sigma T6793 monoclonal antibody) was used to label cilia to identify segments of the first proximal/intermediate segment sinus zone loop. Furthermore, Dr Cutler's Lab had previously determined that high levels of staining were found with AQP3, AQP4 and AQP15 antibodies in the late distal tubule sinus zone loop. Hence the acetylated-tubulin, AQP3 and AQP4 were used with AQP3-2, UT-1 and NCC antibodies to determine which nephron loop in the sinus zone staining was localized to.

For the peptide blocking experiment, as the AQP3-2 antibody staining was weak, there was concern the staining might be coming from a cross reaction of the AQP3-2 antibody with the AQP3 protein whose staining was relatively much stronger. To confirm that the AQP3-2 antibody is binding the AQP3-2 protein rather than the AQP3 protein, the peptide that the AQP3 antibody was made against was used to block the AQP3-2 antibody (both antibodies were made against the C-terminal end of each respective protein). If the AQP3-2 antibody was really cross reacting and binding AQP3 instead of AQP3-2, the peptide blocking would abolish the staining. If not, it might have diminished the staining somewhat

(because it will probably block some of the antibodies up with the AQP3 peptide), but there should still be significant staining. AQP3 and AQP3-2 share 4 amino acids out of 14 (of the AQP3-2 peptide; AQP3 peptide is actually 20 amino acids long), However, they also have a 4 amino acid motif NVKL in common (as underlined in the antibody production information above).

The block solution was prepared by adding 2µl AQP3-2 antibody to 3.9µl AQP3 peptide and 194.1µl PBS (corresponding to 50µg/ml peptide). The AQP3 peptide was added to the AQP3-2 antibody and incubated for 1hour before adding the primary antibodies to the AQP3-2 slides. Additionally, similar control slides were produced where the primary antibodies (against dogfish AQP3/2, UT-1 or NCC proteins), were blocked with the corresponding peptides used to make these polyclonal antibodies in rabbits. The tubulin commercial antibody (anti-Acetylated alpha tubulin mouse monoclonal antibody (Sigma T6793)) was used to label cilia in dogfish shark nephrons, to differentiate the proximal and intermediate nephron segments (with cilia) from the late distal tubule segment (without cilia).

**cDNA production and qPCR**

Quantitative polymerase chain reaction (*qPCR*) is a method of quantifying DNA based on PCR. qPCR tracks target DNA molecule concentration as a function of the number of PCR cycles to derive a quantitative estimate of the initial target template concentration in a sample. As with conventional PCR, it uses a polymerase, dNTPs, and two primers designed to match sequences within the target template. Complementary DNA (cDNA) templates are synthesized or manufactured from messenger RNA (mRNA) templates. cDNA is synthesized in a reaction that is catalyzed by a modified version of the Maloney Murine Leukemia Virus (MMLV) reverse transcriptase with the commercial name Superscript IV (Life Technologies/Thermofisher). Reverse Transcription (RT reaction) is a process in which single-stranded RNA is reverse transcribed into cDNA using total cellular RNA or poly ($A^+$) RNA as a template, Superscript IV RT enzyme, a primer, dNTPs and a Superase In RNase Inhibitor (Life Technologies/Thermofisher). The resulting cDNA can be used for various purposes including RT-PCR or qPCR reactions.

qPCR was used to quantify the expression of AQP3-2 and its spliceoform, UT-1 long and short splice variants, Brain UT, NCC and a RPL-P0 housekeeping control gene. Pre-existing total RNA samples obtained from the kidneys of six sharks per group acclimated to 75%, 100% and 120% SW in three stages over the course of one week were used to make cDNA for qPCR. Two sets of cDNA samples were used for the qPCR experiment. The first set of RNA samples (experiment 1) had been previously produced by other students in Dr. Cutler's lab from a previous experiment and stored in a -80˚C freezer. The second set of total RNA samples (experiment 2) were extracted using the total cellular RNA extraction protocol as described above. Both sets of samples were normalized and RNA gel electrophoresis was used to determine which of the samples were partially or wholly degraded during the storage of the initial tissue homogenates (experiment 2 samples). Six samples (from Expt. 2) that were partially or completely intact and normalized were used for qPCR this was done to see how the results from Expt. 2 compared to those from Expt. 1 Samples.

**RNA gel electrophoresis and normalization of samples from experiment 1 and experiment 2**

A 1.5% gel was made by weighing 2.03g of agarose into a conical flask and adding 105ml d $H_2O$ (a high concentration of agarose was used to prevent formaldehyde from breaking the gel apart). The flask was covered with double-layered cling-wrap and a small hole was pierced on top with a pen to allow air escape when boiling. The mixture was then heated in the microwave for about 45sec on full power, followed by 1 min on 30% power. The flask was carefully swirled using the thermally protective gloves. The gel flask was then taken to the fume hood where 6.75ml of 20X MOPS was added (to give a 1X final concentration) followed by 23.035ml of 37% (w/v) Formaldehyde (to give a 17.5% final concentration). The flask was placed in a water bath at 45˚C to cool to pouring temperature. 13.5µl of the Gel red DNA stain (a UV florescent dye that intercalates into nucleic acid strands and gives out orange light following UV illumination) was added to the gel flask in the water bath. While the flask was cooling in the water bath, the gel tray was assembled by taping up the sides of the gel tray with masking tape. Once the gel cooled for 15 minutes in the water bath, it was poured into the tray placed on a flat and leveled part in the

fume hood. The comb with the thickest teeth was immediately inserted into the slot at the end of the gel. While the gel was cooling, the RNA stock was gotten from the freezer and defrosted by putting the tube in between the fingers and vortexing. After defrosting, the tube was put in the dry block heater set at 65˚C for 3 minutes. The mixture was vortexed and placed on ice.

Two sets of 0.5ml tubes were labeled appropriately. The first set was For Expt. 1 samples, obtained from sharks acclimated to 75 % (6 tubes), 100% (6 tubes) and 120% (6 tubes) seawater. The second set was for Expt. 2 samples obtained from sharks acclimated 75 % (6 tubes), 100% (6 tubes) and 120% (6 tubes) seawater. 2.5µl of RNA from the stock tube was added to each tube and 10µl of formamide was added to each tube to give the RNA sample a 50% final concentration. 3.5µl of formaldehyde was added so that the formaldehyde solution added is 17.5% of the RNA sample final volume. Finally, 1µl of 20X MOPS was added to the mixtures in both tubes to give a final concentration of 1X. All these were done under the fume hood because of the tetratogenic nature of the chemicals used. The samples were heated in the thermocycler at 65˚C for 5 minutes. After 5 minutes, the tubes were collected and placed on ice. 1µl of loading dye was then added to the samples. 250ml of 1X MOPS (the gel running buffer) was prepared by measuring 12.5ml of 20X MOPS into a measuring cylinder and making it up to a final volume of 250ml with d $H_2O$. The solution was carefully inverted to mix, (using stretched parafilm over the cylinder mouth and holding it at the top to prevent leakage). The gel tray containing the gel was then placed inside the electrophoresis tank and the 1xMOPS buffer running buffer prepared above was then poured inside the tank until it covered the gel by around 1mm. The samples were loaded into individual gel wells by pipetting using new tips for each sample. After loading the samples into the gel, the gel remaining buffer was poured to cover the gel surface and the tank was covered with the lid. The gel ran at 150 volts for 1hour. The intensity of the 28S and 18S bands were quantified using the gel doc camera (see Figure 3).

For the normalization process, Experiment 1 samples were run out on a gel thrice and the Experiment 2 samples twice. A sample from each set (3 replicates each) was also run to be able to

normalize the levels of Expt 1 and 2 together. Also, to counteract the effect of variability of the gel doc camera across its width, two rows of the same samples were done each time. The second row had the samples half reversed such that those samples on the outside of the row were now in the middle and vice versa

e.g.

1 2 3 4 5 6

4 5 6 1 2 3

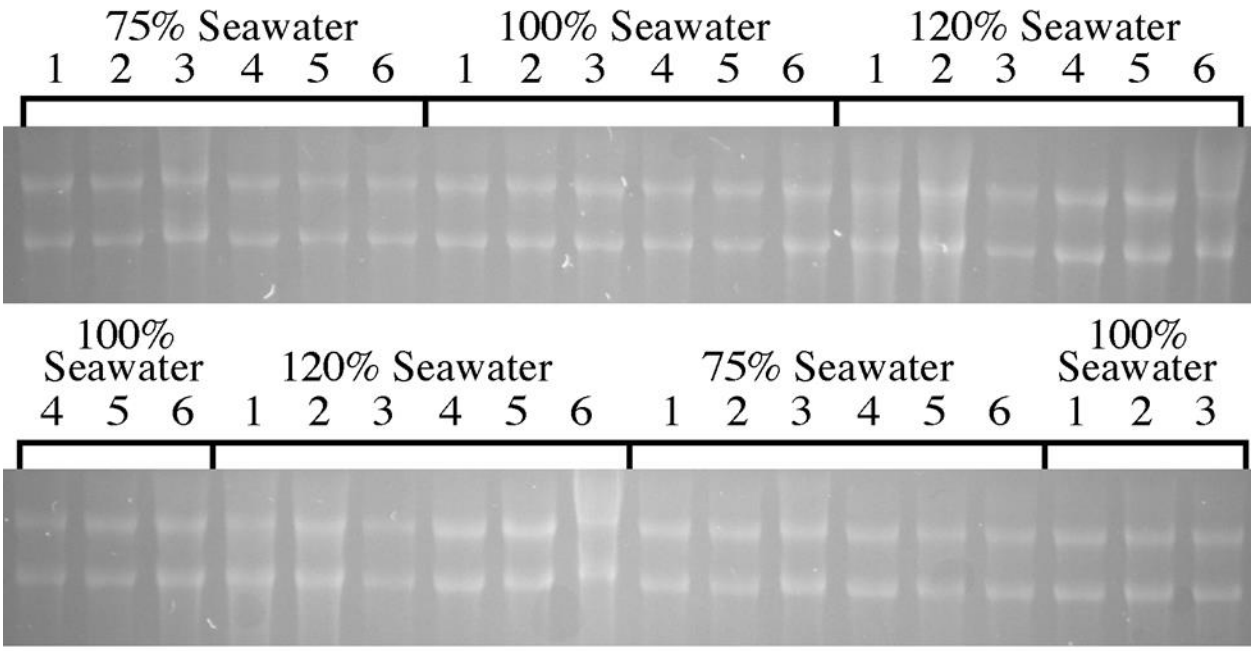


**Figure 3:** Agarose gel electrophoresis of *Squalus acanthias* kidney Expt.1 samples.

The housekeeping gene (RPL P0) was used to assess the gel electrophoresis normalization process of the total RNA samples and potentially to be used to correct for any variability if necessary. The concept of using a housekeeping gene such as RPL P0, is that it should be expressed in equal amounts between organisms and each tissue and in principle would not be affected by salinity. Theoretically, by comparing the expression of biological replicates of RP-LP0 to the average RP-LP0 expression of all samples, one may adjust for any variation produced during the preparation of the samples.

Calculations for processing the data and additionally normalizing data using RPL P0 data were made using Excel. For Expt. 1 samples, obtained from sharks acclimated to 75%, 100% and 120% seawater, there were 6 biological replicates (fish) per group. For Expt. 2 samples obtained from sharks acclimated to 100% and 120% seawater, there were 3 biological replicates (fish) per group. For each sample 3 technical replicates were performed for the qPCR experiments to increase the accuracy of the data.

**Complementary DNA (cDNA) synthesis for qPCR**

The total RNA samples for experiment 1 were made previously and were hence available for qPCR experiments. (See above for the RNA extraction of experiment 2). The cDNA from both experiment 1 and 2 total RNA samples were processed together (24) total RNA samples from kidney tissues were diluted to 222ng/µl by adding a fixed 10µl of RNA to a tube and varying the volume of water added to adjust the concentration correctly. This reduced the error produced by variably pipetting different volumes of RNA (which tend to be sticky and difficult to pipette accurately). Diluted RNA samples were defrosted and heated at 65˚C to re-dissolve and denature the RNA. Samples were kept at 0˚C or on ice at all other times except when being used. A mastermix of 26µl of 100µM Oligo (dT) $_{37}$, 26µl of 10mM dNTPs and 13µl of SUPERase in thermostable RNAse inhibitor (20U/µl; Life Technologies) was produced and 2.5µl of this mastermix was added to 24, labelled 200µl PCR tubes. 4.5µl of each diluted total RNA sample was added to its respective tube of mastermix. The tubes were then heated in a thermocycler at 65˚C for 5 minutes and cooled to 4˚C. Meanwhile, a second mastermix of

52 µl of 5x Superscript IV RT buffer, 13µl of 100mM Dithiothreitol (DTT) and 13µl of Superscript IV reverse transcriptase (200U/µl) was created. 3µl of this mastermix was then added to each tube in the thermocycler (final reaction volume per tube was 10µl). The tubes were then heated to 45˚C for 30 seconds to anneal the oligo dT primer and then the temperature was raised to 55˚C for 30 minutes for cDNA synthesis. After this time the temperature was finally raised to 80˚C for 10 minutes to heat inactivate the reverse transcriptase.

The cDNAs were then diluted by the addition of 190µl of d $H_2O$ to each tube. These sub-stocks of diluted cDNA were then used (4.5µl) in each 10µl qPCR reaction.

**PCR fragments and standards production for qPCR**

Standards were made for absolute qPCR of the AQP3-2 and its spliceoform, UT-1 long and short splice variants, Brain UT, NCC and RPL-P0 genes. These standards were produced by running PCR reactions on kidney (most gene fragments) and brain (Brain UT) cDNA samples. The resulting PCR reactions for each gene were run on a 2% agarose gel and quantified (to give concentrations in ng/µl; (see earlier)). Once the concentration of each fragment was determined, standards were produced by dilution and the calculations for which were performed by first calculating the fraction of a mole present in each sample per µl. This was done by dividing the concentrations calculated from the quantification experiment by the molecular weights of each gene's fragment. The answer was then multiplied by Avogadro's number ($6.02214076 \times 10^{23}$ ) to get the number of molecules in that fraction of a mole per µl.

The number of billion molecules per µl for each fragment was then used to calculate how to dilute each fragment to 1 billion molecules per 4.5µl the volume of template used for qPCR reactions). Each standard fragment was then serially diluted down using a 1:10 dilution to 10 molecules per 4.5µl. In the qPCR process itself, standards were replicated twice per plate.

For qPCR, a LUNA 2x mastermix (New England Biolabs) was used, it contains a hot-start taq polymerase and uses a SYBR green-like fluorescent dye that intercalates into double-stranded DNA. For

qPCR assays a QuantStudio6 Flex Real-Time PCR instrument (Applied Biosystems/Thermofisher) was used. A mastermix of 0.25µl of each 10µM primer and 5µl of LUNA 2x Mastermix was created for the number of samples being run, 5.5µl of this mix was pipetted into the wells of the plates and 4.5µl of each cDNA was added to each well of the plate used (new tips were used for both steps). qPCR experiment was also carried out to confirm that genomic DNA was not being amplified (-RT), these reactions used a total RNA sample diluted to the same extent as the amount of RNA used to make the equivalent amount of cDNA used in the actual qPCR reactions. This was carried out by adding 5.5µl of the mastermix and 4.5µl of RNA and running it under the same conditions as the cDNA experiments. The plate was sealed with a microamp optically adhesive film cover (Applied Biosystems/Thermofisher) and centrifuged at 1200RPM for 2minutes in a Beckman J30i centrifuge using a JS5.9 swinging-bucket rotor before running the plate in the qPCR machine. An Excel spreadsheet (Microsoft) containing the results was exported from the QuantStudio6 instrument after the completion of each qPCR run.

A formula for the relationship between the standard concentration (X; molecules per reaction) and the Ct value (Y) of the standard reactions (i.e., $Y = mX + B$) was created, as the instrument performs regression analysis and generates a Slope (m) and Intercept value (B) from the standard reactions. The equation generated was then applied to the data (Ct values) of each unknown sample to obtain the number of template molecules in each reaction. The three replicates for each sample were then averaged, and then averages and standard deviations were calculated for each group of three (Expt. 2) or six (Expt. 1) fish in the experiment. Statistically significant changes in gene expression were evaluated using an ANOVA statistical test with subsequent post hoc analysis.

# CHAPTER 3

# RESULTS

## RT-PCR of samples from different tissue

The mRNA expression of the following genes, AQP3-2, UT-1 long and short splice variants, Brain UT, NCC and the RPL- P0 (housekeeping control gene) was determined in a variety of dogfish shark (*Squalus acanthias*) tissues (gill, rectal gland, kidney, esophagus, stomach, intestine, brain, muscle, eye, and liver) using RT-PCR and agarose gel electrophoresis (Figure 4). Multiple AQP3-2 bands were seen in kidney and brain (the biggest two bands from kidney were cloned and sequenced to confirm their identity). UT-1 short and long splice variants were also only expressed in brain and kidney. The recently identified Brain UT gene, had a band of the correct size on the gel in most tissues except in the gill and stomach. High levels of expression were seen in brain and eye. But there were also larger and smaller bands present in the intestine, brain, eye, and liver of unknown identity. The NCC cotransporter was mainly expressed in the kidney but with faint DNA bands also in intestine and brain. RPL-P0 was ubiquitously expressed in all tissue as expected for a housekeeping gene.

These genes were cloned and sequenced after confirming their expressions in *Squalus acanthias* especially the kidney (for information concerning gene sequence results see the Appendix).

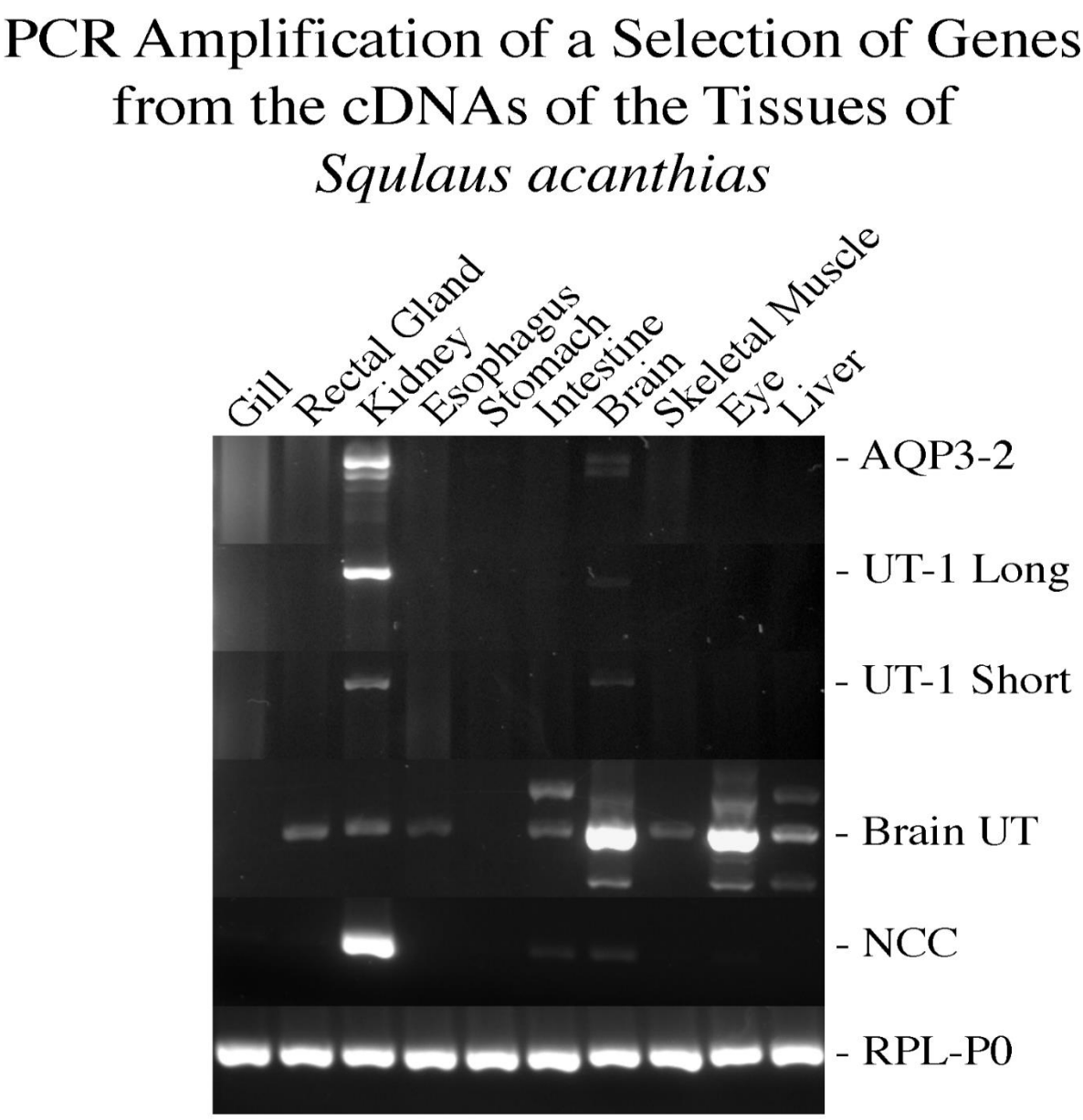


**Figure 4:** Agarose gel electrophoresis of the PCR amplification products of the AQP3-2, UT-1 long, and short splice variant versions, Brain UT, NCC and housekeeping control (RPL-P0) genes in the gill, rectal gland, kidney, esophagus, stomach, intestine, brain, skeletal muscle, eye, and liver tissues of *Squalus acanthias*. The image is a composite of multiple gels and in each case the sizes of products was determined using 2-log ladder DNA markers (NEB; not shown).

## Western Blots result

### *Squalus acanthias* AQP3-2 western blot using crude plasma membrane protein

The three antibodies produced (AQP3-2, UT-1 and NCC/2) by Genosphere (Paris, France) each had been produced in two rabbits (A1 and A2), the results from these appeared identical and so they were often used interchangeably in Western blotting (and Immunohistochemistry).

Initial blots with the AQP3-2 antibodies (Figure 5) were carried out using kidney and brain crude membrane protein extracts as the PCR tissue gel (Figure 4) showed expression in these tissues. These blots (e.g. Figure 5) showed no signal in the the kidney, but the brain sample had a low molecular weight band at 19 kDa.

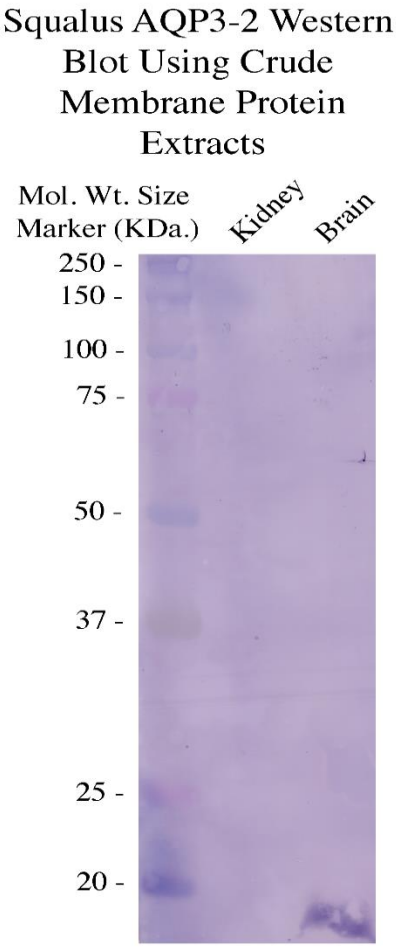


**Figure 5**: Western blot for AQP3-2 antibody (A1) using crude membrane protein extracts (400µg), the blot was incubated in NBT/BCIP enzyme substrate (Peirce) for 8 minutes. The Western blot was made to confirm the expression of AQP3-2 protein in kidney and brain tissues of *Squalus acanthias*. Kaleidescope protein molecular weight marker (Biorad) and its visible bands (kDa) are labeled.

### *Squalus acanthias* AQP3-2 western blot using purified plasma membrane protein

In the AQP3-2 blot made using purified plasma membrane protein, protein bands are seen between 25 KDa and 37 KDa markers sizes (Figure 6 suggesting that there may be multiple N-glycosylated versions of both the splice variant (expected size 27kDa) and the complete version (expected size 32kDa) of the protein. These bands had sizes estimated to be 26 KDa, 27 KDa, 29 KDa, 30 KDa, 31 KDa, and 32 KDa. Possible dimer and trimer bands were seen at 56 KDa and 83 KDa.

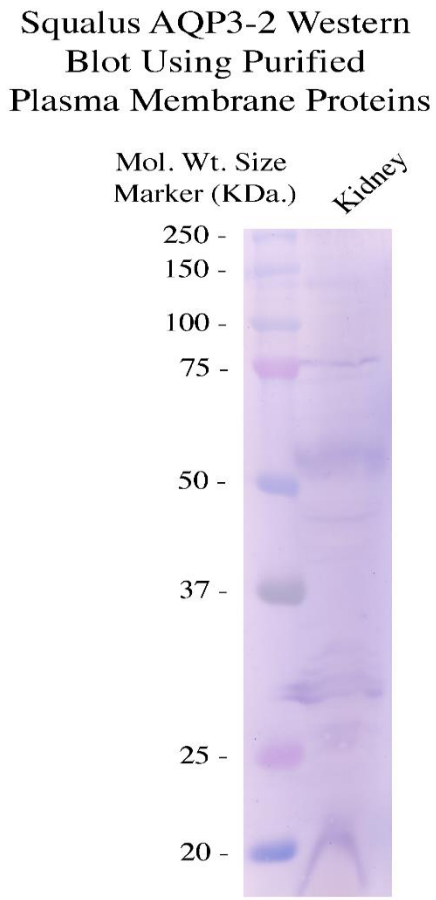


**Figure 6**: Western blot for AQP3-2 antibody (A1) using purified plasma membrane protein extracts (300µg). The blot was incubated in NBT/BCIP enzyme substrate (Peirce) for 5 minutes and was performed to confirm AQP3-2 protein expression in the Kidney of *Squalus acanthias*. Kaleidescope protein molecular weight marker (Biorad) and its visible bands are labeled. Note: The AQP3-2 protein sequence has an N-glycosylation motif and assuming that was utilized, it would make the proteins larger than expected on the Western blot and could potentially produce multiple bands.

### *Squalus acanthias* UT-1 western blot using crude membrane protein extracts

Western blots were also produced using kidney and brain crude membrane protein extracts as the PCR tissue gel (Figure 4) showed that UT-1 was expressed in these tissues. The blots were incubated with the UT-1 A1 and A2 antibodies. (Figure 7). Two main protein bands of around the correct size were obtained with the UT-1 antibodies and these were seen at 53.5 KDa and 45.5 KDa. These bands probably represent an N-glycosylated version of the UT-1 long and short spliceoforms (non-glycosylated sizes are 51.5kDa and 43.5 kDa respectively). Faint bands were seen at 52 KDa, 39.5 KDa, and 26 KDa. The peptide blocked samples showed no bands.

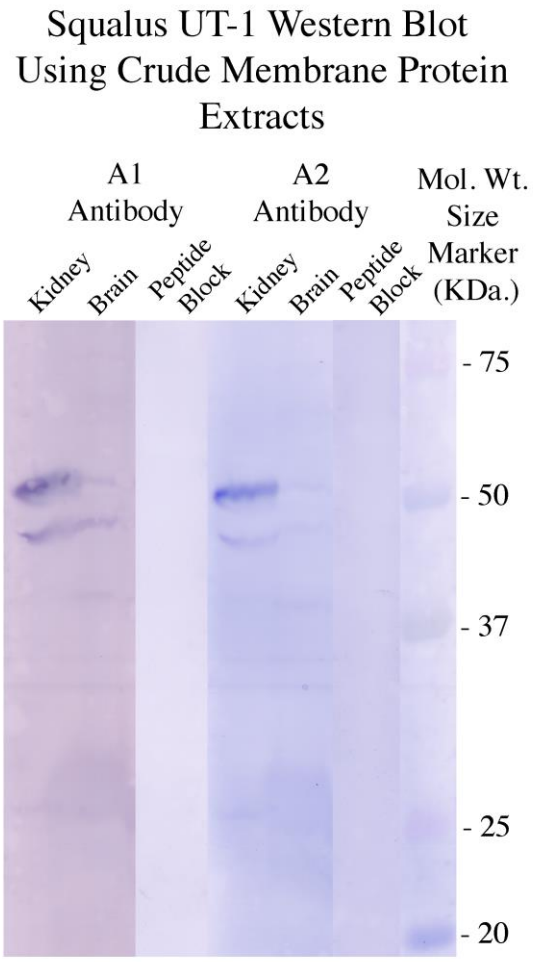


**Figure 7**: Western blot for UT-1 A1 and A2 Antibodies using crude membrane protein extracts (400µg). The blot was incubated in NBT/BCIP enzyme substrate (Peirce) for 5 minutes. For the peptide blocked control blots, the UT-1 antibodies were pre-incubated with the peptide antigen used to make the antibodies (50µg/ml) for >1 hour. The Western blot was made to confirm the expression of UT-1 protein in the kidney and brain of *Squalus acanthias*. Kaleidescope protein molecular weight marker (Biorad) and its visible bands are labeled. Note: The UT-1 short and long protein sequences have 3 or 4 N-glycosylation motifs respectively and assuming that one or more than one of these was utilized this would make the proteins larger than expected on the Western blot and could potentially produce multiple bands.

### *Squalus acanthias* NCC/2 western blot using crude membrane protein extracts

Western blots were additionally produced using kidney crude membrane protein extract as the PCR tissue gel (Figure 4) showed NCC expression was predominantly located in this tissue. The blots were incubated with the NCC/2 A2 antibody (see Figure 8). Main protein band of around 45kDa was obtained. Faint bands seen at 60 kDa. Both the main protein band and faint protein band are too small to represent the complete NCC protein (115+ kDa). The peptide-blocked antibody blot eliminated the bands seen in the normal NCC/2 antibody blot, showing the staining was specific to the antibody.

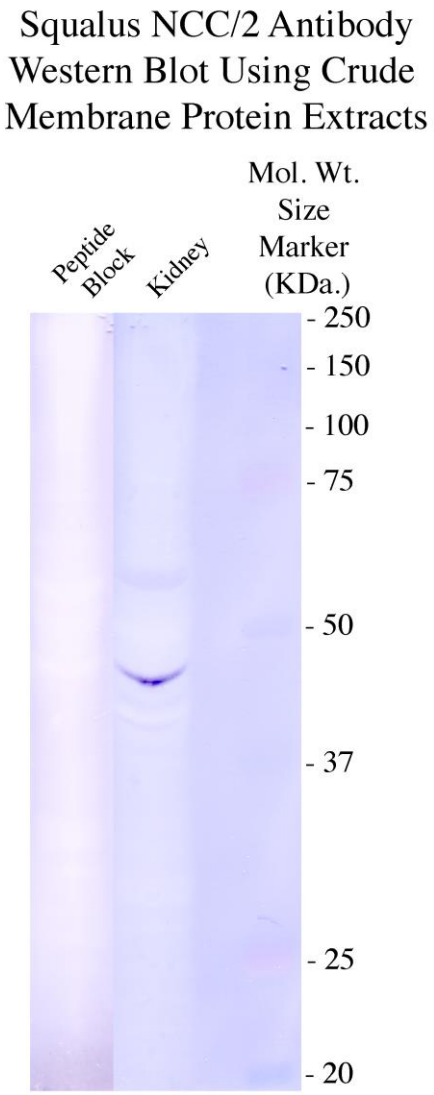


**Figure 8**: Western blot for NCC/2 (A2) antibody using a crude kidney membrane protein extract. The blot was incubated in NBT/BCIP enzyme substrate (Peirce) for 8 minutes. For the peptide blocked control blot the NCC/2 antibody was pre-incubated with the peptide antigen used to make the antibody (50µg/ml) for >1 hour. The Western blot was made to confirm the expression of NCC protein in the kidney of *Squalus acanthias*. Kaleidescope protein molecular weight marker (Biorad) and its visible bands are labeled.

## Immunohistochemistry

### AQP3 and AQP3-2 Immunohistochemistry results

Three antibodies were raised against AQP3-2, UT-1 and NCC transporter proteins. Initial experiments using a standard immunohistochemistry technique yielded no specific signals when the slides were viewed under the microscope. So, it was decided to purchase a tyramide amplification fit (Thermofisher) which could amplify signals up to 200x. Use of the tyramide kit was with the AQP3-2 (Figures 9, 11 and 12) and UT-1 antibodies (Figures 13-16). The results with both AQP3-2 antibodies (A1 and A2) showed staining in narrow tubules in the sinus zone of the kidney (Figure 9A and B) and in the EDT segment in tubules of the convoluted bundle zone (Figure 9C and D). Close ups of the EDT using the confocal microscopes Airyscan super-resolution module showed that the basal membrane of the EDT is a complex structure with numerous invaginations which stain with the AQP3-2 antibody (Figure 9E and F). Control (no primary antibody) sections of the sinus zone (Figure 9G) and convoluted bundle zone (Figure 9H) showed no similar staining.

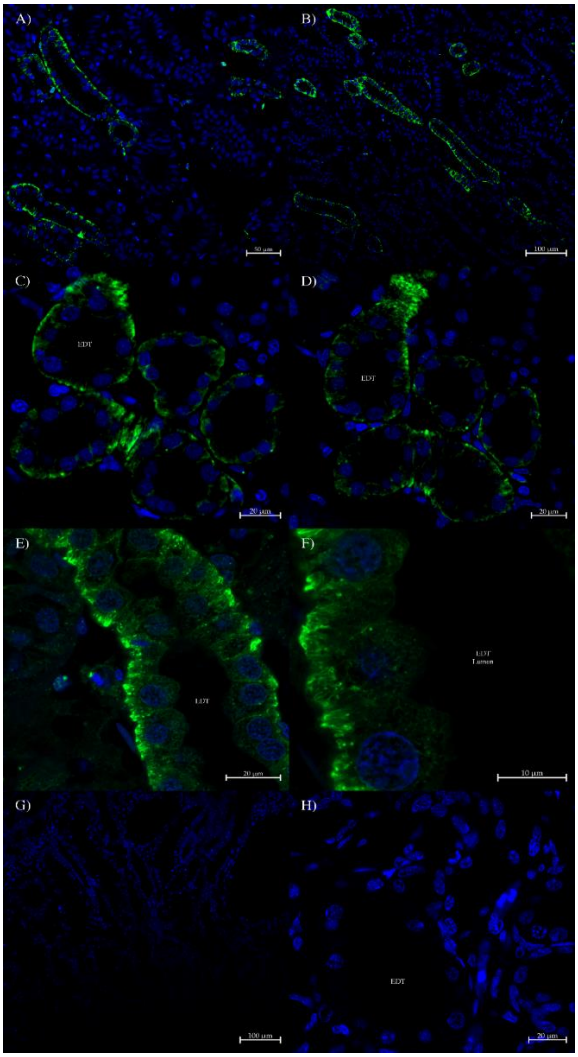


**Figure 9**: Initial kidney section immunohistochemical images labeled with the AQP3-2 A1 (A and C) and A2 (B, D, E, and F) antibodies and no-primary-antibody control sections. Sections A and B are of the sinus zone and both antibodies show basolateral AQP3-2 staining (green) of narrow nephron tubules. Serial sections C and D show convoluted bundle zones with 5 EDT tubules, where the AQP3-2 antibodies stain (green) the basolateral pole/ membranes of the EDT nephron tubules. Sections E and F were Airyscan super-resolution images, produced using a 40x oil (E) or 100x oil (F) lens. Sections G and H were control sections processed without the primary antibody, with a typical image of the sinus zone (G) and bundle zone (H) with an EDT nephron tubule indicated. Dapi labels nuclei blue. Magnification indicated by scale bars.

The narrow tubules of the sinus zone, the intermediate segment I (IS-I) of the first sinus zone loop or late distal tubules (LDT) of the second sinus zone loop look similar on fluorescent microscope images. Hence the laboratory had previously developed a way to identify each type of narrow tubule. The proximal part of the tubule including IS-I tubules generally have cilia which were hence labeled with a mouse anti-acetylated tubulin antibody (Sigma; Figure 10; orange staining) and the start (sLDT) or end (eLDT) of the LDT were labeled with an AQP4 (AQP4/2; Figure 10B; green staining) or AQP3 (Figure 10A; green staining) antibodies respectively but also the (distal) LDT tubules have no cilia. The middle of the LDT (mLDT) expresses moderate levels of both AQP3 and AQP4. The AQP4/2 and AQP3 antibodies were subsequently labeled with a CF633 (red; Biotium) antibody labeling kit for use in in subsequent co-localization experiments.

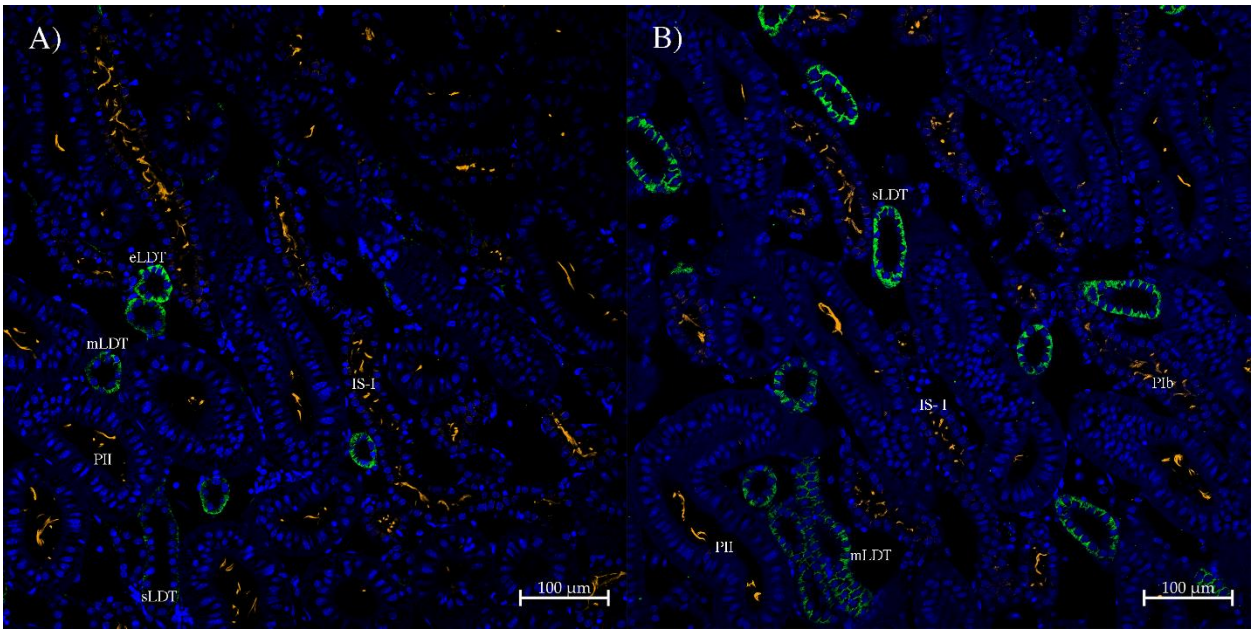


**Figure 10**: Immunohistochemistry images of sinus zone. A) AQP3 antibody (green) B) AQP4/2 antibody (green). Both with the mouse acetylated-Tubulin antibody, orange. Dapi was the blue nuclear counterstain. The start (sLDT), middle (mLDT) and end (eLDT) of the late distal tubule (LDT) are indicated, as are proximal Ib (PIb), proximal II (PII) and intermediate segment I (IS-I) tubules. Magnification indicated by scale bars.

As the initial AQP3-2 tyramide amplified slides showed staining for AQP3-2 in narrow sinus zone tubules, a further series of slides was prepared (Figure 11) using the mouse anti-acetylated tubulin antibody (orange) and the AQP3 or AQP4/2 antibodies (both red). These serial sections (Figure 11A and B) show that the AQP3-2 stains the LDT and not IS-I tubules. AQP3-2 staining (green) co-localizes with AQP3 staining in the mLDT (Figure 11A) but AQP3 staining was absent from the sLDT. However, AQP3-2 staining also co-localizes with AQP4/2 staining in the sLDT and mLDT (Figure 11B). The sections also show the AQP3-2 staining in the EDT (Figure 11C and D). Figure 11C shows that the AQP3 antibody does not cross react with the AQP3-2 protein (no red staining in figure 11C). AQP3-2 and AQP4/2 staining both occur in the EDT but without out much overlap (which would show up as yellow). In other words where AQP3-2 is strongly present there is little or no AQP4 and vice versa.

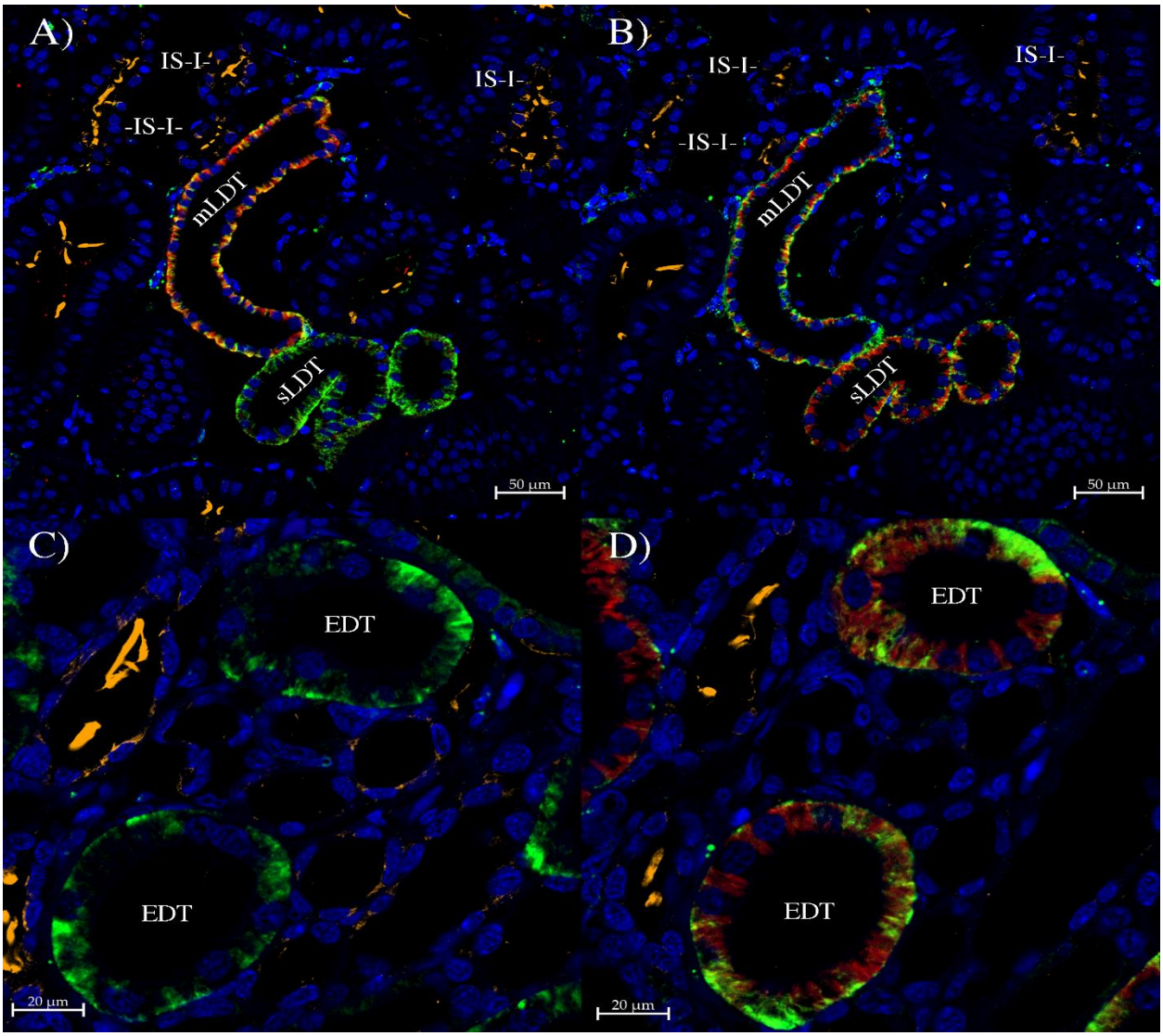


**Figure 11**: Immunohistochemistry images of AQP3-2 antibody staining (Green) on serial sections of the sinus zone LDT; A and B (A1 antibody) and convoluted bundle zone; C and D (A2 antibody). A) And C) are also stained with AQP3 (Red). B) and D) are also stained with the AQP4/2 antibody (Red). Where EDT = early distal tubule; sLDT = start of late distal tubule mLDT = middle of late distal tubule and IS-I = intermediate segment I. Dapi labels nuclei blue. Magnification indicated by scale bars.

Finally, some control slides were produced where the AQP3-2 antibody was blocked using the peptide antigen used to produce the antibody (Figure 12B, D and F) and this almost completely abolished the AQP3-2 staining compared to serial sections produced with unblocked AQP3-2 antibody (Figure 12A, C and E). To identify whether the AQP3-2 antibody was cross-reacting and binding to AQP3 protein in the LDT. The AQP3-2 antibody was blocked with the AQP3 peptide antigen Figure 12G and H) and this failed to block the AQP3-2 staining.

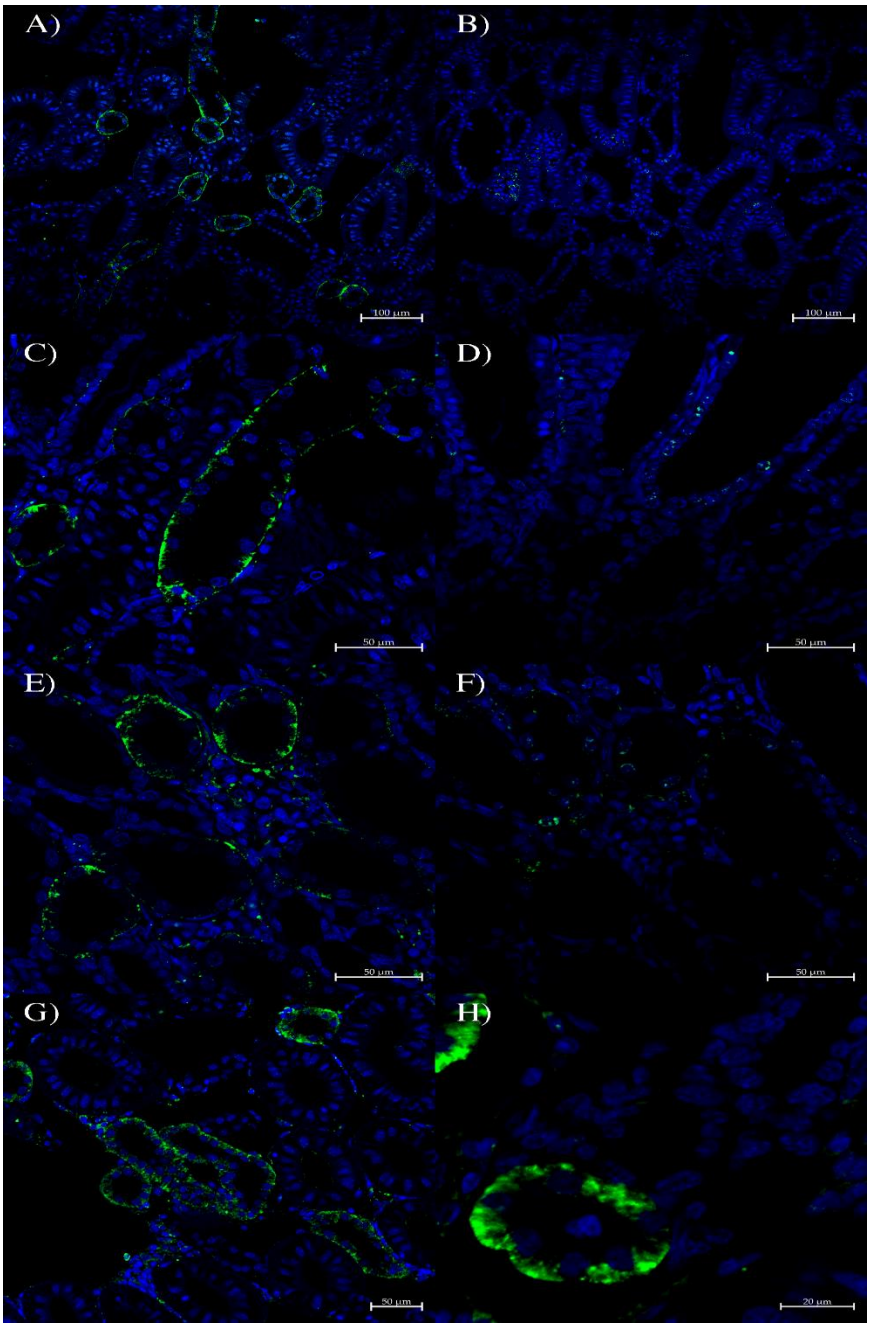


**Figure 12**: AQP3-2 antibody staining (Green) in the sinus zone (A, B and G), the straight bundle zone (C and D) and the convoluted bundle zone (E, F and H). A, C and E are labeled with AQP3-2 antibody, B, D and F are serial sections labeled with the AQP3-2 antibody blocked by its peptide antigen. Sections G and H are labeled with AQP3-2 antibody blocked with the AQP3 peptide antigen. Dapi labels nuclei blue. Magnification indicated by scale bars.

**UT-1 Immunohistochemistry results**

The UT-1 antibody also gave no fluorescent signals on initial slides using a standard immunohistochemical approach. So as with the AQP3-2 antibody, a tyramide amplification kit was used with the UT-1 antibody (Figure 13). On serial sections of the sinus zone (Figure 13A and B), the UT-1 antibody labeled proximal Ib (PIb) tubules with strong punctate staining and proximal II tubules (PII) with diffuse and (lower levels of) punctate staining. Some narrow tubules, that might be intermediate I (IS-1) or late distal tubules (LDT), showed weak diffuse staining. In the convoluted bundle zone (Figure 13C), at least 4 of the 5 tubules (including the early distal tubule; EDT as indicated) showed punctate UT-1 staining. A higher resolution image taken using the Airyscan module (Figure 13D) showed that the punctate staining in the PIb) appeared to be located in large membranous structures within the cells, around the nucleus and in the apical pole of cells.

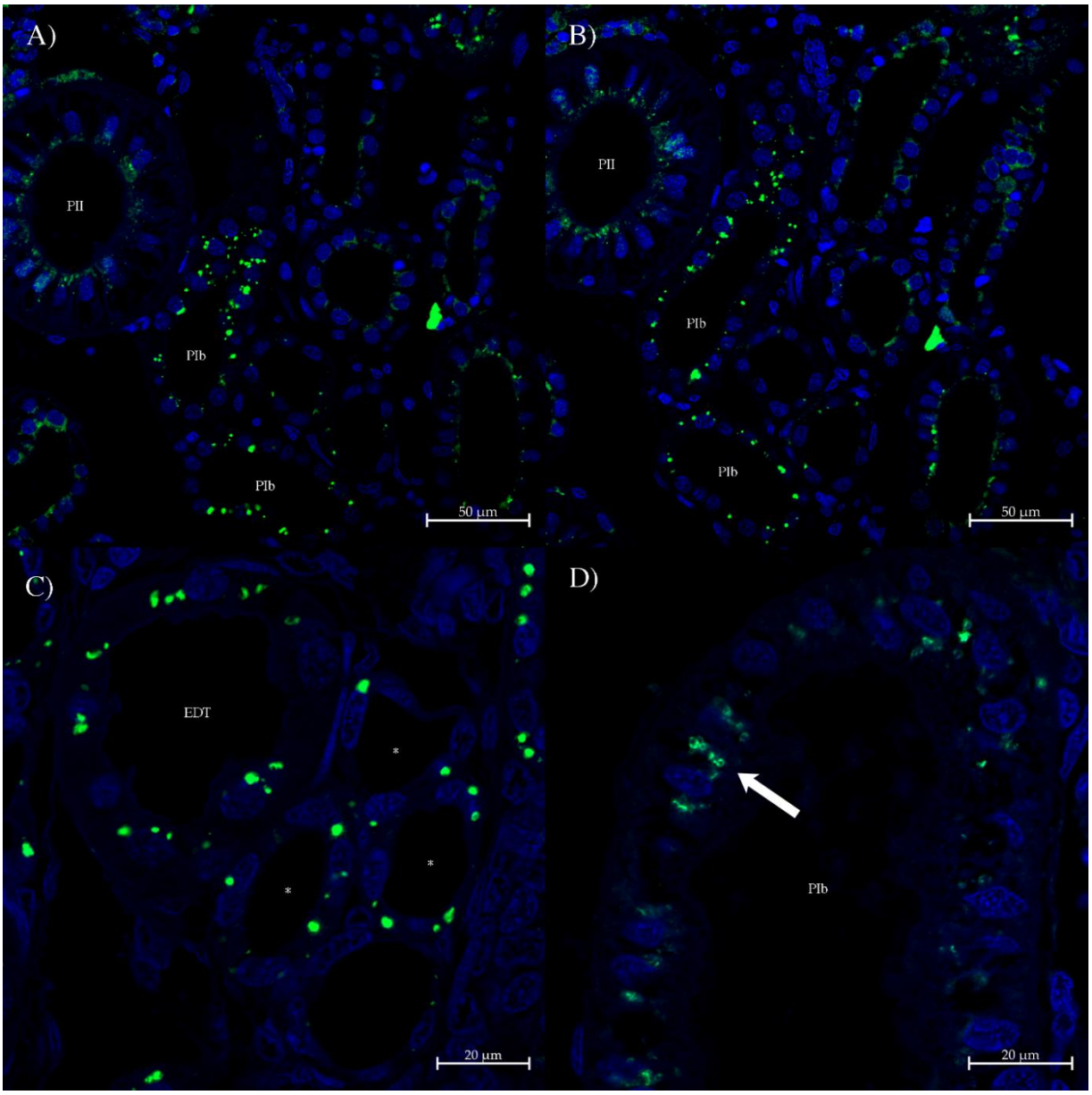


**Figure 13**: Immunohistochemistry image of initial kidney sections labeled with the UT-1 A1 (A, C and D) and A2 (B) antibodies. A and B are serial sections of the sinus zone with UT-1 staining (green) which occurred on the apical side of the nuclei of cells in multiple types of nephron segments as indicated. Panel C) shows UT-1 staining (green) tubules in the convoluted bundle zone. Section D was produced using the confocal microscope's Airyscan super-resolution module, using a 40x oil lens and shows a PIb tubule with UT-1 punctate staining (Arrow). Where EDT = early distal tubule; PIb = proximal tubule Ib and PII = proximal tubule II. Dapi labels nuclei blue. Magnification indicated by scale bars.

To determine whether the UT-1 staining in narrow tubules in the sinus zone was in IS-I or LDT tubules, the UT-1 antibody staining was co-localized with that of the cilia-staining mouse anti-acetylated tubulin antibody (orange) and the AQP3 or AQP4/2 antibodies (both red; Figure 14). In Figures 14A and B, UT-I staining (green) did occur in IS-I tubules with cilia, but also in sLDT (weak red AQP3 staining) with punctate staining but not in the eLDT (Strong AQP3 staining). The staining intensity was variable depending on the gain used for the photomultiplier detector (i.e., how much light was collected). With AQP4/2 antibody staining (red; Figures 14C and D), UT-1 staining was again seen in sLDT tubules, with lower levels in mLDT tubules (with less AQP4/2 staining) and was almost non-existent in eLDT tubules (those with very low AQP4/2 red staining). Part of the straight bundle zone (bottom left of Figure 14C) was also visible, showing a tubule transitioning between PIa (straight bundle zone with some punctate UT-1 staining and a row of luminal multi-cilia ribbons) and PIb (sinus zone with strong punctate UT-1 staining) The PIa tubule appeared to have less punctate UT-1 staining than the PIb tubule segment.

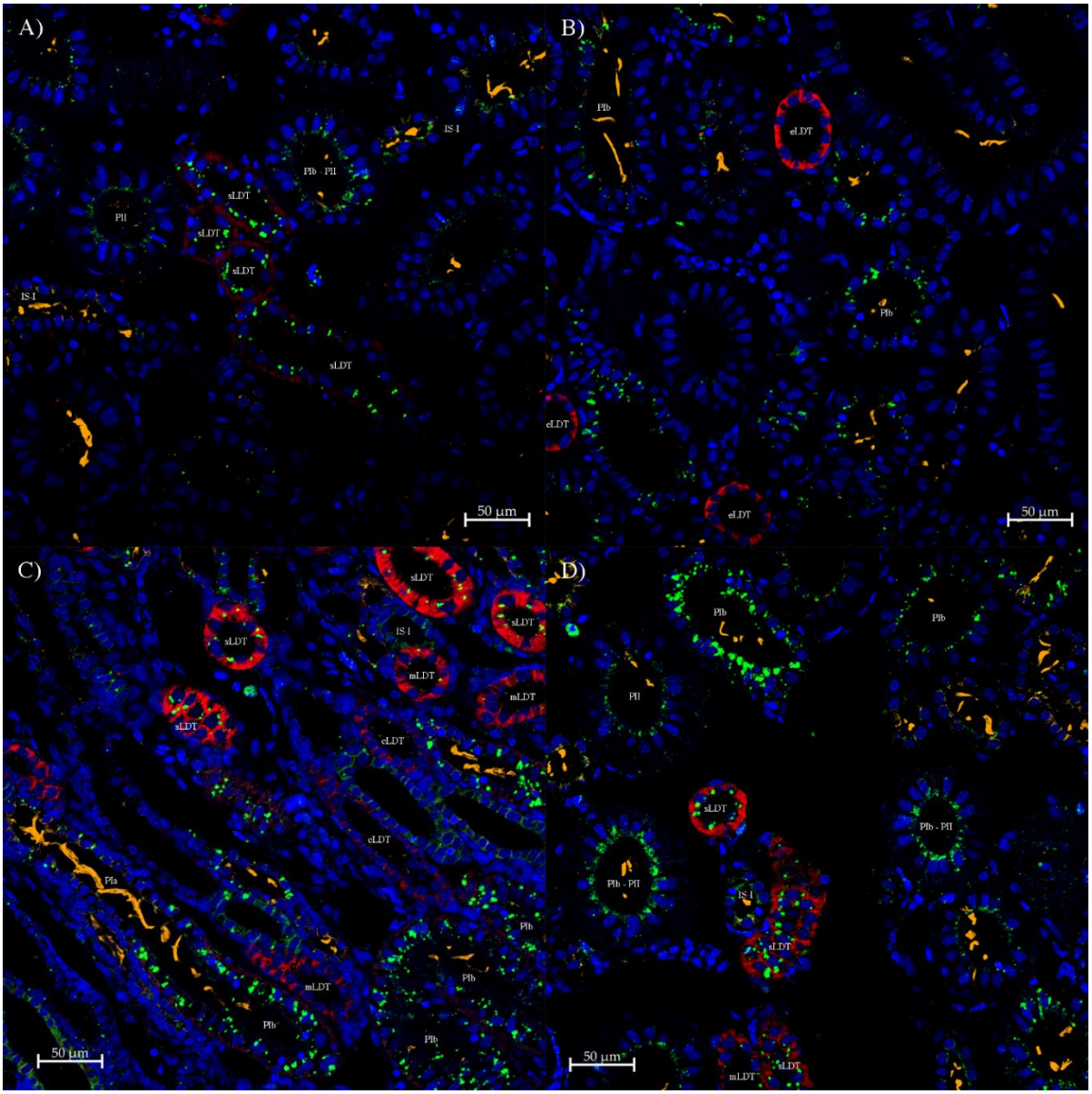


**Figure 14**: Immunohistochemistry image of the sinus zone showing UT-1 staining (green) and is also labeled with either AQP3 (red, A and B) or AQP4/2 (red, C and D) antibodies. Tubulin antibody (orange). Dapi (blue). Panel A) show punctate UT-1 staining in tubules and weak AQP3 staining at the start of the LDT (sLDT). Panel B) shows UT-1 staining (green) and strong AQP3 staining in the end of the LDT (eLDT). Panel C) and D) Shows LDT tubules (indicated by sLDT, mLDT and eLDT) with different levels of UT-1 (green) and AQP4 (red) staining. Where PIa = proximal tubule Ia; PIb = proximal tubule Ib; PII = proximal tubule II and IS-I = intermediate tubule I. Magnification indicated by scale bars.

In convoluted bundle zone (Figure 15A). UT-1 staining was seen in the early distal tubule (EDT) and three out of the four other tubules of the bundle. The three tubules that stain for UT-1 also had cilia (staining orange) in their lumens (c) but despite this there is still no way to identify for sure which tubule doesn't stain with the UT-1 antibody i.e., whether it's the neck segment (NS), proximal Ia (PIa), intermediate segment II (IS-II) or collecting tubule (CT). The squashed structure on the right of the image labeled CV? Maybe the central vessel that takes absorbed fluid away from the bundle or it may be a capillary, however it shows some UT-1 in Figure 15B. It should also be noted that the AQP3 antibody (red) (Figure 15A) did not stain any of the convoluted bundle zone tubules. In the straight bundle zone (Figure 15 C and D) the section was again prepared with the AQP4/2 antibody (red), and this labels the EDT as before. There are two other tubules without multi-cilia ribbons, which are hence distal tubules i.e., the intermediate II and collecting tubules (IS-II and CT), one is labeled with UT-1 antibody (green), and one is unlabeled. There should also be two more proximal tubules with cilia which would be proximal Ia (PIa) and the neck segment (NS) but there is no current way to distinguish these two from each other.

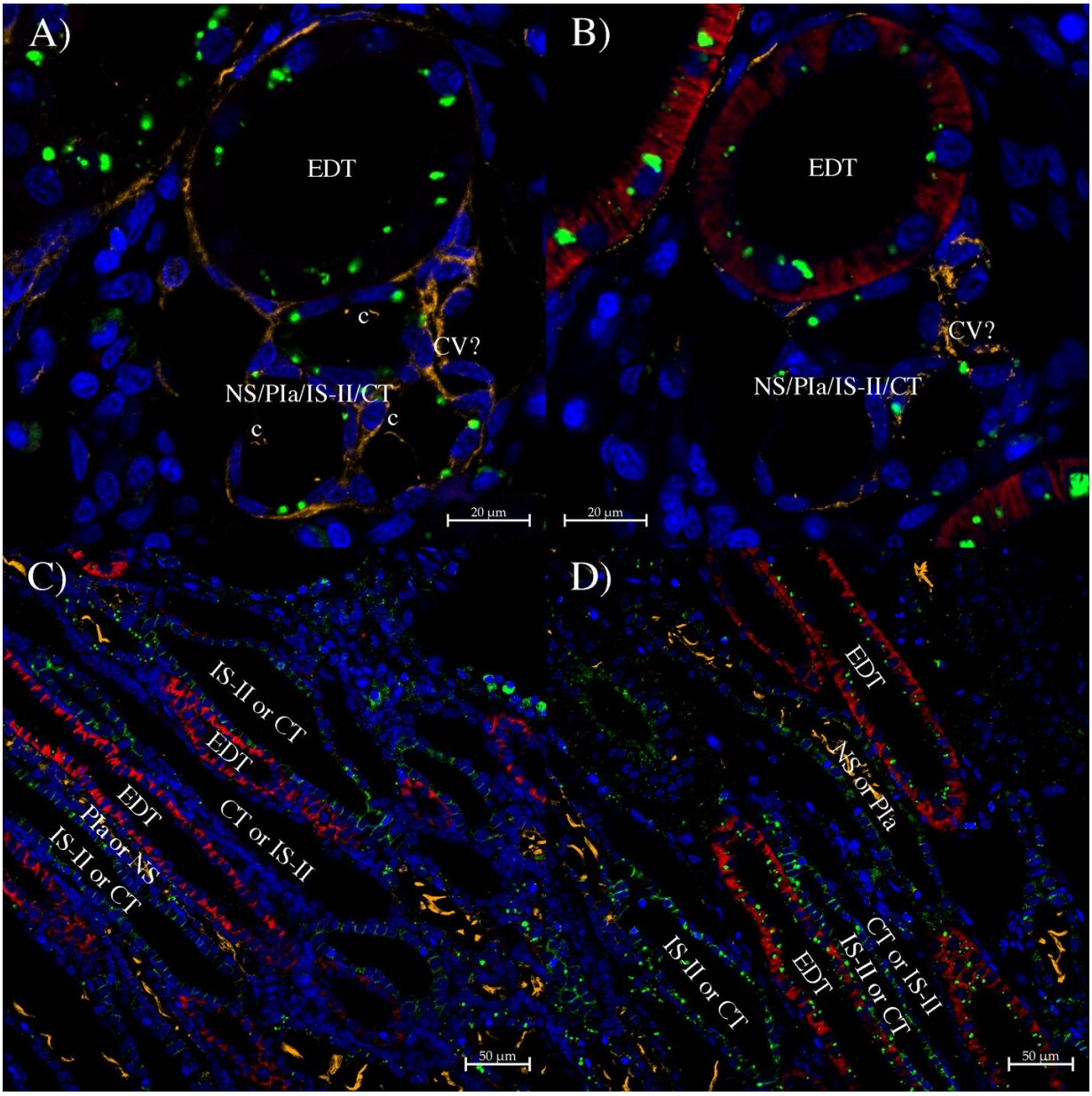


**Figure 15**: Immunohistochemistry image of UT-1 staining (green) in the bundle zone. A) And B) are serial sections of the convoluted bundle zone with 'bundles' of 5 tubules; Panel A) is stained with AQP3 (red). C) and D) are of the straight bundle zone stained with the AQP4/2 antibody (Red). The sections were also stained with the mouse anti-acetylated tubulin antibody (orange) to label cilia. Where EDT = early distal tubule; CV? = possible central vessel; NS = neck segment; Pia = proximal Ia segment; IS-II = intermediate II segment; CT = collecting tubule. Dapi labels nuclei blue. Magnification indicated by scale bars.

To confirm that the UT-1 staining was specific to the antibody, the UT-1 antibody was blocked with the peptide antigen used to produce it (as in Figure 16B and D; sinus zone and convoluted bundle zone respectively). This showed the UT-1 staining was abolished in comparison to serial sections stained with unblocked UT-1 antibody (Figures 16A and C respectively). Some possible auto-fluorescence was seen at the bottom right of Figure 16A and B.

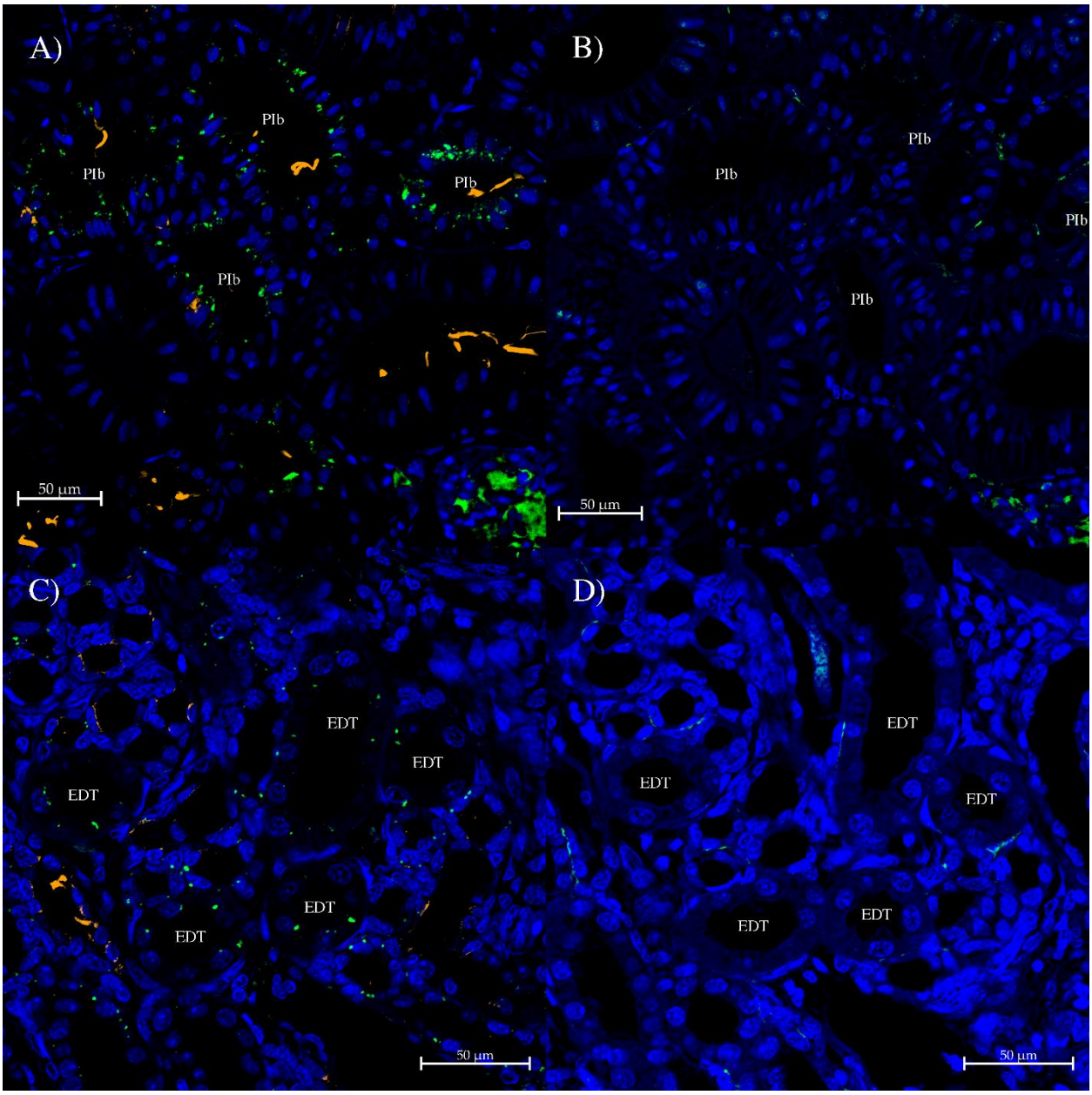


**Figure 16**: Immunohistochemistry image of UT-1 staining (A1 antibody) in the sinus zone (panels A and B) and convoluted bundle zone (panels C and D) Panels B and D were incubated with the UT-1 antibody that had been blocked by the peptide antigen used to produce it. Cilia are labeled orange (A and C). Where EDT = early distal tubule; PIb = proximal tubule Ib. Dapi labels nuclei blue. Magnification indicated by scale bars.

**NCC/2 Immunohistochemistry results**

The NCC/2 antibody (A1 or A2) gave strong enough staining to not need tyramide amplification. Serial sections were produced that co-localized the NCC/2 antibody (green) with either the AQP3 (Figure 17A and C) or AQP4/2 antibodies (Figures 17B and D). As can be seen in figure 17, the NCC/2 antibody labeled proximal Ib tubules (PIb) with strong cytoplasmic staining and the start of the late distal tubule (sLDT) but not the middle of the LDT (mLDT). Figures 17C and D show the straight bundle zone on the left-hand side. Transitions between the PIa (little or no NCC/2 staining; green) to PIb (strong NCC/2 staining) can be seen in both serial sections. Control sections where the NCC/2 antibody was blocked with peptide antigen used to produce it (Figure 17E) or without the primary NCC/2 antibody (Figure 17F) showed no NCC/2 antibody staining. The renal corpuscle (glomerulus; RC) and connected neck segment (NS), proximal II tubules (PII) and Intermediate I tubules (IS-I) are labeled and appear unstained.

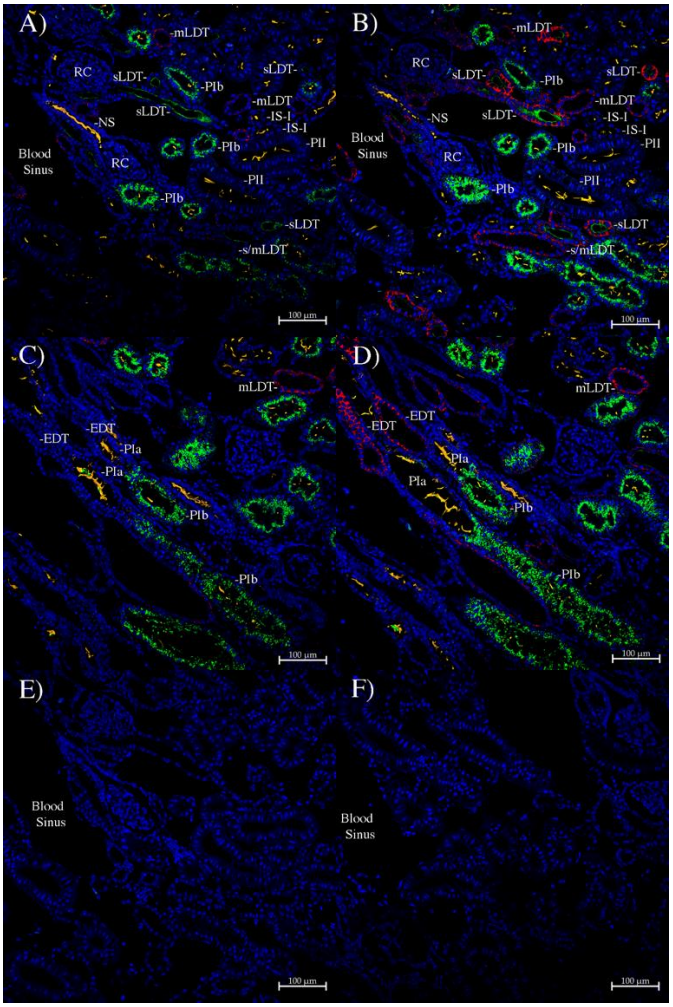


**Figure 17**: Immunohistochemistry image of NCC/2 antibody staining (green). Panels A, B, E and F are serial sections of approximately the same region of the kidney. Panels C and D are also serial sections. Panel A) and C) are additionally labeled with AQP3 antibody (red). Panels B) and D) are additionally labeled with the AQP4 (AQP4/2) antibody (red). Panels A- D has cilia stained (with the mouse acetylated-tubulin antibody; orange). Panel E shows a control section where NCC/2 antibody had been blocked with its peptide antigen. Panel F is a similar control section but incubated without the primary NCC/2 antibody. Where EDT = early distal tubule; sLDT=start of the Late distal tubule; mLDT = middle of the late distal tubule; Pia = proximal tubule Ia; PIb = proximal tubule Ib; PII = proximal tubule II; IS-I = intermediate segment I; NS = neck segment, RC = renal corpuscle. A blood sinus is also indicated. Dapi labels nuclei blue. Magnification indicated by scale bars.

## qPCR Result

### *Squalus acanthias* AQP3 qPCR results

Quantitative PCR was performed on samples from 2 experiments, experiment 1 where sharks were acclimated from seawater (100%SW) to 120% or 75% SW, and experiment 2 where sharks were acclimated from 100% SW to 120% SW but where some of the samples were partially degraded. Total RNA levels (28S and 18S rRNA bands) were normalized on agarose electrophoresis gels prior to production of the cDNA (by reverse transcription) for experiments. Statistical testing for each gene was performed using ANOVA with a Bonnferroni/Dunn post hoc test on $\log_{10}$ transformed data for experiment 1 and a t-test for experiment 2 data.

The first figure (Figure 18.) shows the results for amplifications involving AQP3. This gene was measured (it had already been measured previously by Northern blotting) to be able to compare it to its duplicate gene copy, AQP3-2. Although no groups in experiment one were statistically different, AQP3 mRNA expression showed a unique trend in the means for each, group. AQP3 expression was lowest in the 75% SW group and highest in the 120% SW group. As with all other genes measured, the 120% SW group in experiment 2 was slightly lower than the 100% SW group.

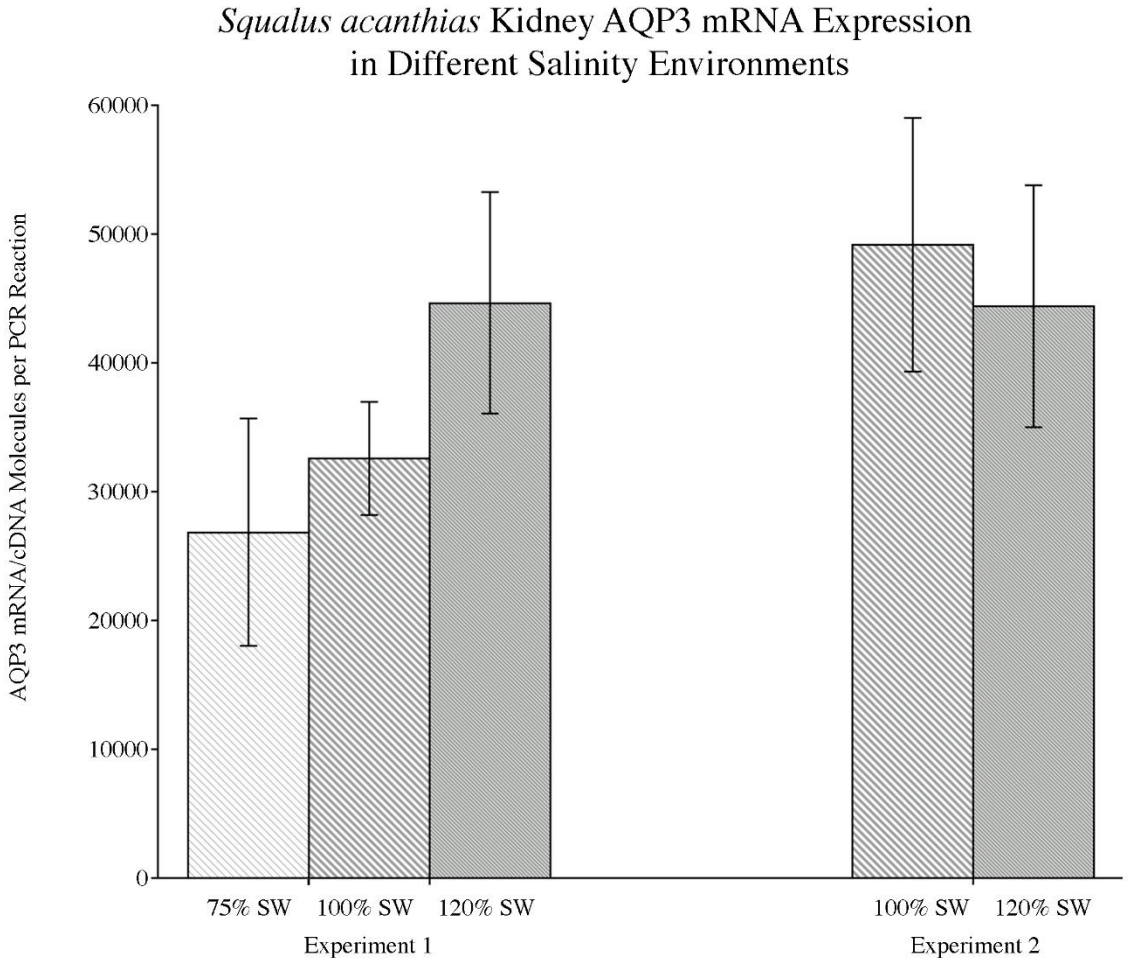


**Figure 18**: Graph comparing the number of AQP3 mRNA/cDNA molecules from qPCR analysis of *Squalus acanthias* kidney tissue cDNAs from the 75%, 100% and 120% SW groups in experiment 1 and the corresponding 100% and 120% SW groups in experiment 2. Data is expressed as mean ± standard error of means (SEM). Statistical significance between 75% and 100% SW P= 0.2449, 75% and 120% SW P= 0.0709, 100% and 120% SW P= 0.4746 groups in experiment 1. Also, between 100% SW and 120% SW in experiment 2, P= 0.72.

### *Squalus acanthias* AQP3-2 qPCR results

For AQP3-2 (Figure 19) the groups in experiment 1 (or 2) were not statistically different to one another but the trend in the means for each group in experiment 1 showed decreasing AQP3-2 mRNA expression from the 75% SW group to the 120% SW group which was the opposite trend to that of AQP3.

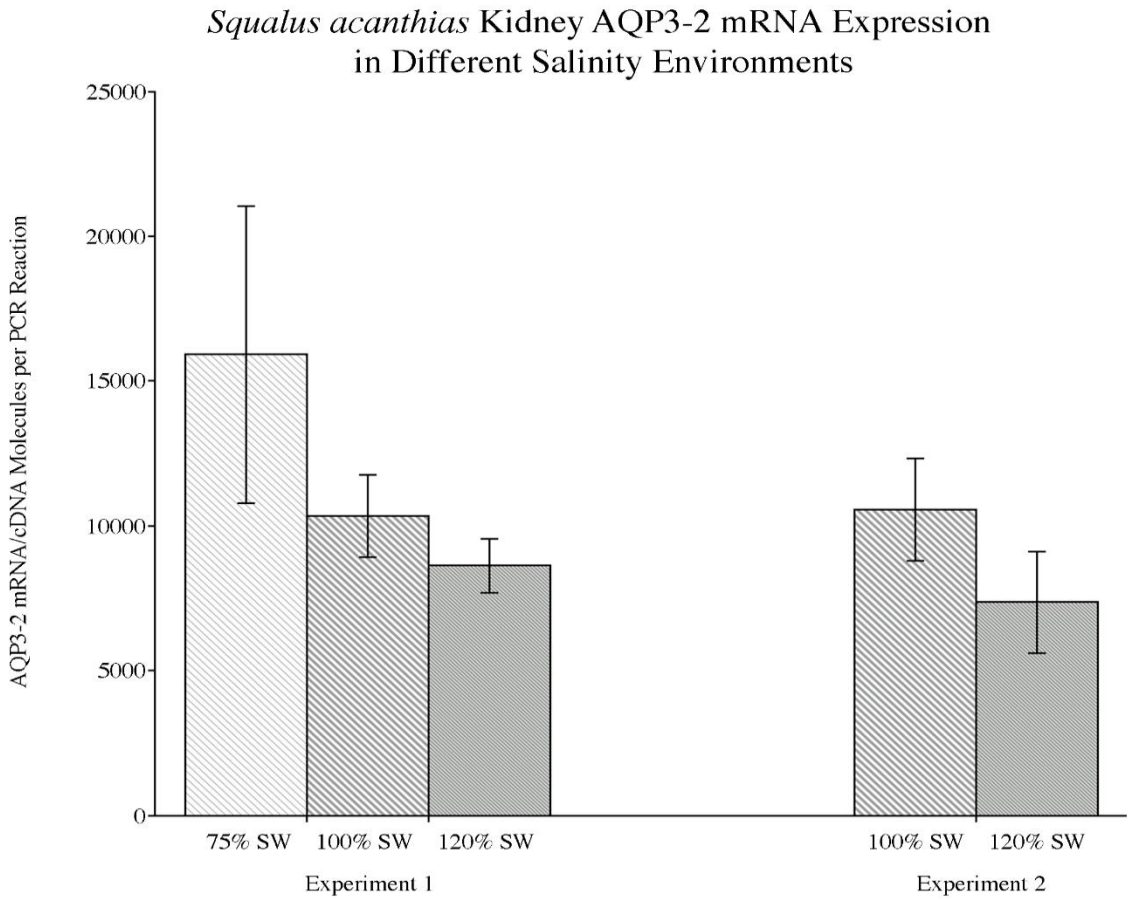


**Figure 19**: Graph comparing the number of AQP3-2 mRNA/cDNA molecules from qPCR analysis of for 75%, 100% and 120% SW groups in experiment 1 and the corresponding 100% and 120% SW groups in experiment 2 in *Squalus acanthias* kidney tissue. Data is expressed as mean ± standard error of means (SEM). Statistical significance between 75% and 100% SW P= 0.2997, 75% and 120% SW P= 0.1249, 100% and 120% SW P= 0.5895 in experiment 1. And between 100% SW and 120% SW in experiment 2 P= 0.2804.

### *Squalus acanthias* AQP3-2 spliceoform qPCR results

For the splice variant of AQP3-2 (Figure 20) the trends in data were the same as for the full-length gene in figure 19. However, the 120% SW group in experiment 1 showed a large and statistically significant decrease compared to the 75% SW or 100% SW groups. The variation between individuals in the 120% SW group was also remarkably small (see error bar).

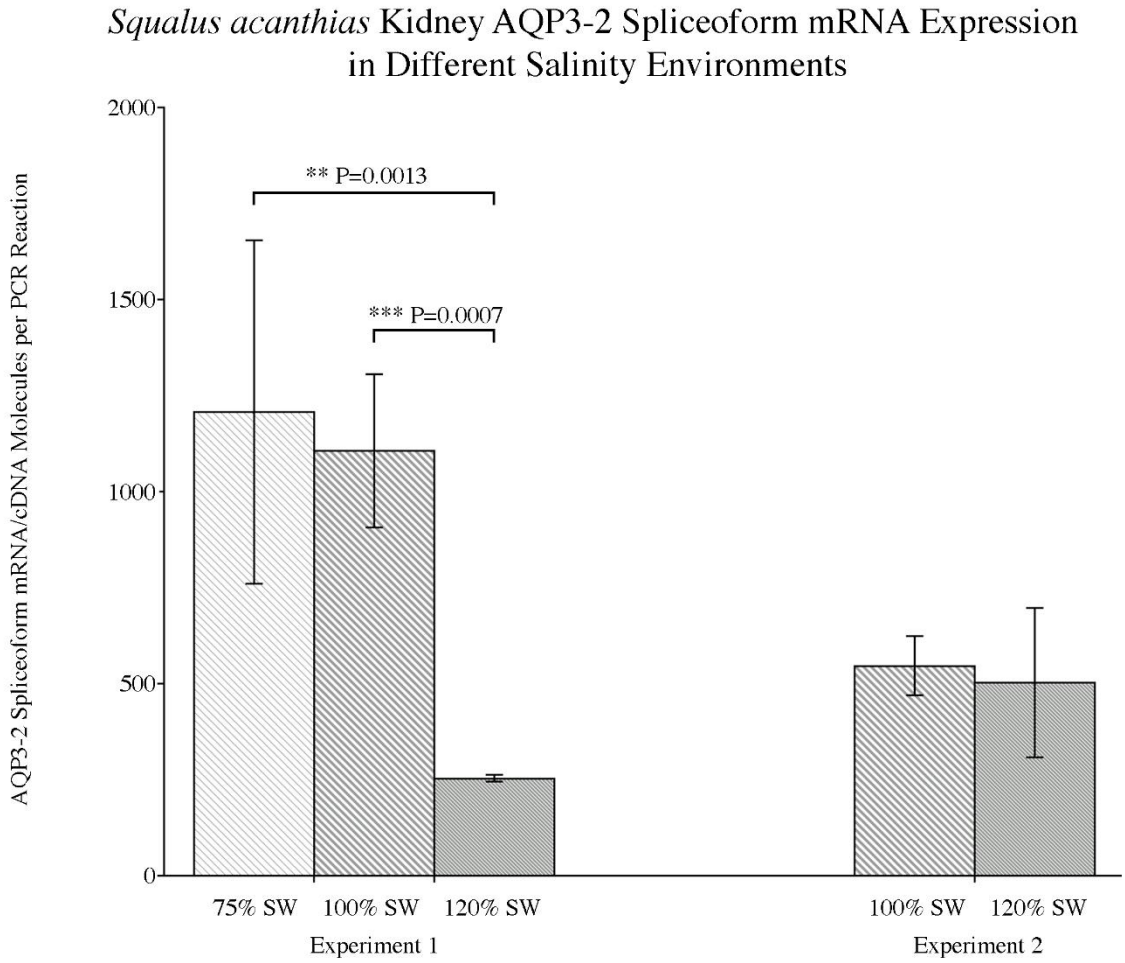


**Figure 20**: Graph comparing the number of AQP3-2 Spliceoform mRNA/cDNA molecules from qPCR analysis of for 75%, 100% and 120% SW groups in experiment 1 and the corresponding 100% and 120% SW groups in experiment 1 in *Squalus acanthias* kidney tissue. Data is expressed as mean ± standard error of means (SEM). Statistical significance between 75% and 100% SW P= 0.7595, 75% and 120% SW P= 0.0013, 100% and 120% SW P= 0.0007 in experiment 1. And between 100% SW and 120% SW in experiment 2, P= 0.6188. Statistically significant probabilities shown on the graph where **P<0.01 and ***P<0.001.

### *Squalus acanthias* Brain UT qPCR results

The urea transport genes (Brain UT and UT-1) show the same trends between groups as the majority of other genes (data not shown; information courtesy of Dr Cutler). The level of expression in experiment one groups was higher in the 75% SW and 120% SW groups than in the 100% SW group, although for the Brain UT gene, the 75% SW group mean was only slightly higher than the 100%%SW group mean, and the Brain UT groups were not statistically significantly different (Figure 21).

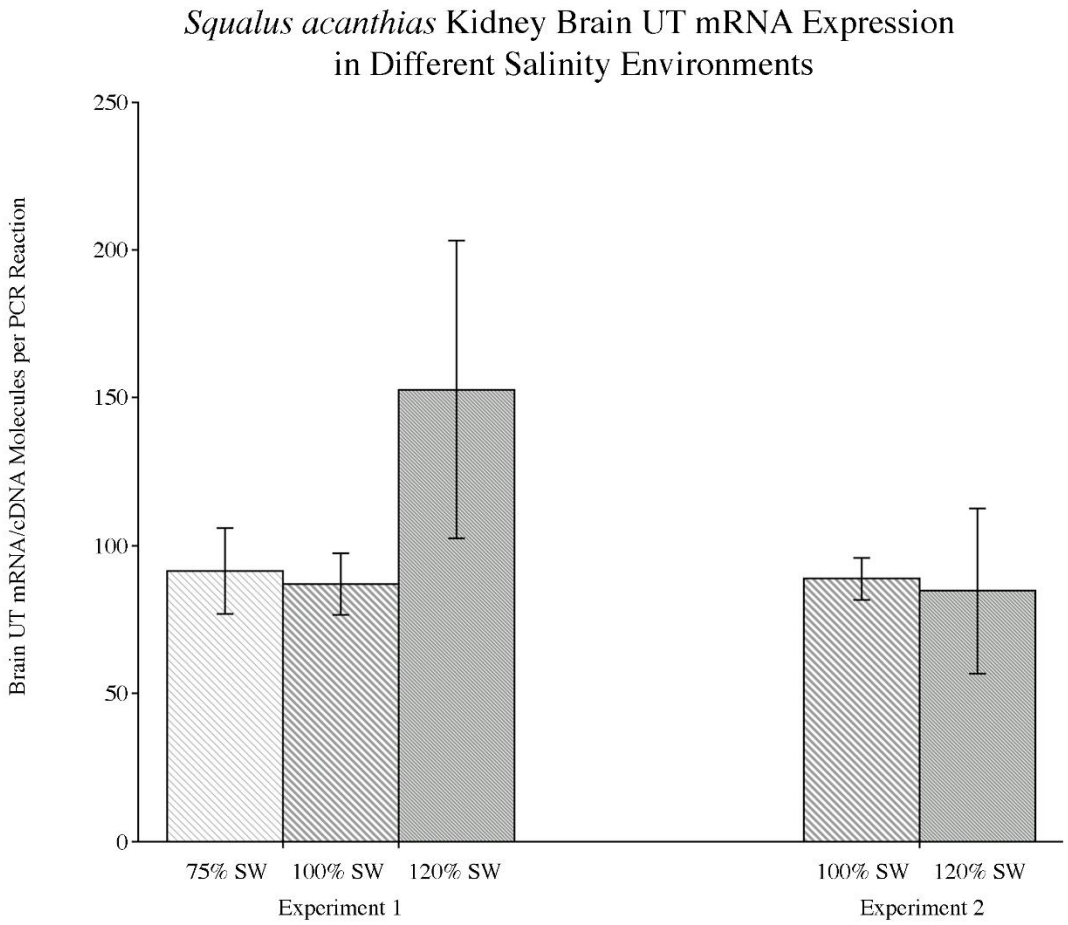


**Figure 21**: Graph comparing the number of Brain UT mRNA/cDNA molecules from qPCR analysis of for 75%, 100% and 120% SW groups in experiment 1 and the corresponding 100% and 120% SW groups in experiment 2 in *Squalus acanthias* brain tissue. Data is expressed as mean ± standard error of means (SEM). Statistical significance between 75% and 100% SW P= 0.9194, 75% and 120% SW P= 0.1438, 100% and 120% SW P= 0.1207 in experiment 1. And between 100% SW and 120% SW in experiment 2, P= 0.6819.

### *Squalus acanthias* Kidney UT-1 long spliceoform qPCR results

For the UT-1 long splice variant (Figure 22), the 75% SW group in experiment 1 was significantly increased compared to the 100% SW group, the 120% SW group was also quite a lot higher, but the difference was not great enough to be statistically significant (figure 22).

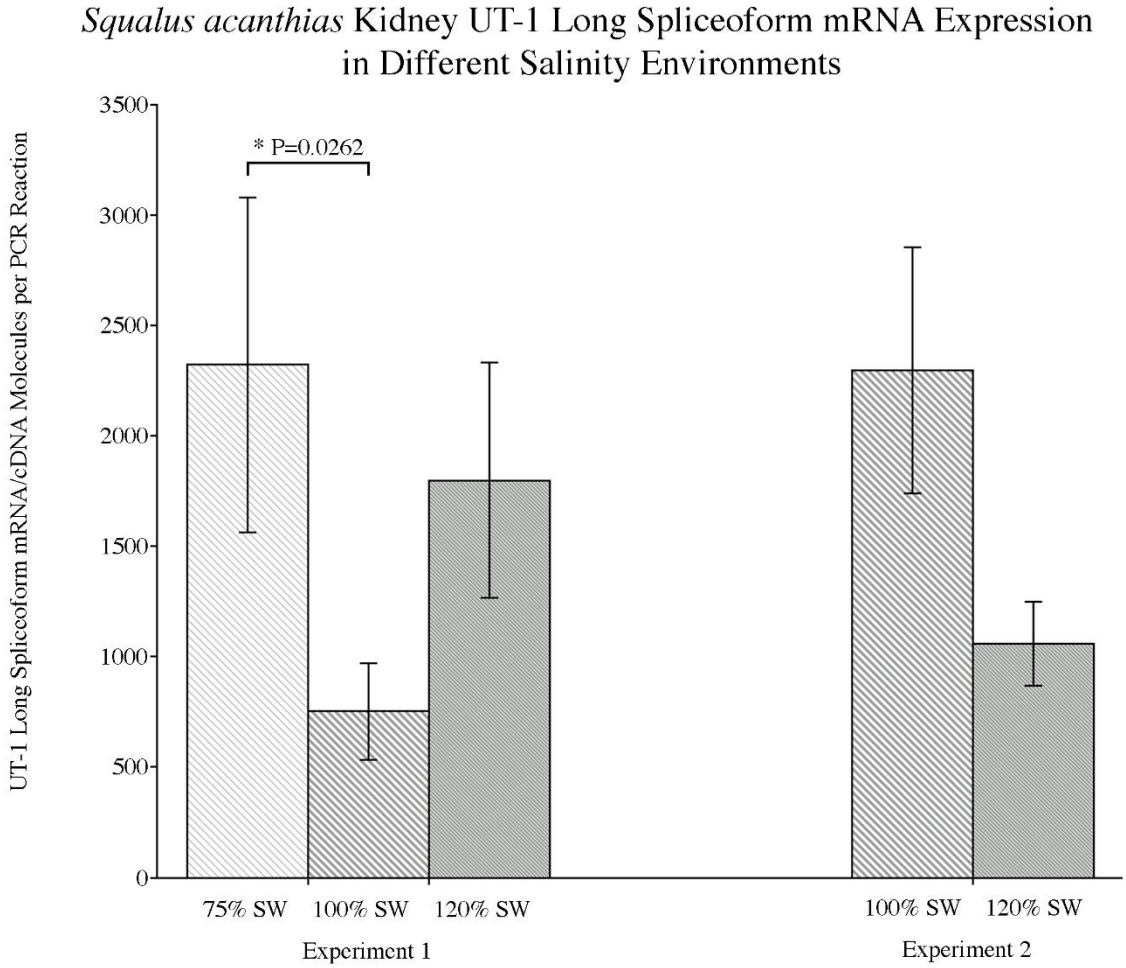


**Figure 22**: Graph comparing the number of UT-1 long spliceoform mRNA/cDNA molecules from qPCR analysis of for 75%, 100% and 120% SW groups in experiment 1 and the corresponding 100% and 120% SW groups in experiment 2 in *Squalus acanthias* kidney tissue. Data is expressed as mean ± standard error of means (SEM). Statistical significance between 75% and 100% SW P= 0.0262, 75% and 120% SW P= 0.679, 100% and 120% SW P= 0.0589 in experiment 1. And between 100% SW and 120% SW in experiment 2, P= 0.0985. Statistically significant probabilities shown on the graph where *P<0.05.

### *Squalus acanthias* Kidney UT-1 short spliceoform qPCR results

For the UT-1 short splice variant, the trend of the group means in experiment 1 (and 2) were similar to UT-1 long but the differences between groups were not large enough to be statistically significant. Still the mean of the 75% SW group was almost double that of the 100% SW group (Figure 23).

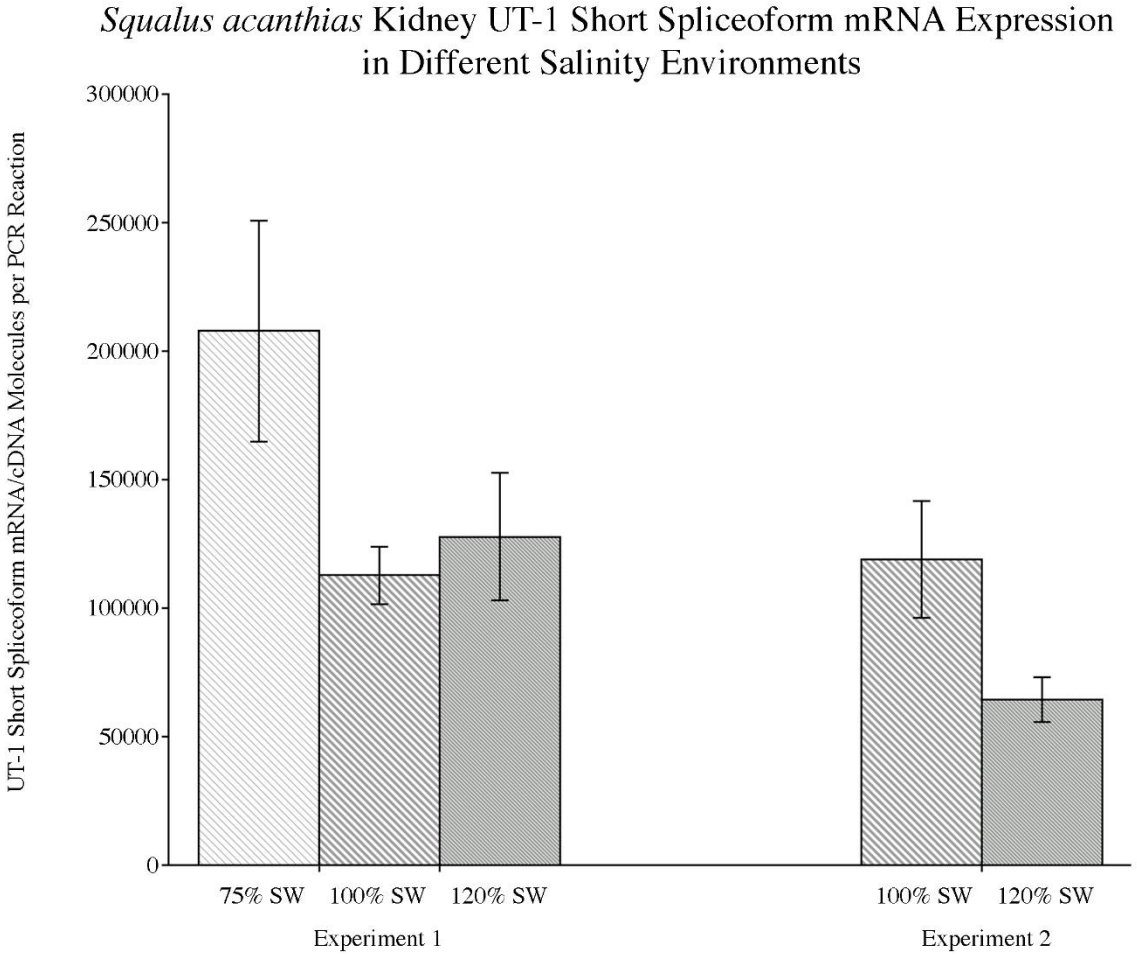


**Figure 23**: Graph comparing the number of UT-1 short spliceoform mRNA/cDNA molecules from qPCR analysis of for 75%, 100% and 120% SW groups in experiment 1 and the corresponding 100% and 120% SW groups in experiment 2 in *Squalus acanthias* kidney tissue. Data is expressed as mean ± standard error of means (SEM). Statistical significance between 75% and 100% SW P= 0.0902, 75% and 120% SW P= 0.1141, 100% and 120% SW P= 0.8956 in experiment 1. And between 100% SW and 120% SW in experiment 2, P= 0.0524.

### *Squalus acanthias* Kidney NCC qPCR results

The NCC cotransporter gene showed similar trends in its group means to AQP3-2 in that mRNA expression decreased with increasing salinity, although the differences between groups were not large enough to be statistically significant (Figure 24).

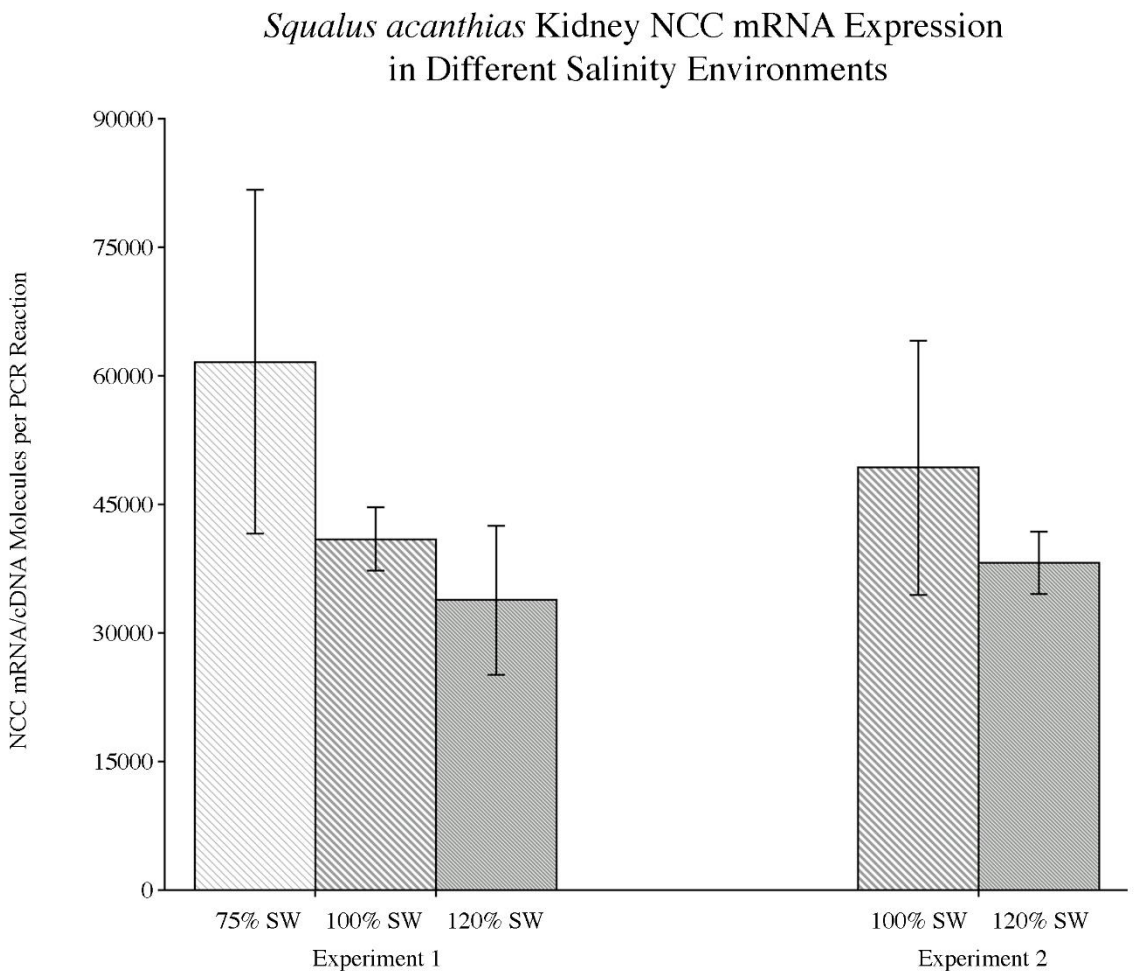


**Figure 24**: Graph comparing the number of NCC/2 mRNA/cDNA molecules from qPCR analysis of for 75%, 100% and 120% SW groups in experiment 1 and the corresponding 100% and 120% SW groups in experiment 2 in *Squalus acanthias* kidney tissue. Data is expressed as mean ± standard error of means (SEM). Statistical significance between 75% and 100% SW P= 0.6022, 75% and 120% SW P= 0.1207, 100% and 120% SW P= 0.2833 in experiment 1. And between 100% SW and 120% SW in experiment 2, P= 0.5654.

### *Squalus acanthias* RPL-P0 qPCR results

The RPL-P0 gene showed fairly large differences between the different groups in experiment one, and although the differences were not statistically different, they were very close to that (Figure 25). The large changes in expression suggest that RPL-P0 gene does not represent a good housekeeping gene for any further normalization of the data that might be carried out, and hence this was not done.

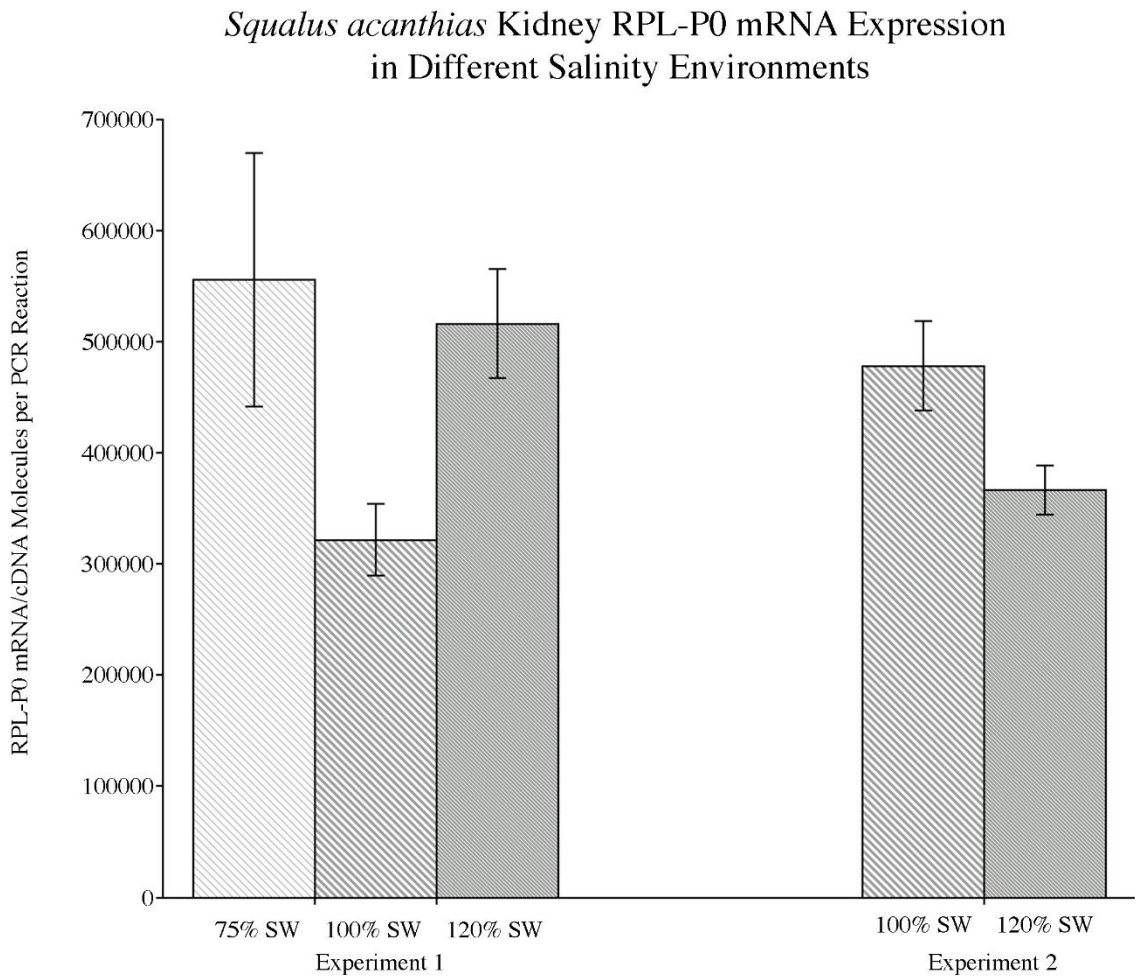


**Figure 25**: Graph comparing the number of RPL-P0 housekeeping mRNA/cDNA molecules from qPCR analysis of for 75%, 100% and 120% in experiment 1 and the corresponding 100% and 120% SW groups in experiment 2 *Squalus acanthias* kidney tissue. Data is expressed as mean ± standard error of means (SEM). Statistical significance between 75% and 100% SW P= 0.0654, 75% and 120% SW P= 0.8892, 100% and 120% SW P= 0.0502 in experiment 1. And between 100% SW and 120% SW in experiment 2, P= 0.6044.

# CHAPTER 4

# DISCUSSION

RT-PCR was done to confirm the expression of the genes being studied in *Squalus acnathias*. The housekeeping gene RPL-P0 was expressed in all the tissues investigated as expected (Figure 4). An alignment of the sequences of Elephant fish *(Callorhinchus mili*), Cat shark (*Scyliorhinus canicula*) and Whale shark (*Rhincodon typus*) was created (see A3 in Appendix), the sequences used, were obtained from the gene bank. The alignment was used to design primers for the amplification of a *Squalus acanthias* RPL-P0 fragment since there was no corresponding sequence in the gene bank at the time of this study. The *Scyliorhinus canicula* RPL-P0 sequence was found have 90.96% nucleotide homology to *Squalus acanthias* (see A3.4 in Appendix). This was the most similar of all the RPL-P0 sequences in the genebank. The large differences in RPL-P0 expression (see Figure 25) between the different groups (which were almost but not quite statistically significantly different), suggest RPL-P0 is changing expression and hence not a good 'housekeeping gene' in this experiment/circumstance. Because the expectation for a housekeeping gene is that its expression between groups should be more or less flat and then the variation between each individual animal can be used to normalize the data and adjust for any small errors in pipetting or variation in the efficiency of the RT-PCR. Consequently, RPL-P0 wasn't used to further normalize the data as it would have caused major distortions to the results of the experimental groups for the other genes measured (AQP3/2, AQP3/2 spliceoform, UT-1 long, UT-1 short, brain UT and NCC/2). The change in RPL-P0 suggests that the fish may be under stress (due to the change in salinity) causing a requirement to make new proteins, therefore as RPL-P0 is a ribosomal protein, more RPL-P0 mRNA and proteins may have been needed to make more ribosomes. To get a better housekeeping control gene, another gene such as beta actin or GAPDH or some other gene could be tried to see if they are homogenously expressed between the groups, but as there is no genome for *Squalus acanthias*, this is not necessarily a straightforward situation of merely looking up gene sequences in the gene bank and this was consequently outside the scope of this study. Concerning the qPCR experiments,

the results from Experiment 2 were very curious in that every gene seemed to show slightly lower expression in 120% SW. The fact that these samples were partially degraded probably in some way affected the results and hence the remainder of the discussion will only consider the results from Experiment 1 samples.

This study was able to confirm the duplicate copy of AQP3 (AQP3-2) as reported by a recent genomic and transcriptomic paper (Chana-Munoz *et al.* 2017). A novel spliceoform of the gene was also found to be expressed by *Squalus acanthias.* The amino acid homology of 60.68% between *Squalus acanthias* AQP3 and AQP3-2 translated gene sequences, while higher than that for other ancient gene duplications (such as AQP3-AQP9 =48.2% or AQP3-2-AQP9 =42.4%), the relatively low level of homology, suggests that the AQP3 gene must have been duplicated a considerable time ago during evolution (producing AQP3-2). The homology of 60.68% for some proteins would be low enough to consider AQP3-2 as a completely different aquaporin with its own name (as opposed to merely being a duplicate of AQP3). Of course, it also suggests the transport characteristics and regulation of AQP3-2 are most likely distinct from that of AQP3 itself.

Regarding the tissue PCR electrophoresis gel (Figure 4), multiple AQP3-2 bands were seen in kidney and brain cDNA amplifications. The two largest bands from kidney were cloned and sequenced to confirm their identity and to generate the complete and accurate coding-region sequences of *Squalus acanthias* AQP3-2 and its splice variant. The spliceoform (AQP3-2) is unlikely to be a water (or osmolyte) channel as it is missing the first (of the two) NPA domain(s) required for water channel pore formation. That of course implies that it has some other functions and as mentioned in the introduction, AQP3 is known to have a number of other functions outside of water/osmolyte transport. Humans also express a splice variant of AQP3 (see accession number NP_001305073.1) but this has a different C-terminal amino acid sequence and is not a missing internal exon/sequence (as AQP3-2 spliceoform is). This suggests that the *Squalus acanthias* AQP3-2 spliceoform may be unique in that regard. On the tissue PCR electrophoresis gel, the brightest bands are suspected to be AQP3-2 and its splice variant. These two

bands closest to the actual size of the gene and were excised for cloning and sequencing. The presence of other faint bands of smaller sizes implies that there may be other splice variants of the gene that were considered to be beyond the scope of this study.

The AQP3-2 Western blot (Figure 6) showed multiple bands between 25kDa and 37kDa as well as some high molecular weight bands, particularly strong bands at about 55kDa and 80kDa. This potentially implies the presence of other splice variants (as also seen in the tissue PCR amplification (figure 4)). The band sizes seen for both AQP3-2 and APQ3-2 spliceoform were as expected (32kDa and 27kDa respectively) but these may be post translationally modified with the N-terminal sequence removed by proteases (appears smaller) or N glycosylated (appears bigger), and there may also be multimer versions as seen with other aquaporins (Hasler *et al.* 1998, Jin *et al.* 2011, Mathai and Agre 1999, Rodriguez *et al.* 2019). The smaller 19kDa/21kDa band maybe a protease cut version as seen with for instance AQP0 (Gonen *et al.* 2004). Or again this band may possibly represent a smaller splice variant. Additionally, the sizes measured on SDS-page gels are at best approximate as the measured sizes depend on how well the SDS interacts with proteins as to how quickly or slowly they run in comparison to their actual size. The AQP3-2 immunohistochemistry showed a different localization for the protein expression of AQP3 vs AQP3-2. AQP3-2 just like AQP4 is located in the basolateral membranes of the EDT but no apical aquaporins have been identified in this segment and there is supposed to be low water permeability in the EDT (or "diluting segment" as it is also known (Friedman and Hebert 1990)). This suggests these aquaporins may be involved in cell volume regulation or some other non-transport function and/or AQP3-2 might also be involved in glycerol transport in the EDT. Interestingly the parts of the EDT in the convoluted bundle zone where AQP4 staining was strong, AQP3-2 staining was weak and vice versa (Figure 11D) and that suggest there is a switch in expression between the two aquaporins, although the reason for this is not currently apparent. AQP3-2 and AQP4 seen at the start of the LDT (together with AQP15 apical expression; unpublished data courtesy of Dr Cutler) suggest this is the site of water permeability of the LDT, as was also suggested by Friedman and Hebert (1990).

Statistical Analysis of the qPCR results show that the trends of changes in mRNA expression for AQP3-2 and AQP3-2 spliceoform were higher in 75%SW and lower in 120%SW, which is the exact opposite of what is expected from a gene responding to the need for decreased or increased urea reabsorption respectively (Figures 19 and 20). An interesting contrast was seen in the case of AQP3 (lower by 17.6% in 75% SW and higher by 37% in 120% SW; see Figure 18). i.e., AQP3 expression increased as salinity increased. The trends observed for AQP3, and AQP3-2 suggest a form of interchanging balance in the expression of these genes; as one increases the other decreases in expression and vice versa, even though they are not located in exactly the same place (AQP3 protein expression is limited and is mostly found at the end of the LDT whereas AQP3-2 protein expression is found in the whole of the LDT and the EDT (see figure 11). Interestingly despite the more limited distribution of AQP3 protein compared to that of AQP3-2, the level of AQP3 mRNA was around three times that of AQP3-2 in qPCR experiments (e.g., experiment 1, 100%SW), hence there must be a much higher intensity of AQP3 expression at the end of the LDT. Of course, the changes in expression were not statistically different except for that of the AQP3-2 spliceoform in 120% SW fish compared to 100% SW fish. It's interesting that there is such a significant decrease in AQP3-2 spliceoform expression in 120% SW. This suggests that whatever its actual function is that it must be relatively important for it to be eradicated in higher salinity environments.

Brain UT which was originally discovered in the brain (Chana-Munoz *et al.* 2017), but the RT-PCR showed that its mRNA expression also occurs in the kidney (Figure 4). The 3' RACE PCR was carried out to get the complete sequence, and in the process a splice variant of the gene was identified which has never been reported previously (see A2 in Appendix). The Brain UT spliceoform exhibits a different C-terminal end to its amino acid sequence (see A2.1 in Appendix) and while it is clearly present in brain cDNA, it could not be amplified from kidney cDNAs during qPCR experiments. The full-length Brain UT sequence obtained was similar to the UT-1 short version of UT-1 (see A2.4 in Appendix). The PCR amplification of the 5' end fragment of Brain UT (see A2 in Appendix) was similar to but not the

same as the Brain UT sequence from the transcriptomics paper (Chana-Munoz *et al.* 2017) as there were nine nucleotide differences between the sequences that are probably polymorphisms. Multiple bands of brain UT were seen in the RT-PCR for brain and other tissues (Figure 4) potentially implying multiple splice variants of the gene. Although, the larger bands may be genomic copies that amplified because their introns were small enough to allow that to occur. It can be speculated that the presence of AQP3-2 and its spliceoform, UT-1 long, UT-1, short, Brain UT and NCC proteins in the brain is to sense the circulating levels of $H_2O$, urea and NaCl, to allow their homeostatic regulation via the modulation of regulatory hormones.

The sequences for UT-1 long, UT-1 short splice variants, and NCC were already available in the gene bank so cloning experiment were not needed. Initial RT-PCR reactions were able to amplify UT-1 long and short bands in kidney and brain. Curiously, there was a bit less (fainter band) of UT-1 short than the UT-1 long spliceoform in the tissue PCR gel result (Figure 4). The UT-1 long splice variant appeared to amplify better in the kidney on the tissue PCR gel than the short variant. However, the qPCR results (Figures 22 and 23) show there is actually many more copies of the short variant. But the short variant having more copies is consistent with the original cloning where only the short variant was identified (Smith and Wright 1999). Brain UT amplified in most tissues except in the gill and stomach, but band intensity was strongest in the brain and eye cDNA samples. As there was some Brain UT mRNA expressed in the kidney, qPCR was done to further investigate this, but no significant differences were found for renal Brain UT mRNA expression across different salinity environments (Figure 21). Regarding the sequences and the production of the UT-1 antibody, the antibody was produced before the work on Brain UT was carried out, but comparison of the C –terminal amino acid sequences show 8 out 14 amino acids are common to Brain UT and UT-1 in the C-terminal end region used to make the UT-1 antibody. The common amino acids are spread throughout the sequence, and this coupled with the relatively low level of renal Brain UT expression suggests the antibody signals either on Western blots or in

immunohistochemistry experiments are unlikely to show cross-reaction of the UT-1 antibody with Brain UT protein.

The Western blots using the UT-1 antibody (Figure 7) had two main bands of 45.5 and 53.5 kDa in size. The smaller band is likely to be that of UT-1 short (expected size 43.5 kDa). The larger 53.5kDa band may be that of UT-1 long (expected size 51.5 kDa) but that is not certain because the qPCR results showed that there is around 100x less UT-1 long mRNA than UT-1 short mRNA expressed in the kidney and therefore the level of UT-1 long protein would be expected to be very much lower than that of UT-1 short, but on the Western blot the 53.5 kDa band is actually stronger than the 45.5 kDa band. Additionally, similar but fainter bands (compared to kidney samples) were seen in the brain crude membrane extracts. A faint band at around 25 kDa may result from another splice variant or from protease cutting. Urea transporter/transport (UT-1) localization with the antibody in immunohistochemistry (Figure 13-16) gives a totally different localization to that found in the Euryhaline Bullshark (*Carcharhinus leucas*; (Imaseki *et al.* 2019)) and the Houndshark (*Triakis scyllium*; (Yamaguchi *et al.* 2009)) where it is only expressed in the collecting tubule (CT).

In this study in *Squalus acanthias*, immunohistochemistry results show that it is not impossible that there may not be any expression of it in the CT at all (see Figure 15), although it's not possible to be sure (as one of the five tubules in the bundle was unstained and the end of the LDT connected to the CT was unstained). This and the localization of UT-1 protein in most other parts of the nephron, implies that UT-1 in *Squalus acanthias* kidney may be involved in urea absorption prior to the CT and that there might also consequently be some other unknown urea re-absorption mechanism operating in the CT instead. Interestingly, in *Squalus acanthias*, urea absorption has been shown to occur in lock step with NaCl reabsorption, which is not true in other Elasmobranch species (Schmidt-Nielsen *et al.* 1972) and therefore this suggests the possibility that some form of Na-urea cotransporter may exist in the *Squalus acanthias* which is possibly expressed in the CT. In any case other authors (Schmidt-Neilsen and Bankir, 2003 and Brown and Green, 1987) have given evidence for the presence of urea reabsorption in proximal

regions of the nephron and this would be consistent with the present study (See. Figure 13-16). One possible explanation for the results is that there is some UT-1 expression in the CT (i.e., the absence of UT-1 staining was in another bundle zone segment) and that the expression of UT-1 showing up in other areas is a matter of sensitivity. The 200x tyramide (kit) amplification used for the immunohistochemistry is much more inclined to show low level signals than the techniques employed by Imaseki et al., (2019) or Yamaguchi et al., (2009). In many ways absorption of urea in proximal segments make sense, as other osmolytes (sugars, amino acids, and nucleotides etc.) and $H_2O$ are absorbed, that will concentrate the urea allowing some urea absorption to occur. That absorption of urea (and some $H_2O$) would then in turn help the absorption of further (other) osmolytes. Another curious feature of the UT-1 immunohistochemistry results is that there is no sign of UT-1 staining in the apical membrane. A possible explanation is that the region of UT-1 binding the UT-1 antibody, may be modified by phosphorylation (or in some other way) when UT-1 is located in the apical membrane, and that that modification blocks the antibody binding. The antigen/antibody binding site contains a tyrosine residue that might be phosphorylated.

Other transport proteins such as Brain UT, AQP3 and AQP3-2 may also be involved in urea reabsorption. Although the role of Brain UT is likely to be minor due to its relatively low level of expression. AQP3-2 might be involved in urea absorption in the LDT as there is also some UT-1 expression at the start of the LDT (sLDT) in the apical pole, with hence the possibility of having UT-1 in the apical membrane. AQP3 is interesting as it seems to take over where the level of UT-1 leaves off in LDT (i.e., at the end of the LDT; eLDT) but consequently if basolateral AQP3 was involved in any urea uptake, the apical entry route for the urea in the eLDT is unknown. Recent studies showed that the mRNA expression of UT-1 in Bullshark (*Carcharinhus leucas*) (Imaseki *et al.* 2019) and Houndshark (*Triakis syllium*) (Yamaguchi *et al.* 2009) kidney was not significantly changed by acclimation of the fish to low salinity environments (FW and 30% SW respectively), although interestingly the trends in mRNA levels in the two species were in opposite directions (Imaseki *et al.* 2019, Yamaguchi *et al.* 2009). In this case, the study on Bullshark (*Carcharinhus leucas*) had similar trends to this study, with higher UT-1 mRNA

expression in low salinities, whereas the Houndshark (*Triakis syllium*) generally had decreased mRNA expression in lower salinities and specifically had lower levels of UT-1 protein in the apical membrane of tubule cells.

The NCC cotransporter mRNA expression was mostly seen in the kidney (Figure 4) as it has been reported by other studies (Imaseki *et al.* 2019, Yamaguchi *et al.* 2009). However, Takabe *et al* (Takabe *et al.* 2019) reported the expression of a NCC in the gills of Houndshark (*Triakis syllium*) but in this study there was no RT-PCR amplification from the gill of *Squalus acanthias*. The NCC antibody staining was localized to the LDT (where studies in other sharks have localized it and therefore this staining may actually represent correct NCC staining) but also staining in PIb, which may be related to the low molecular weight bands seen on the Western blot (figure 8). The bands seen for the NCC/2 were not as expected (>114 kDa). The band seen at around 45kDa probably suggests incorrect binding of the antibody to some other target protein, although the existence of a splice variant version of NCC should not be discounted in the LDT or P1b. The peptide blocking for all the genes worked as expected and abolished most if not all the (therefore) specific antibody staining. NCC qPCR expression matches what was seen in bullshark and houndshark with higher levels of expression in lower salinities, this suggests that NCC may be involved in conserving (absorbing) NaCl especially in low salinity environments.

There was not a lot of statistically significant changes in the expression of the genes studied. However, some trends in the changes in gene expression were interesting even though it isn't certain that the changes are real rather than due to random variations. RPL-P0, UT-1 long, UT-1 short and Brain UT mRNA levels, were higher in 75% SW and 120% SW than they were in 100% SW. This suggests the potential of the response to salinity changes as a stressor with a more general increase in expression of many osmoregulatory genes/proteins. Most of the genes showed higher expression in 120%SW in Experiment 1 samples, except for AQP 3-2 spliceoform (-77.20%), NCC (-17.40%), and AQP3-2 (-16.70%). These three genes/variants also showed similar trends as they all showed decreased mRNA expression as salinity increased. Whether there is any connection between the decreases in these three

gene versions is hard to ascertain. The two genes that showed statistically significant differences were AQP3-2 spliceoform (-77.20% in 120% vs 100% SW) and UT-1 long (208.90% higher in 75% vs 100% SW). The fact that many of the genes in the salinity acclimation experiment showed no statistically different changes in expression, suggests that in future experiments more fish may be needed (greater n per group) and/or the salinity challenges should be greater (less than 75% and more than 120% SW). One study has more recently shown that dogfish can tolerate at least 70% SW (Wright *et al.* 2014). Future work could also be to produce further independent antibodies against the various transporter proteins to confirm the immunohistochemistry and Western blotting results. Further antibodies would also allow immunoprecipitation experiments, where one antibody is used to immunoprecipitate the protein, and the second antibody is used to detect the protein. This would improve the certainty of results especially for NCC.

The only qPCR result that correlates completely with the hypothesis of this study is that of AQP3 (see above). The qPCR results for the other genes either showed higher (rather than lower) mRNA expression in 75% SW or lower levels (rather than higher) of mRNA expression in 120% SW. This suggests for the most part, that other factors are in play to make the adjustments needed by the fish to acclimate to the different salinity environments. As mentioned in the introduction, sharks seem to absorb (in low salinity environments) or lose (in higher salinity environments) water across the gills and increase or decrease their body mass as a result. Also, there may be changes to the urea synthesis rate, drinking rate, rectal gland secretion rate, renal glomerular filtration rate and nephron fluid secretion rate, which together with the changes to the osmolyte and water transporter gene expression described here, allow dogfish to acclimate to different environmental salinities.

# REFERENCES

Anderson, G.W., Nawata, M., Wood, C.M., Piercey-Normore, M.D. and Weihrauch, D. 2012. Body fluid osmolytes and urea and ammonia flux in the colon of two chondrichthyan fishes, the ratfish, Hydrolagus colliei, and spiny dogfish, *Squalus acanthias. Comp. Biochem. Physiol.* 161: 27-35.

Anderson, P.M. 2001. Urea and glutamine synthesis: environmental influences on nitrogen excretion. Pp. 239–278 in P.A. Wright and P.M. Anderson, eds. Fish Physiology. Vol. 20. Nitrogen Excretion. Academic Press, San Diego, CA.

Anderson, W.G., Taylor, J.R., Good, J.P., Hazon, N., Grosell, M. 2007. Body fluid volume regulation in elasmobranch fish. *Comp Biochem Physiol A Mol Integr Physiol*; 148(1):3-13.

Bagnasco, S.M. 2005. Role and regulation of urea transporters. *Pflügers Arch* 450: 217–226.

Bankir, L., Chen, K., Yang, B. 2004. Lack of UT-B in vasa recta and red blood cells prevents urea-induced improvement of urinary concentrating ability. *Am. J. Physiol. Renal Physiol.* 286, F144–F15110.1152.

Berger, U. V., Tsukaguchi, H., Hediger, M. A. 1998. Distribution of mRNA for the facilitated urea transporter UT3 in the rat nervous system. *Anat. Embryol.* 197, 405–41410.1007/s004290050152.

Beyenbach, K.W., Frömter, E. 1985. Electrophysiological evidence for Cl secretion in shark renal proximal tubules. *Am J Physiol.*; 248(2 Pt 2): F282-95.

Boylan, J.W. 1972. A model for passive urea reabsorption in the elasmobranch Kidney. *Comp Biochem Physiol* 42A, 27–30.

Brown, J.A., Green, C. 1987. Single nephron function of the lesser spotted dogfish, Scyliorhinus canicula, and the effects of adrenaline. *J Exp Biol.*; 129:265-78.

Burger, J.W, Hess, W.N. 1960. Function of the rectal gland in the spiny dogfish. *Science* 131:670–671.

Burger, J.W. 1965. Roles of the rectal gland and kidneys in salt and water excretion in the spiny dogfish. *Physiol. Zool*. 38:191–196.

Chana-Munoz, A., Jendroszek, A., Sønnichsen, M. Kristiansen, R., Jensen, J., Andreasen, P., Bendixen C., Panitz, F. 2017. Multi-tissue RNA-seq and transcriptome characterisation of the spiny dogfish shark (Squalus acanthias) provides a molecular tool for biological research and reveals new gene involved in osmoregulation. *PLoS ONE* 12(8): e0182756.

Chomczynski, P. and Sacchi, N. 1987. Single-step method of RNA isolation by acid guanidinium thiocyanate-phenol-chloroform extraction. *Anal. Biochem*. 162, 156–159.

Chou, C. L., Knepper, M. A. 1989. Inhibition of urea transport in inner medullary collecting duct by phloretin and urea analogues. *Am. J. Physiol.* 257, F359–F365.

Cutler, C. P. 2006. Cloning of aquaporin 1e gene homologues in the dogfish shark (*Squalus acanthias*) and hagfish (*Myxine glutinosa*). *Bull. Mt. Desert Isl. Biol. Lab.* 45, 40–41.

Cutler, C. P. 2007. Cloning and identification of four aquaporin genes in the dogfish shark (*Squalus acanthias*). *Bulletin Mount Desert Island Biological Laboratory* **46**: 19-20.

Cutler, C., and Cramb, G. 2008. Differential expression of absorptive cation-chloride cotransporters in the intestinal and renal tissues of the European eel (*Anguilla anguilla*). *Comparative Biochemistry and Physiology* 149: 63-73.

Cutler, C., MacIver, B., Cramb, G., and Zeidel, M. 2012. Aquaporin 4 is a ubiquitously expressed isoform in the dogfish (*Squalus acanthias*) shark. *Frontiers in Physiology* 2: 107, 1-9.

Cutler, C.P., Anne-Sophie Martinez, A-S. And Cramb, G. 2007. The role of aquaporin 3 in fish. *Comp. Biochem. Physiol.* 148: 82-91.

Cutler, C.P., Meischke, L. and Cramb, G. 2005. Evolutionary and comparative analysis of aquaporin water channel genes in fish. Bull. Mt. Des. Isl. Biol. Lab. 44: 55.

Dantzler, WH. 2005. Challenges and intriguing problems in comparative renal physiology. *J Exp Biol*.; 208(Pt 4):587-94.

Echevarrı́a, M., Windhager, E. E., Tate, S. S., and Frindt, G. 1996. Selectivity of the Renal Collecting Duct Water Channel Aquaporin-3. *The journal of biological chemistry*. 271 (41) 25079 –25082.

Evans, D.H. 1979. Chapter 6. Fish. In: G.M.O. Moloiy (Ed.), Comparative physiology of osmoregulation in animals. *Academic Press, Orlando*, Vol. 1 pp. 305-370.

Evans, DH, Piermarini, PM, Choe, KP. 2004. Homeostasis: Osmoregulation, pH regulation, and nitrogen excretion. In: Carrier JC, Musick JA, Heithaus MR, editors. Biology of sharks and their relatives. Boca Raton, Florida: CRC Press.

Fenton, R. A., Howorth, A., Cooper, G. J., Meccariello, R., Morris I. D., Smith, C. P. 2000. Molecular characterization of a novel UT-A urea transporter isoform (UT-A5) in testis. *Am. J. Physiol. Cell Physiol.* 279, C1425–C1431.

Fenton, R. A., Knepper, M. A. 2007. Urea and renal function in the 21st century: insights from knockout mice. *J. Am. Soc. Nephrol.* 18, 679–68810.1681.

Fenton, R.A., Hewitt, J.E., Howorth, A, Cottingham, C.A., Smith, C.P. 1999. The murine urea transporter genes Slc14a1 and Slc14a2 occur in tandem on chromosome 18. *Cytogenet Cell Genet* 87: 95–96.

Finn, R.N., Chauvigné, F., Hlidberg, J.B., Cutler, C.P. and Cerdà, J. 2014. The lineage-specific evolution of aquaporin gene clusters facilitated tetrapod terrestrial adaptation. *PLoS ONE* 9 (11): e113686 p1-38.

Friedman, P.A., Hebert, S.C. 1990. Diluting segment in kidney of dogfish shark I. Localization and characterization of chloride absorption. *Am. J. Physiol*. 258: R398–408.

Gallucci, E, Micelli, S, Lippe, C. 1971. Non-electrolyte permeability across thin lipid membranes. *Arch Int Physiol Biochim Biophys* 79: 881–887.

Gamba, G. 2005. Molecular physiology and pathophysiology of electroneutral cation chloride cotransporters. *Physiological Reviews*, 85(2), 423–493.

Gamba, G., Miyanoshita, A., Lombardi, M., Lytton, J., Lee, W. S., Hediger, M. A. 1994. Molecular cloning, primary structure, and characterization of two members of the mammalian electroneutral sodium-(potassium)-chloride cotransporter family expressed in kidney. *The Journal of Biological Chemistry*, 269(26), 17713–17722.

Gangnon, E., Forbush, B., Flemmer, A., Gimenez, I., Caron, L., Isenring, P. 2002. Functional and molecular characterization of the shark renal Na-K-Cl cotransporter: novel aspects. *Am J Physiol Renal Physiol* 283: F1046–F1055.

Gonen, T., Cheng, Y., Kistler J, Walz, T. 2004. Aquaporin-0 membrane junctions form upon proteolytic cleavage. *J Mol Biol*. 342(4):1337-45.

Gorin, M., Yancy, B., Cline, J., Revel, J., Horwitz, J. 1984. The major intrinsic protein (MIP) of the bovine lens fiber membrane: Characterization and structure based on cDNA cloning. *Cell* 39(1): 49-59.

Gregory, M. Preston and Peter, A. 1991. Isolation of the cDNA for erythrocyte integral membrane protein of 28 kilodaltons: Member of an ancient channel family. *Proc. Nati. Acad. Sci. USA*. 88: 11110-11114.

Hammerschlag, N. 2006. Osmoregulation in elasmobranchs: a review for fish biologists, behaviourists and ecologists. *Marine and Freshwater Behaviour and Physiology*; 39(3): 209–228.

Hasler, L, Walz T, Tittmann P, et al. 1998. Purified lens major intrinsic protein (MIP) forms highly ordered tetragonal two-dimensional arrays by reconstitution. *Journal of Molecular Biology*. 279(4):855-864.

Haywood, G.P. 1973. Hypo-osmotic regulation coupled with reduced metabolic urea in the dogfish Poroderma africanum: An analysis of serum osmolarity, chloride, and urea. *Biol*. 23:121–127.

Hazon, N. Tierney, M.L., Anderson, W.G., Mackenzie, S., Cutler, C.P. and Cramb, G. 1997. Chapter 5. Ion and Water balance in elasmobranch fish. In: Hazon, N, Eddy, F.B. and Flik, G. (Eds.) Ionic Regulation in Animals. Springer Verlag, Heidelberg, Germany pp. 70-87.

Hazon, N. Wells, A., Pillans, R.D., Good, J.P., Anderson, W.G., Franklin, C.E. 2003. Urea based osmoregulation and endocrine control in elasmobranch fish with special reference to euryhalinity. *Comp. Biochem. Physiol*. B. 136:685–700.

Hentschel, H. 1987. Renal architecture of the dogfish *Scyliorhinus caniculus* (Chondrichthyes, Elasmobranchii). *Zoomorphology* 107, 115–125.

Hentschel, H. 1988. Renal blood vascular system in the elasmobranch, Raja erinacea Mitchill, in relation to kidney zones. *Am J Anat*; 183 (2):130-47.

Hentschel, H. 1991. Developing nephrons in adolescent dogfish, *Scyliorhinus caniculus* (L.), with reference to ultrastructure of early stages, histogenesis of the renal countercurrent system, and nephron segmentation in marine elasmobranchs. *Am. J. Anat.*, *190*, 309–333.

Hentschel, H., Storb, U., Teckhaus, L. and Elger, M. 1998. The central vessel of the renal countercurrent bundles of two marine elasmobranchs – dogfish (Scyliorhinus caniculus) and skate (Raja erinacea) – as revealed by light and electron microscopy with computer-assisted reconstruction. *Anat. Embryol*. 198, 73-89.

Hyodo, S., Fumi, K., Toyoji, K. and Yoshio, T. 2003. A facilitative urea transporter is localized in the renal collecting tubule of the dogfish *Triakis scyllia*. *The Journal of Experimental Biology* 207, 347-356.

Hyodo, S., Keigo, K., Wataru, T., Kumi, H., and Yoko, Y. 2014. Morphological and functional characteristics of the kidney of cartilaginous fishes: with special reference to urea reabsorption. *Am J Physiol Regul Integr Comp Physiol* 307: R1381–R1395.

Imaseki, I., Wakabayashi, M., Hara, Y., Wantanabe, T., Takabe, S., Kakumura, K., Honda, Y., Ueda, K., Murakumo, K., Matsumoto, R., Matsumoto, Y., Nakamura, M., Takagi, W., kuraku, S., Hyodo, S. 2019. Comprehensive analysis of genes contributing to euryhalinity in the bull shark, Carcharhinus leucas; Na+-Cl− co-transporter is one of the key renal factors upregulated in acclimation to low-salinity environment. *Journal of Experimental Biology*. 222, jeb201780.

Inoue, H., Jackson, S. D., Vikulina, T., Klein, J. D., Tomita, K., Bagnasco, S. M. 2004. Identification and characterization of a Kidd antigen/UT-B urea transporter expressed in human colon. *Am. J. Physiol. Cell Physiol.* 287, C30–C3510.1152.

Ishibashi, K., Morinaga, T., Kuwahara, M., Sasaki, S. and Imai, M. 2002. Cloning and identification of a new member of water channel (AQP10) as aquaglyceroporin. *Biochim. Biophys. Acta* 1576, 335-340.

Itaru, I., Midori, W., Yuichiro, H., Taro, W., Souichirou, T., Keigo, K., Yuki, H., Keiichi, U., Kiyomi, M., Rui, M., Yosuke, M., Masaru, N., Wataru, T., Shigehiro, K., Susumu, H. 2019. Comprehensive analysis of genes contributing to euryhalinity in the bull shark, Carcharhinus leucas; Na+-Cl− co-transporter is one of the key renal factors upregulated in acclimation to low-salinity environment. *J. Exp. Biol. 222*: In press.

Jin, B.J., Rossi, A., Verkman, A.S. 2011. Model of aquaporin-4 supramolecular assembly in orthogonal arrays based on heterotetrameric association of M1-M23 isoforms. *Biophys J*. 22;100(12):2936-45.

Kajimura, M., Walsh, P.J. Mommsen, T.P. and Wood, C.M. 2006. The dogfish shark (*Squalus acanthias*) increases both hepatic and extrahepatic ornithine urea cycle enzyme activities for nitrogen conservation after feeding. *Phys. Biochem. Zool.* 79: 602-613.

Kakumura, K., Watanabe, S., Bell, J., Donald, J., Toop, T., Kaneko, T., Hyodo, S. 2009. Multiple urea transporter proteins in the kidney of holocephalan elephant fish (*Callorhinchus milii*) *Comparative Biochemistry and Physiology*, Part B 154; 239–247.

Kakumura, K., Takabe, S., Takagi, W., Hasegawa, K., Konno, N., Bell, J.D., Toop, T., Donald, J.A., Kaneko, T., Hyodo, S. 2015. Morphological and molecular investigations of the holocephalan elephant fish nephron: the existence of a countercurrent-like configuration and the two separate diluting segments in the distal tubule. *Cell and Tissue Research,* 362 (3): 677-688.

Kempton, R.T. 1953. Studies on the elasmobranch kidney. II. Reabsorption of Urea by the smooth dogfish, *Mustelus canis*. *Biol Bull* 104: 45–56.

Klein, J.D., Blount, M.A, Sands, J.M. 2011. Urea transport in the kidney. *Compr Physiol* 1: 699–729.

Lacy, E. R. and Reale, E. 1985a. The elasmobranch kidney II. Sequence and structure of the nephrons. *Anat. Embryol.* 173, 163-186.

Lacy, E.R., Reale, E. 1986.The elasmobranch kidney. The elasmobranch kidney III. Fine structure of the peritubular sheath. *Anat Embryol* 173, 299–305.

Lacy, R., Reale E. 1985b. The elasmobranch kidney. The elasmobranch kidney I. Gross anatomy and general distribution of nephrons. *Anat Embryol* 173**,** 23–34.

Lacy, R., Reale, E., Schlusselberg, D., Smith, W., and Woodward, D. 1985. A Renal Countercurrent System in Marine Elasmobranch Fish: A Computer-Assisted Reconstruction. *Science, New Series*, Vol. 227, No. 4692, pp. 1351-1354.

Lacy, E.R. and Reale, E. 1995. Functional morphology of the elasmobranch nephron and retention of urea In: Wood C. M. and Shuttleworth T.J. (Eds.). Cellular and Molecular Approaches to Fish Ionic Regulation, Fish Physiology. Vol. 14 pp. 107–146.

Laemmli, U. K. 1970. Cleavage of structural proteins during the assembly of the head of bacteiophage T4. *Nature* 227, 680–685.

Lei, T., Zhou, L., Layton, A. T., Zhou, H., Zhao, X., Bankir, L., Yang, B. 2011. Role of thin descending limb urea transport in renal urea handling and the urine concentrating mechanism. *Am. J. Physiol. Renal Physiol.* 301, F1251–F125910.1152.

Levin, E. J., Quick, M., Zhou, M. 2009. Crystal structure of a bacterial homologue of the kidney urea transporter. *Nature* 462, 757–76110.1038.

Lucien, N., Bruneval, P., Lasbennes, F., Belair, M. F., Mandet, C., Cartron, J. P., Bailly, P., Trinh-Trang-Tan, M. M. 2005. UT-B1 urea transporter is expressed along the urinary and gastrointestinal tracts of the mouse. *Am. J. Physiol. Regul. Integr. Comp. Physiol.* 288, R1046–R105610.1152.

Lucien, N., Sidoux-Walter F, Olivès B, Moulds J, Le Pennec P-Y, Cartron J-P, Bailly P. 1998. Characterization of the gene encoding the human Kidd blood group/urea transporter protein: evidence for splice site mutations in Jknull individuals. *J Biol Chem.*; 273:12973–12980.

Ma, T., Song Y., Yang B., Gillespie A., Carlson E. J., Epstein C. J. 2000. Nephrogenic diabetes insipidus in mice lacking aquaporin-3 water channels. *Proc. Natl. Acad. Sci. USA* 97: 4386–4391.

Madsen, S., Engelund, M., and Cutler, C.P. 2015. Water transport and the functional dynamics of aquaporins in osmoregulatory organs of fishes. *Biol. Bull.* 229: 1, 70-92.

Martin, RA. 2005. Conservation of freshwater and euryhaline elasmobranchs: A review. *J. Mar. Biol. Assoc. UK*. 85:1049–1073.

Mathai, J., Agre P. 1999. Hourglass pore-forming domains restrict aquaporin-1 tetramer assembly *Biochemistry* 38 (3), 923-928

MacIver, B., Cutler, C., Yin, J., Hill, M., Zeidel, M., and Hill, W. 2009.Expression and functional characterization of four aquaporin water channels from the European Eel (*Anguilla anguilla)*. *Journal of Experimental Biology* **212**: 2856-2863.

Moreno, E., de Los Heros, P., Plata, C., Cutler, C., Vega-Mateos, A., Vázquez, N., Gamba. G. 2019. Structure-function relationships in the renal NaCl cotransporter (NCC). *Curr Top Membr.*; 83:177-204.

Morgan, R.L., Ballantyne J.S., and Wright, P.A. 2003. Regulation of a renal urea transporter with reduced salinity in a marine elasmobranch, Raja erinacea. *J Exp Biol* 206:3285–3292.

Olives, B., Mattei, M. G., Huet, M., Neau, P., Martial, S., Cartron, J. P., Bailly, P. 1995. Kidd blood group and urea transport function of human erythrocytes are carried by the same protein. *J. Biol. Chem.* 270, 15607–1561010.1074/jbc.270.26.15607.

Olives, B., Neau, P., Bailly P, Hediger, M.A., Rousselet, G., Carton, J.P., Ripoche, P. 1994. Cloning and functional expression of a urea transporter from human bone marrow cells. *J Biol Chem* 269: 31649 –31652.

Pallone, T. L. 1994. Characterization of the urea transporter in outer medullary descending vasa recta. *Am. J. Physiol.* 267, R260–R267.

Pannabecker, T.L. 2013. Comparative physiology and architecture associated with the mammalian urine concentrating mechanism: role of inner medullary water and urea transport pathways in the rodent medulla. *Am J Physiol Regul Integr Comp Physiol* 304: R488–R503.

Pannabecker T.L. Danzler W.H. 2005. Renal gene expression in Squalus acanthius following hyposmotic stress. Mt. Desert Isl. Bio. Lab. Bull. 44, 78-79.

Perlman, D. F., Goldstein, L. 1988. Nitrogen metabolism. In Physiology of Elasmobranch Fishes (ed. T. J. Shuttleworth). Berlin: Springer-Verlag.pp. 253–276.

Pfaffl, M.W. 2004. Quantification strategies in real-time PCR. In: Bustin SA, editor. *The Real-Time PCR Encyclopedia A–Z of Quantitative PCR.* International University Line; La Jolla, CA: 2004. pp. 87–112.

Piermarini, P.M, Evans, D.H. 2000. Effects of environmental salinity of Naþ/Kþ-ATPase in the gills and rectal gland of a euryhaline elasmobranch (*Dasyatis sabina*). *J. Exp. Biol.* 203:2957–2966.

Robertson, J.D. 1975. Osmotic constituents of the blood plasma and parietal muscle of *Squalus acanthias. L. Biol. Bull*. 148:303–319.

Rodriguez, R.A, Liang, H., Chen, L.Y., Plascencia-Villa, G., Perry, G. 2019. Single-channel permeability and glycerol affinity of human aquaglyceroporin AQP3. *Biochim Biophys Acta Biomembr*. 1; 1861(4):768-775.

Rojek, A, Praetorius, J., Frokiaer, J., Nielsen, S., Fenton, R.A. 2008. A current view of the mammalian aquaglyceroporins. *Annu Rev Physiol* 70: 301– 327.

Sands, J.M. 2003. Mammalian urea transporters. *Annu Rev Physiol* 65: 543– 556.

Sawyer, D.B., Beyenbach, K.W. 1985. Mechanism of fluid secretion in isolated shark renal proximal tubules. *Am J Physiol*.; 249(6 Pt 2): F884-90.

Schmidt-Nielsen B., Truniger, B., Rabinowitz, L. 1972. Sodium-linked urea transport by the renal tubule of the spiny dogfish *Squalus acanthias*. *Comp Biochem Physiol. 42A: 13–25.*

Schmidt-Nielsen, B., and Bankir, L. 2003. Dilution of urine through renal fluid secretion: anatomo-functional convergence in marine elasmobranches and oligochaetes. *Bull Mt Desert Isl Biol Lab Salisb Cove Maine* 42: 2–9, 21.

Shayakul, C., Steel, A., Hediger, M. 1996. Molecular cloning and characterization of the vasopressin-regulated urea transporter of rat kidney collecting ducts. *J Clin Invest.* 98(11):2580-2587.

Shayakul, C., Steel, A., Hediger, M. 2013. The urea transporter family (SLC14): Physiological, pathological, and structural aspects. *Molecular Aspects of Medicine* 34: 313–322.

Smith, C. P., Fenton, R. A. 2006. Genomic organization of the mammalian SLC14a2 urea transporter genes. *J. Membr. Biol.* 212, 109–117.

Smith, C.P. and Wright, P.A. 1999. Molecular characterization of an elasmobranch urea transporter. *Am. J. Physiol.* 276: R622-626.

Smith, H.W. 1931. The absorption and excretion of water and salts by the elasmobranch fishes. I. Freshwater elasmobranchs. *Am. J. Physiol*. 98:296–310.

Takabe, S., Inokuchi, M., Yamaguchi, Y., Hyodo, S. 2016. Distribution and dynamics of branchial ionocytes in houndshark reared in full-strength and diluted seawater environments. *Comparative Biochemistry and Physiology*, Part A 198: 22–32.

Thorson, T.B. 1962. Partitioning of body fluids in the Lake Nicaragua shark and three marine sharks. *Science,* 138:688–690.

Timmer, R. T., Klein, J. D., Bagnasco, S. M., Doran, J. J., Verlander, J. W., Gunn, R. B., Sands, J. M. 2001. Localization of the urea transporter UT-B protein in human and rat erythrocytes and tissues. *Am. J. Physiol. Cell Physiol.* 281, C1318–C1325.

Trinh-Trang-Tan, M.M., Geelen, G., Teillet, L., Corman, B. 2003. Urea transporter expression in aging kidney and brain during dehydration. *Am J Physiol Regul Integr Comp Physiol*; 285(6): R1355-65.

Tsukaguchi H., Shayakul, C., Berger, U. V., Tokui, T., Brown, D., Hediger, M. A. 1997. Cloning and characterization of the urea transporter UT3: localization in rat kidney and testis. *J. Clin. Invest.* 99, 1506–151510.1172/JCI119313.

Verkman, A.S., 2005. More than just water channels: unexpected cellular roles of aquaporins. *J. Cell Sci.* 118, 3225–3232.

Villalobos A.R.A., and Renfro J.L. 2007. Trimethylamine oxide suppresses stress-induced alteration of organic anion transport in choroid plexus. *J. Exp. Biol.* 210, 541-552.

Wang, W., Li, C, Yang, B. 2017. Molecular Biology of Aquaporins. Aquaporins. *Dordrecht, Springer* Netherlands: 1-34.

Wood, C., Part, P, Wright, P. 1995. Ammonia and urea metabolism in relation to gill function and acid-base balance in a marine elasmobranch, the spiny dogfish (*Squalus acanthias*). *J Exp Biol.* 198(Pt 7):1545-58.

Wood, C.M., Matsuo, A., Gonzalez R.J., Wilson, R.W., Patrick, M.L., Val, A.L. 2002. Mechanisms of ion transport in Potamotrygon, a stenohaline freshwater elasmobranch native to the ion-poor blackwater of the Rio Negro. *J. Exp. Biol.* 205:3039–3054.

Wright, P., Lawrence, M., Currie, S., MacLellan, R., Wood, C., Edwards, S. 2014. Rhesus glycoproteins in dogfish shark (*Squalus acanthias*) in response to hypo-osmotic stress. *The Bulletin, MDI Biological Laboratory* V. 53.

Xu, Y., Olives, B., Bailly, P., Fischer, E., Ripoche, P., Ronco, P., Cartron, J. P., Rondeau, E. 1997. Endothelial cells of the kidney vasa recta express the urea transporter HUT11. *Kidney Int.* 51, 138–14610.1038/ki.1997.17.

Xu, J., Lytle, C., Zhu, T., Payne, J., Benz, E., Forbush, B. 1994. Molecular cloning and functional expression of the bumetanide-sensitive Na-K-Cl cotransporter. *Proc. Nati. Acad. Sci. USA.* 91; 2201-2205.

Yamaguchi, Y., Takaki, S., Hyodo, S. 2009. Subcellular distribution of urea transporter in the collecting tubule of shark kidney is dependent on environmental salinity. *Journal of experimental zoology*. 311A: 705–718.

Yang, B., Bankir L. 2005. Urea and urine concentrating ability: new insights from studies in mice. *Am. J. Physiol. Renal Physiol.* 288, F881–F89610.1152.

You, G., Smith, C.P., Kanai, Y., Lee, W.S., Stelzner, M., Hediger, M.A. 1993. Cloning and characterization of the vasopressin-regulated urea transporter. *Nature* 365: 844 –847.

Yu, L., Liu, T., Fu, S., Li, L., Meng, X., Su, X., Xie, Z., Ren, J., Meng, Y., Lv, X., & Du, Y. 2019. Physiological functions of urea transporter B. *Pflugers Archiv: European journal of physiology*, *471*(11-12), 1359–1368.

# APPENDIX

## Sequencing and Cloning Information and Results

### AQP3-2

AQP3-2 and AQP3-2 spliceoform gene were cloned and sequenced, to check that the gene was expressed as suggested by the work of Chana-Munoz (Chana-Munoz *et al.* 2017) and to make accurate primers for qPCR and other experiments. A comprehensive gene study (Finn *et al.* 2014) revealed that the Elasmobranch has 2 copies of AQP3 (see table 3). Subsequently, a transcriptomics study (Chana-Munoz *et al.* 2017) deposited sequence data *et al* for *S. acanthias* for AQP 0, 1, 4, 9, 15 as well as duplicate copies of AQP3 (in this thesis termed AQP3 and AQP3-2), as well as a splice variant of AQP3-2. (Cutler *et al.* 2007, Evans *et al.* 2004, Finn *et al.* 2014, Gamba 2005). But this laboratory had already obtained all of those sequences previously except for that of AQP3-2.

**Squalus AQP3-2 nucleotide sequence**

ATTGATTAAAAATGGGAAAACAAAAAGAGATCCTCATAAAAATGACAACGACACTGAAAGTCCGAAGTATTCTGGTG
AAACAATGTCTTGCTGAATGTTTAGGAACTCTAATTCATACAATGCTTACCTGTGGAGCAATAGCACAATTTACTCT
CGGTTATGGTACACACAAAGAATTTTTGACGGTTACTTTTGCCATCGGATTTGCAGTAGCTCTGGGTATAATGGTAA
CTAGTAAAGTGTCAGGAGCTCACCTGAATCCTGCAGTGACCTTTGCTTTGTGCTTGCTTGCTTGTGAGCCTTGGTTA
AAATTCCCCTTCTTCTTTTTGGCACAAACATTCGGTGCCTTTCTTGGATCAGGAATAATGTTTGGTTTGTATTACTA
TAAATTGTGGCATTATGGTAATAAACAGCTAACAGTAATGGGACCAAACTCTACTGCTGGAATATTTACTACTTATC
CGCCTGAACATTTGAGTGCAGTCAGTGGCATTTTTGATCACGCAATTGGGACGGCAGCTCTGATACTTTGTATCCTT
ATCATTGTGGATCCAATGAACAAGCCAGTGCCAACAGGACTGGAAGCCTTTACCATTGGCTTTGTGGTTCTGATAAT
TGGCTGGTCAATGGATTCAAATTCCCAGTACTCATTAAATCCTGCCAGAGATATTGGACCTCGCTTGTTTACTGCAA
TTGCTGGTTGGGGATCTGAAGTTTTCACTGCTGGAAACTATTGGTTTTGGATCCCACTTGTCAGCCCAATCATTGGT
GCCATTTTTGGTGTTCTGATGTATCTATTCATTGTTGGATTGCGTGTTGAAGCAAGAAGCGGCTGCTCACCCAATGC
AGAACAAAATGTAAAGTTAATGAGCCAGAAACCAAAGGGGAGGCGCTAATGATT

**Squalus AQP3-2 spliceoform nucleotide sequence**

ATTGATTAAAAATGGGAAAACAAAAAGAGATCCTCAGAAAAATGACAACGACACTGAAAGTCCGAAGTATTCTGGTG
AAACAATGTCTTGCTGAATGTTTAGGAACTCTAATTCATACAATGCTTAGCTGTGGAGCAATAGCACAATTTACTCT
CGGTTATGGTACACACAAAGAATTTTTGACGGTTACTTTTGCCATCGGATTTGCAGTAGCTCTGGGTATAATGGTAA
CTAGTAAAGTGTCAG----------
---------- ----------
ATAAATTGTGGCATTATGGTAATAAACAGCTAACAGTAATGGGACCAAACTCTACTGCTGG
AATATTTACTACTTATCCGCCAGAACATTTGAGTGCAGTCAGTGGCATTTTTGATCAGGCAATTGGGACGGCAGCTC
TGATACTTTGTATCCTTATCATTGTGGATCCAATGAACAAGCCAGTGCCAACAGGACTGGAAGCCTTTACCATTGGC
TTTGTGGTTCTGATAATTGGCTGGTCAATGGATTCAAATTCCCAGTACTCATTAAATCCTGCCAGAGATATTGGACC
TCGCTTGTTTACTGCAATTGCTGGTTGGGGATCTGAAGTTTTCACTGCTGGAAACTATTGGTTTTGGATCCCACTTG
TCAGCCCAATCATTGGTGCCATTTTTGGTGTTCTGATGTATCTATTCATTGTTGGATTGCGTGTTGAAGCAAGAAGC
GGCTGCTCACCCAATGCAGAACAAAATGTAAAGTTAATGAGCCAGAAACCAAAGGGGAGGCGCTAATGATT

**A1***: Squalus acanthias* AQP3-2 and AQP3-2 spliceoform nucleotide sequences generated by cloning and the production of colony PCR DNA fragments for sequencing. The exon missing in the spliceoform version is indicated with --- lines and is underlined in the full-length sequence. The qPCR primer sites used are double underlined. Start (**ATG**) and Stop (**TAA**) Codons are bolded and underlined.

Squalus AQP3-2 Sense Phusion Tm = 71°C Product = 934bp

ACCAGCATCG GCTTCTCACA GAA

Squalus AQP3-2 Anti Phusion Tm = 69°C

CTTCAGAGAA TCATAATCCA TGCACTGTCT

**A1.1**: The primers used to generate the complete coding-regions of *Squalus acanthias* AQP3-2 and its splice variant. The PCR fragments produced were then cloned and sequenced. The melting temperature for the primers when using Phusion DNA polymerase (NEB) for PCR are indicated. The expected size of the full-length AQP3-2 is also indicated.

***Squalus acanthias* AQP3s' Amino Acid Alignment**

```
Squalus AQP3       1                          MGKQKAIIRKIEDSFRIRNLLVRQCLAEC     29
                                              |||||.|:||:..:.::|::||:||||||
Squalus AQP3-2     1                          MGKQKEILRKMTTTLKVRSILVKQCLAEC     29

Squalus AQP3      30 LGTLILVLFGCGALAQMTLSRGTHGQFLTVNFAFGFAVMLGVLLAGQVSG     79
                     |||||..:..|||:||.||..|||.:|||||.||.||||.||::::..:|||
Squalus AQP3-2    30 LGTLIHTMLSCGAIAQFTLGYGTHKEFLTVTFAIGFAVALGIMVTSKVSG     79

Squalus AQP3      80 AHLNPAVTFAMCLLAREPWLKFPLYSLAQILGGFLGSGIIFGLYFDAMWD    129
                     ||||||||||:||||.|||||||.:.:|||..|.||||||:||||:|.:|.
Squalus AQP3-2    80 AHLNPAVTFALCLLACEPWLKFPFFFLAQTFGAFLGSGIMFGLYYDKLWH    129

Squalus AQP3     130 FSGQNKLLIYGPNATAGIFATYPSVHLTPLNGFFDQLIGTAALIVCILSI    179
                     : |..:|.:.:|||:|||||.|||..||:.::|.|||.|||||||:|||.|
Squalus AQP3-2   130 Y-GNKQLTVMGPNSTAGIFTTYPPEHLSAVSGIFDQAIGTAALILCILII    178

Squalus AQP3     180 VDKFNNPVPKGLEAFTVGFTVLVIGLSMGFNSGYAVNPARDFGPRLFTSL    229
                     ||..|.|||.||||||:||.||:||.||..||.|::|||||.|||||::
Squalus AQP3-2   179 VDPMNKPVPTGLEAFTIGFVVLIIGWSMDSNSQYSLNPARDIGPRLFTAI    228

Squalus AQP3     230 AGWGAEVFIAGNYWFWIPIFAPLLGSVLGILVYQLMIGIHLEPENHNSPI    279
                     ||||:|||.|||||||||:.:|::|::.|:|:|..::|:.:|..:..||.
Squalus AQP3-2   229 AGWGSEVFTAGNYWFWIPLVSPIIGAIFGVLMYLFIVGLRVEARSGCSPN    278

Squalus AQP3     280 GEENVKLANVKLRESS    295
                     .|:||||.:.:|.:...
Squalus AQP3-2   279 AEQNVKLMSQKPKGRR    294
```

**A1.2**: An Amino acid homology and sequence alignment of *Squalus acanthias* AQP3 and AQP3-2. Identical amino acids are indicated with a | symbol, chemically similar amino acids have a : symbol, and other amino acid differences a . symbol. The – symbol represents a gap in the amino acid sequence added to maintain the alignment. Carboxyl-terminal regions used to make peptide antigens for antibody production are underlined. N-glycosylation sites are in **bold**. The exon sequence missing from the AQP3-2 spliceoform is underlined and lies between amino acids 79 and 124. The Amino acid homology between AQP3 and AQP3-2 = 60.68%.

**BRAIN UT**

The transcriptomics paper (Chana-Munoz *et al.* 2017) included the 5' end sequence of Brain UT (as well as a version probably including some introns) but the sequence was not complete as it was missing its 3'end (i.e., the end of the coding sequence). The Brain UT cDNA was amplified by PCR in two overlapping pieces and then these were then cloned and sequenced and aligned (using EBI EMBOSS Needle alignment tool) to generate the sequences for the purpose of this thesis. The PCR amplification of the 3' end fragment of Brain UT generated two products which aligned with one but not the other of the two sequences from the transcriptomics paper (Chana-Munoz *et al.* 2017). One of these two sequences generated appeared to be missing an exon at position 777-876 bp in comparison to the more complete version (see A2).

```
     10    20    30    40    50    60    70    80    90    100
     |     |     |     |     |     |     |     |     |     |
ATGAAGAATTTAGCACCGAGCTCTCATTCTGCGCAACAGCGAATCCATCAGTTCACTTTCAGTGTTCAGCCAAGCAAGAGAAGACCAATGTTTGATTCGA
••••••••••••••••••••••••••••••••••••••••••••••••••••••••••••••••••••••••••••••••••••••••••••••••••••••••
ATGAAGAATTTAGCACCGAGCTCTCATTCTGCGCAACAGCGAATCCATCAGTTCACTTTCAGTGTTCAGCCAAGCAAGAGAAGACCAATGTTTGATTCGA
     |     |     |     |     |     |     |     |     |     |
     10    20    30    40    50    60    70    80    90    100

     110   120   130   140   150   160   170   180   190   200
     |     |     |     |     |     |     |     |     |     |
AGCTGGTCCAGCTGGAGACAAATTCATTCATGCAGCAAATGGTACCAGTATGTATTGAAGAGAACACAGCCGTCCAACAAGATAACAACAAGAATGTCTA
••••••••••••••••••••••••••••••••••••••••••••••••••••••••••••••••••••••••••••••••••••••••••••••••••••••••
AGCTGGTCCAGCTGGAGACAAATTCATTCATGCAGCAAATGGTACCAGTATGTATTGAAGAGAACACAGCCGTCCAACAAGATAACAACAAGAATGTCTA
     |     |     |     |     |     |     |     |     |     |
     110   120   130   140   150   160   170   180   190   200

     210   220   230   240   250   260   270   280   290   300
     |     |     |     |     |     |     |     |     |     |
CTGTAATTGTGAACGTATTGTACAATTCCCTGATAAAATCAGAAAGTTTGGTGATTGGCTCAAAGAGCAGAACATTATCTTTCTATTTATTGACTGGAAC
••••••••••••••••••••••••••••••••••••••••••••••••••••••••••••••••••••••••••••••••••••••••••••••••••••••••
CTGTAATTGTGAACGTATTGTACAATTCCCTGATAAAATCAGAAAGTTTGGTGATTGGCTCAAAGAGCAGAACATTATCTTTCTATTTATTGACTGGAAC
     |     |     |     |     |     |     |     |     |     |
     210   220   230   240   250   260   270   280   290   300

     310   320   330   340   350   360   370   380   390   400
     |     |     |     |     |     |     |     |     |     |
TTACGTGGTGCCGCTCAGGTGATGTTTGTCAACAACCCATTGAGTGGGCTTATTATTTTAGTCGGGCTGATTGTACAGAATCCATGGTGGGCACTGAATG
••••••••••••••••••••••••••••••••••••••••••••••••••••••••••••••••••••••••••••••••••••••••••••••••••••••••
TTACGTGGTGCCGCTCAGGTGATGTTTGTCAACAACCCATTGAGTGGGCTTATTATTTTAGTCGGGCTGATTGTACAGAATCCATGGTGGGCACTGAATG
     |     |     |     |     |     |     |     |     |     |
     310   320   330   340   350   360   370   380   390   400

     410   420   430   440   450   460   470   480   490   500
     |     |     |     |     |     |     |     |     |     |
GCTTCGTGGGAACAGTGTTCTCAACTCTGGCAGCACTTTTGCTCAGTCAGAACAGATCTAAAATTGCAGCAGGGCTTCATGGGTACAATGGCATCTTGGT
••••••••••••••••••••••••••••••••••••••••••••••••••••••••••••••••••••••••••••••••••••••••••••••••••••••••
GCTTCGTGGGAACAGTGTTCTCAACTCTGGCAGCACTTTTGCTCAGTCAGAACAGATCTAAAATTGCAGCAGGGCTTCATGGGTACAATGGCATCTTGGT
     |     |     |     |     |     |     |     |     |     |
     410   420   430   440   450   460   470   480   490   500

     510   520   530   540   550   560   570   580   590   600
     |     |     |     |     |     |     |     |     |     |
TGGCCTTCAACTGGCTGTGTTTTCTAATAAAGGAGATTGGTATTGGTGGCTACTACTGCCTGTGATTGTCGTGTCAATAGTGTGCCCTGTGCTTTCAAGT
••••••••••••••••••••••••••••••••••••••••••••••••••••••••••••••••••••••••••••••••••••••••••••••••••••••••
TGGCCTTCAACTGGCTGTGTTTTCTAATAAAGGAGATTGGTATTGGTGGCTACTACTGCCTGTGATTGTCGTGTCAATAGTGTGCCCTGTGCTTTCAAGT
     |     |     |     |     |     |     |     |     |     |
     510   520   530   540   550   560   570   580   590   600

     610   620   630   640   650   660   670   680   690   700
     |     |     |     |     |     |     |     |     |     |
GCCTTGGCCTCTGTGATGGAAAGATGGGATCTGCCTGTTTTCACGCTGCCTTTTAATATTGCTCTGTCGGTGTATATGGCCGCAACAGGACACGACAACC
••••••••••••••••••••••••••••••••••••••••••••••••••••••••••••••••••••••••••••••••••••••••••••••••••••••••
GCCTTGGCCTCTGTGATGGAAAGATGGGATCTGCCTGTTTTCACGCTGCCTTTTAATATTGCTCTGTCGGTGTATATGGCCGCAACAGGACACGACAACC
     |     |     |     |     |     |     |     |     |     |
     610   620   630   640   650   660   670   680   690   700

     710   720   730   740   750   760   770   780   790   800
     |     |     |     |     |     |     |     |     |     |
AGCATTTTCCCCAGGTTCTTATTCAACCCATGACAGCACCATTAAACACCACATGGCCAGATCTCAGTGTTTCAATGCTTCTGAGAGCTATCCCAGTGGG
••••••••••••••••••••••••••••••••••••••••••••••••••••••••••••••••••••••••••••••••••••••••••••••••••••••••
AGCATTTTCCCCAGGTTCTTATTCAACCCATGACAGCACCATTAAACACCACATGGCCAGATCTCAGTGTTTCAAT----------------------
     |     |     |     |     |     |     |
     710   720   730   740   750   760   770

     810   820   830   840   850   860   870   880   890   900
     |     |     |     |     |     |     |     |     |     |
TGTTGGGCAGGTGTATGGCTGCGACAATCCCTGGACTGGTGGCATTTTCCTTATTGCATTAATTATCTCATCTCCAGTCATATGTCTGCATGCTGCAATT
                                  ••••••••••••••••••••••••
----------------------------------------------------------------------------GTCATATGTCTGCATGCTGCAATT
                                       |     |     |
                                       780   790   800

     910   920   930   940   950   960   970   980   990   1000
     |     |     |     |     |     |     |     |     |     |
GGATCCTGTCTCGGTATACTGGCAGGATTATCCCTGGCTTCACCATTCCAGAAAATCTATGATGGATTATGGAGCTACAACTGTGTTCTGGCCTGTACTG
```

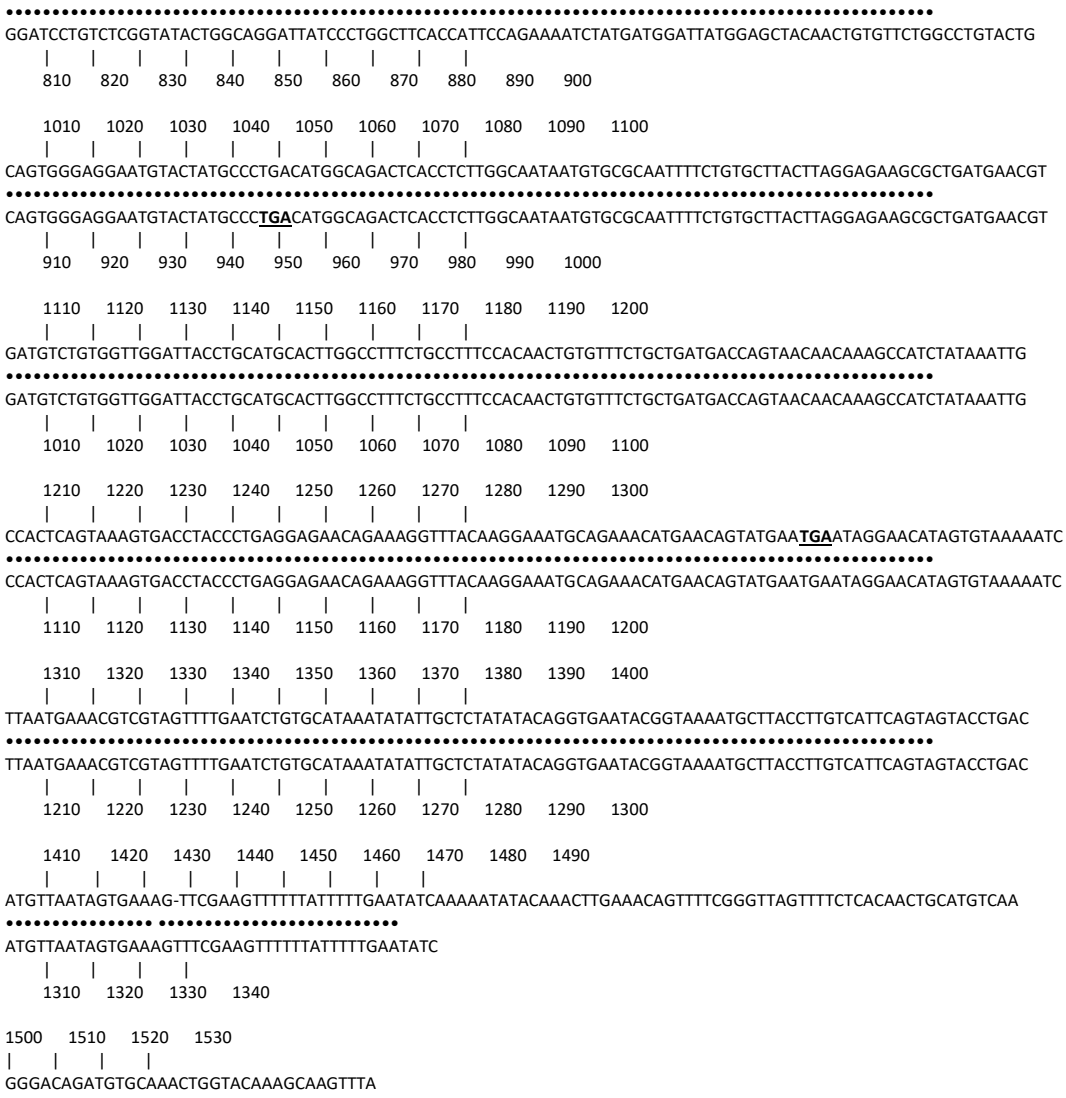


**A2:** Aligned sequences of *Squalus acanthias* Brain UT and its spliceoform. - = missing exon, and short underlines (top sequence) are bases (9) that are different to the transcriptomics study (Chana-Munoz *et al.* 2017) sequence (polymorphisms or sequencing errors). Long underlines represent primer sites. These were located at:- 1) for Tissue PCR, Sense 170-204 bp, Antisense 660-683 bp, 2) for 3' RACE, GSP1 483-512bp, GSP2 532-561 bp and 3) for QPCR, Sense 571-594, Antisense 808-830 bp (within the exon missing in the splice variant). Start (ATG) and Stop (TGA) codons are also underlined. Start codon and the two different stop codons for normal and spliced versions are underlined and bolded.

**Brain UT**

MKNLAPSSHS AQQRIHQFTF SVQPSKRRPM FDSKLVQLET NSFMQQMVPV CIEENTAVQQ
DNNKNVYCNC ERIVQFPDKI RKFGDWLKEQ NIIFLFIDWN LRGAAQVMFV NNPLSGLIIL
VGLIVQNPWW ALNGFVGTVF STLAALLLSQ NRSKIAAGLH GYNGILVGLQ LAVFSNKGDW
YWWLLLPVIV VSIVCPVLSS ALASVMERWD LPVFTLPFNI ALSVYMAATG HDNQHFPQVL
IQPMTAPLNT TWPDLSVSM**L LRAIPVGVGQ VYGCDNPWTG GIFLIALIIS SPVICLHAAI
GSCLGILAGL SLASPFQKIY DGLWSYNCVL ACTAVGGMYY ALTWQTHLLA IMCAIFCAYL
GEALMNVMSV VGLPACTWPF CLSTTVFLLM TSNNKAIYKL PLSKVTYPEE NRKVYKEMQK
HEQYE**

**Brain UT splice variant**

MKNLAPSSHS AQQRIHQFTF SVQPSKRRPM FDSKLVQLET NSFMQQMVPV CIEENTAVQQ
DNNKNVYCNC ERIVQFPDKI RKFGDWLKEQ NIIFLFIDWN LRGAAQVMFV NNPLSGLIIL
VGLIVQNPWW ALNGFVGTVF STLAALLLSQ NRSKIAAGLH GYNGILVGLQ LAVFSNKGDW
YWWLLLPVIV VSIVCPVLSS ALASVMERWD LPVFTLPFNI ALSVYMAATG HDNQHFPQVL
IQPMTAPLNT TWPDLSVSM**S YVCMLQLDPV SVYWQDYPWL HHSRKSMMDY GATTVFWPVL
QWEECTMP**

**A2.1:** Translated amino acid sequence (single letter amino acid codes) of *Squalus acanthias* Brain UT and its spliceoform respectively. (Different –COOH ends are bolded). Brain UT (top) = 425Amino acids. Brain UT spliceoform (bottom) = 308 amino acids.

```
     Met Lys Asn Leu Ala Pro Ser Ser His Ser Ala Gln Gln Arg Ile His Gln     17
   1 ATG AAG AAT TTA GCA CCG AGC TCT CAT TCT GCG CAA CAG CGA ATC CAT CAG
     Phe Thr Phe Ser Val Gln Pro Ser Lys Arg Arg Pro Met Phe Asp Ser Lys     34
  52 TTC ACT TTC AGT GTT CAG CCA AGC AAG AGA AGA CCA ATG TTT GAT TCG AAG
     Leu Val Gln Leu Glu Thr Asn Ser Phe Met Gln Gln Met Val Pro Val Cys     51
 103 CTG GTC CAG CTG GAG ACA AAT TCA TTC ATG CAG CAA ATG GTA CCA GTA TGT
     Ile Glu Glu Asn Thr Ala Val Gln Gln Asp Asn Asn Lys Asn Val Tyr Cys     68
 154 ATT GAA GAG AAC ACA GCC GTC CAA CAA GAT AAC AAC AAG AAT GTC TAC TGT
     Asn Cys Glu Arg Ile Val Gln Phe Pro Asp Lys Ile Arg Lys Phe Gly Asp     85
 205 AAT TGT GAA CGT ATT GTA CAA TTC CCT GAT AAA ATC AGA AAG TTT GGT GAT
     Trp Leu Lys Glu Gln Asn Ile Ile Phe Leu Phe Ile Asp Trp Asn Leu Arg    102
 256 TGG CTC AAA GAG CAG AAC ATT ATC TTT CTA TTT ATT GAC TGG AAC TTA CGT
     Gly Ala Ala Gln Val Met Phe Val Asn Asn Pro Leu Ser Gly Leu Ile Ile    119
 307 GGT GCC GCT CAG GTG ATG TTT GTC AAC AAC CCA TTG AGT GGG CTT ATT ATT
     Leu Val Gly Leu Ile Val Gln Asn Pro Trp Trp Ala Leu Asn Gly Phe Val    136
 358 TTA GTC GGG CTG ATT GTA CAG AAT CCA TGG TGG GCA CTG AAT GGC TTC GTG
     Gly Thr Val Phe Ser Thr Leu Ala Ala Leu Leu Leu Ser Gln Asn Arg Ser    153
 409 GGA ACA GTG TTC TCA ACT CTG GCA GCA CTT TTG CTC AGT CAG AAC AGA TCT
     Lys Ile Ala Ala Gly Leu His Gly Tyr Asn Gly Ile Leu Val Gly Leu Gln    170
 460 AAA ATT GCA GCA GGG CTT CAT GGG TAC AAT GGC ATC TTG GTT GGC CTT CAA
     Leu Ala Val Phe Ser Asn Lys Gly Asp Trp Tyr Trp Trp Leu Leu Leu Pro    187
 511 CTG GCT GTG TTT TCT AAT AAA GGA GAT TGG TAT TGG TGG CTA CTA CTG CCT
     Val Ile Val Val Ser Ile Val Cys Pro Val Leu Ser Ser Ala Leu Ala Ser    204
 562 GTG ATT GTC GTG TCA ATA GTG TGC CCT GTG CTT TCA AGT GCC TTG GCC TCT
     Val Met Glu Arg Trp Asp Leu Pro Val Phe Thr Leu Pro Phe Asn Ile Ala    221
 613 GTG ATG GAA AGA TGG GAT CTG CCT GTT TTC ACG CTG CCT TTT AAT ATT GCT
     Leu Ser Val Tyr Met Ala Ala Thr Gly His Asp Asn Gln His Phe Pro Gln    238
 664 CTG TCG GTG TAT ATG GCC GCA ACA GGA CAC GAC AAC CAG CAT TTT CCC CAG
     Val Leu Ile Gln Pro Met Thr Ala Pro Leu Asn Thr Thr Trp Pro Asp Leu    255
 715 GTT CTT ATT CAA CCC ATG ACA GCA CCA TTA AAC ACC ACA TGG CCA GAT CTC
     Ser Val Ser Met Leu Leu Arg Ala Ile Pro Val Gly Val Gly Gln Val Tyr    272
 766 AGT GTT TCA ATG CTT CTG AGA GCT ATC CCA GTG GGT GTT GGG CAG GTG TAT
     Gly Cys Asp Asn Pro Trp Thr Gly Gly Ile Phe Leu Ile Ala Leu Ile Ile    289
 817 GGC TGC GAC AAT CCC TGG ACT GGT GGC ATT TTC CTT ATT GCA TTA ATT ATC
     Ser Ser Pro Val Ile Cys Leu His Ala Ala Ile Gly Ser Cys Leu Gly Ile    306
 868 TCA TCT CCA GTC ATA TGT CTG CAT GCT GCA ATT GGA TCC TGT CTC GGT ATA
     Leu Ala Gly Leu Ser Leu Ala Ser Pro Phe Gln Lys Ile Tyr Asp Gly Leu    323
 919 CTG GCA GGA TTA TCC CTG GCT TCA CCA TTC CAG AAA ATC TAT GAT GGA TTA
     Trp Ser Tyr Asn Cys Val Leu Ala Cys Thr Ala Val Gly Gly Met Tyr Tyr    340
 970 TGG AGC TAC AAC TGT GTT CTG GCC TGT ACT GCA GTG GGA GGA ATG TAC TAT
     Ala Leu Thr Trp Gln Thr His Leu Leu Ala Ile Met Cys Ala Ile Phe Cys    357
1021 GCC CTG ACA TGG CAG ACT CAC CTC TTG GCA ATA ATG TGC GCA ATT TTC TGT
     Ala Tyr Leu Gly Glu Ala Leu Met Asn Val Met Ser Val Val Gly Leu Pro    374
1072 GCT TAC TTA GGA GAA GCG CTG ATG AAC GTG ATG TCT GTG GTT GGA TTA CCT
     Ala Cys Thr Trp Pro Phe Cys Leu Ser Thr Thr Val Phe Leu Leu Met Thr    391
1123 GCA TGC ACT TGG CCT TTC TGC CTT TCC ACA ACT GTG TTT CTG CTG ATG ACC
     Ser Asn Asn Lys Ala Ile Tyr Lys Leu Pro Leu Ser Lys Val Thr Tyr Pro    408
1174 AGT AAC AAC AAA GCC ATC TAT AAA TTG CCA CTC AGT AAA GTG ACC TAC CCT
     Glu Glu Asn Arg Lys Val Tyr Lys Glu Met Gln Lys His Glu Gln Tyr Glu    425
1225 GAG GAG AAC AGA AAG GTT TAC AAG GAA ATG CAG AAA CAT GAA CAG TAT GAA
     Stop                                                                  425
1276 TGA ATAGGAACATAGTGTAAAAATCTTAATGAAACGTCGTAGTTTTGAATCTGTGCATAAATATAT
1342 TGCTCTATATACAGGTGAATACGGTAAAATGCTTACCTTGTCATTCAGTAGTACCTGACATGTTAAT
1409 AGTGAAAGTTCGAAGTTTTTTATTTTTGAATATCAAAAATATACAAACTTGAAACAGTTTTCGGGTT
1476 AGTTTTCTCACAACTGCATGTCAAGGGACAGATGTGCAAACTGGTACAAAGCAAGTTTA
```

**A2.2:** *Squalus acanthias* interleaved full length Brain UT nucleotide and amino acid sequences (3 letter amino acid codes; differences to spliceoform underlined).

```
    Met Lys Asn Leu Ala Pro Ser Ser His Ser Ala Gln Gln Arg Ile His Gln     17
  1 ATG AAG AAT TTA GCA CCG AGC TCT CAT TCT GCG CAA CAG CGA ATC CAT CAG
    Phe Thr Phe Ser Val Gln Pro Ser Lys Arg Arg Pro Met Phe Asp Ser Lys     34
 52 TTC ACT TTC AGT GTT CAG CCA AGC AAG AGA AGA CCA ATG TTT GAT TCG AAG
    Leu Val Gln Leu Glu Thr Asn Ser Phe Met Gln Gln Met Val Pro Val Cys     51
103 CTG GTC CAG CTG GAG ACA AAT TCA TTC ATG CAG CAA ATG GTA CCA GTA TGT
    Ile Glu Glu Asn Thr Ala Val Gln Gln Asp Asn Asn Lys Asn Val Tyr Cys     68
154 ATT GAA GAG AAC ACA GCC GTC CAA CAA GAT AAC AAC AAG AAT GTC TAC TGT
    Asn Cys Glu Arg Ile Val Gln Phe Pro Asp Lys Ile Arg Lys Phe Gly Asp     85
205 AAT TGT GAA CGT ATT GTA CAA TTC CCT GAT AAA ATC AGA AAG TTT GGT GAT
    Trp Leu Lys Glu Gln Asn Ile Ile Phe Leu Phe Ile Asp Trp Asn Leu Arg    102
256 TGG CTC AAA GAG CAG AAC ATT ATC TTT CTA TTT ATT GAC TGG AAC TTA CGT
    Gly Ala Ala Gln Val Met Phe Val Asn Asn Pro Leu Ser Gly Leu Ile Ile    119
307 GGT GCC GCT CAG GTG ATG TTT GTC AAC AAC CCA TTG AGT GGG CTT ATT ATT
    Leu Val Gly Leu Ile Val Gln Asn Pro Trp Trp Ala Leu Asn Gly Phe Val    136
358 TTA GTC GGG CTG ATT GTA CAG AAT CCA TGG TGG GCA CTG AAT GGC TTC GTG
    Gly Thr Val Phe Ser Thr Leu Ala Ala Leu Leu Leu Ser Gln Asn Arg Ser    153
409 GGA ACA GTG TTC TCA ACT CTG GCA GCA CTT TTG CTC AGT CAG AAC AGA TCT
    Lys Ile Ala Ala Gly Leu His Gly Tyr Asn Gly Ile Leu Val Gly Leu Gln    170
460 AAA ATT GCA GCA GGG CTT CAT GGG TAC AAT GGC ATC TTG GTT GGC CTT CAA
    Leu Ala Val Phe Ser Asn Lys Gly Asp Trp Tyr Trp Trp Leu Leu Leu Pro    187
511 CTG GCT GTG TTT TCT AAT AAA GGA GAT TGG TAT TGG TGG CTA CTA CTG CCT
    Val Ile Val Val Ser Ile Val Cys Pro Val Leu Ser Ser Ala Leu Ala Ser    204
562 GTG ATT GTC GTG TCA ATA GTG TGC CCT GTG CTT TCA AGT GCC TTG GCC TCT
    Val Met Glu Arg Trp Asp Leu Pro Val Phe Thr Leu Pro Phe Asn Ile Ala    221
613 GTG ATG GAA AGA TGG GAT CTG CCT GTT TTC ACG CTG CCT TTT AAT ATT GCT
    Leu Ser Val Tyr Met Ala Ala Thr Gly His Asp Asn Gln His Phe Pro Gln    238
664 CTG TCG GTG TAT ATG GCC GCA ACA GGA CAC GAC AAC CAG CAT TTT CCC CAG
    Val Leu Ile Gln Pro Met Thr Ala Pro Leu Asn Thr Thr Trp Pro Asp Leu    255
715 GTT CTT ATT CAA CCC ATG ACA GCA CCA TTA AAC ACC ACA TGG CCA GAT CTC
    Ser Val Ser Met Ser Tyr Val Cys Met Leu Gln Leu Asp Pro Val Ser Val    272
766 AGT GTT TCA ATG TCA TAT GTC TGC ATG CTG CAA TTG GAT CCT GTC TCG GTA
    Tyr Trp Gln Asp Tyr Pro Trp Leu His His Ser Arg Lys Ser Met Met Asp    289
817 TAC TGG CAG GAT TAT CCC TGG CTT CAC CAT TCC AGA AAA TCT ATG ATG GAT
    Tyr Gly Ala Thr Thr Val Phe Trp Pro Val Leu Gln Trp Glu Glu Cys Thr    306
868 TAT GGA GCT ACA ACT GTG TTC TGG CCT GTA CTG CAG TGG GAG GAA TGT ACT
    Met Pro Stop                                                          308
919 ATG CCC TGA CATGGCAGACTCACCTCTTGGCAATAATGTGCGCAATTTTCTGTGCTTACTTAGG
983 AGAAGCGCTGATGAACGTGATGTCTGTGGTTGGATTACCTGCATGCACTTGGCCTTTCTGCCTTTCC
1050 ACAACTGTGTTTCTGCTGATGACCAGTAACAACAAAGCCATCTATAAATTGCCACTCAGTAAAGTGA
1117 CCTACCCTGAGGAGAACAGAAAGGTTTACAAGGAAATGCAGAAACATGAACAGTATGAATGAATAGG
1184 AACATAGTGTAAAAATCTTAATGAAACGTCGTAGTTTTGAATCTGTGCATAAATATATTGCTCTATA
1251 TACAGGTGAATACGGTAAAATGCTTACCTTGTCATTCAGTAGTACCTGACATGTTAATAGTGAAAGT
1318 TTCGAAGTTTTTTATTTTTGAATATC
```

**A2.3:** *Squalus acanthias* interleaved Brain UT spliceoform nucleotide and amino acid sequences (3 letter amino acid codes; differences with full version Brain UT underlined).

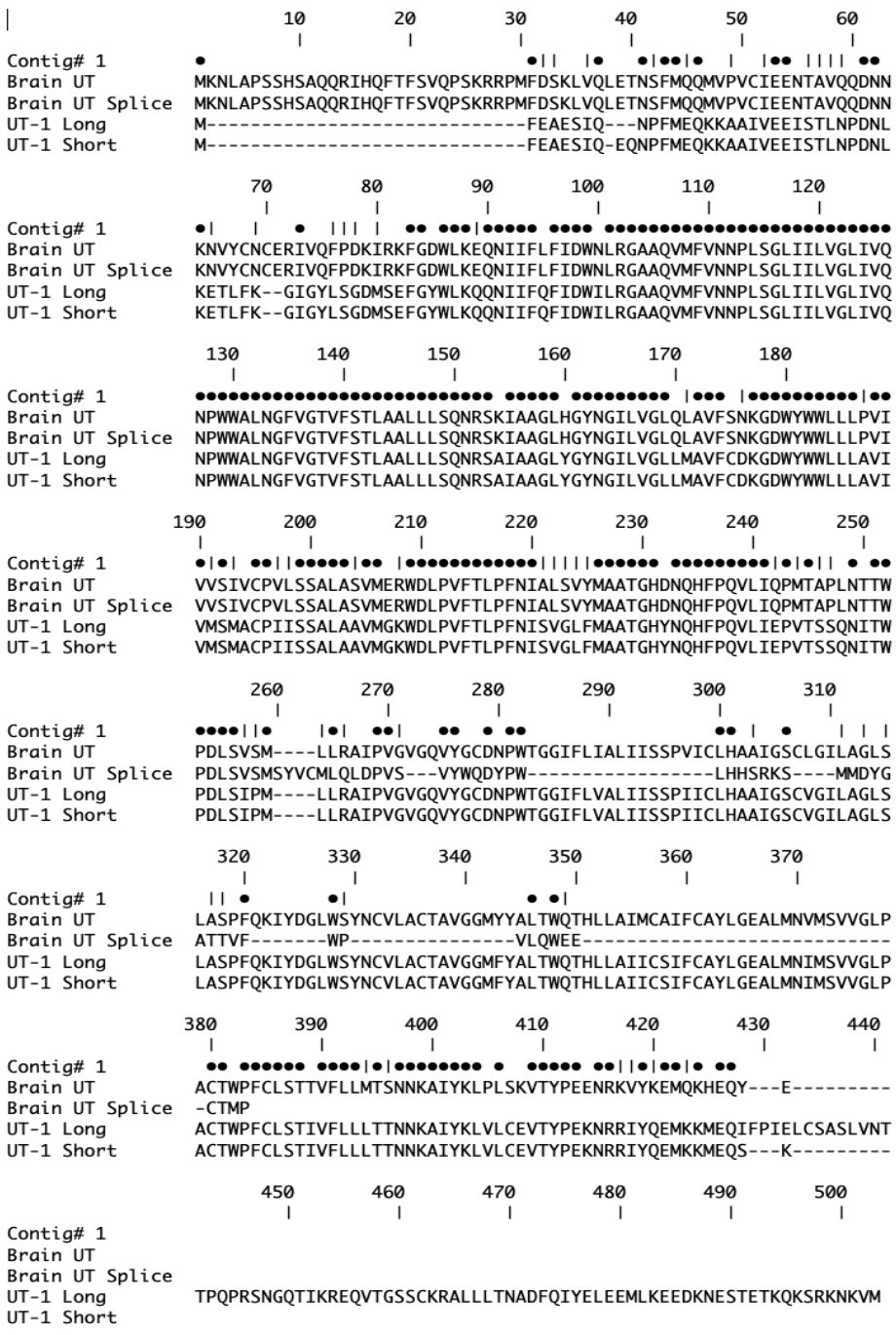


**A2.4:** Amino Acid Sequences of *Squalus acanthias* Brain UT and its spliceoform aligned (Clustal) with the sequences of UT-1 long and short spliceoforms. = The same amino acid in all sequences. | are at positions with chemically similar substitutions. – are added to maintain the spacing of the alignment.

**Initial tissue PCR**

Squal Brain UT sense Phusion Tm = 69˚C Product = 499bp

CCGTCCAACA AGATAACGAC AAGAATGTCT ACTGT

Squal Brain UT Anti Phusion Tm = 70˚C

TGCGGCCATA TACACCGACA GAGCA

**5' End PCR**

Squal brain UT sen 2 (Before start codon) Phusion Tm = 67˚C Product = 718bp

CTCGGGCAAA CATTCCGGCA TTAACTACAG TCTG

Squal Brain UT Anti Phusion Tm = 70˚C (same as above)

TGCGGCCATA TACACCGACA GAGCA

**3' RACE PCR**

Squal brain UT 3R 1 Phusion Tm = 69˚C

GTACAATGGCATCTTGGTTGGCCTTCAACT

Squal brain UT 3R 2 Phusion Tm = 69˚C

GGAGATTGGTATTGGTGGCTACTACTGCCT

**QPCR primers**

Brain UT QPCR3 Sen Taq Tm = 62˚C Product = 260bp

GTGTCAATAG TGTGCCCTGT GCTT

Brain UT QPCR2 Norm Anti Taq Tm = 63˚C

GGATTGTCGC AGCCATACAC CTG

**A2.5:** *Squalus acanthias* Brain UT primer sequences (see also A2). The melting temperature for the primers when using Phusion or Taq DNA polymerases for PCR are indicated. The expected size of the initial tissue PCR product, the 5' end PCR fragment and the QPCR fragment are also as indicated.

**RPL-P0**

At the start of this study there was no sequence in the gene bank for the housekeeping control gene RPL-P0, for *Squalus acanthias*. So RPL-P0 sequences were obtained from the three nearest relatives. These were the Elephant fish *(Callorhinchus mili*), Cat shark (*Scyliorhinus canicula*) and Whale shark (*Rhincodon typus*), were obtained from the gene bank and these were then aligned using Clustal Omega (see A3 above). The alignment was used to design primers for the amplification of a *Squalus acanthias* RPL-P0 fragment (see A3.1). This approach was taken because the RPL-P0 gene has been highly conversed during evolution.

The Ensembl browser for zebrafish/human genomic sequences was used to find conserved intron- junctions. QPCR primers for all genes studied (including RPL-P0) were then designed across the intron-exon junctions to prevent genomic DNA amplification. To achieve this, most of the primers made were located in the outer exon, with only 7-10 (3'end of primer) nucleotides on the other side of the intron-exon junction in the second exon (see A3.2 and A3.3). The cat shark (*Scyliorhinus canicula*) RPL-P0 sequence was found to be the most similar to the *Squalus acanthias* RPL-P0 sequence with which it shares 90.96% nucleotide homology (see A3.4).

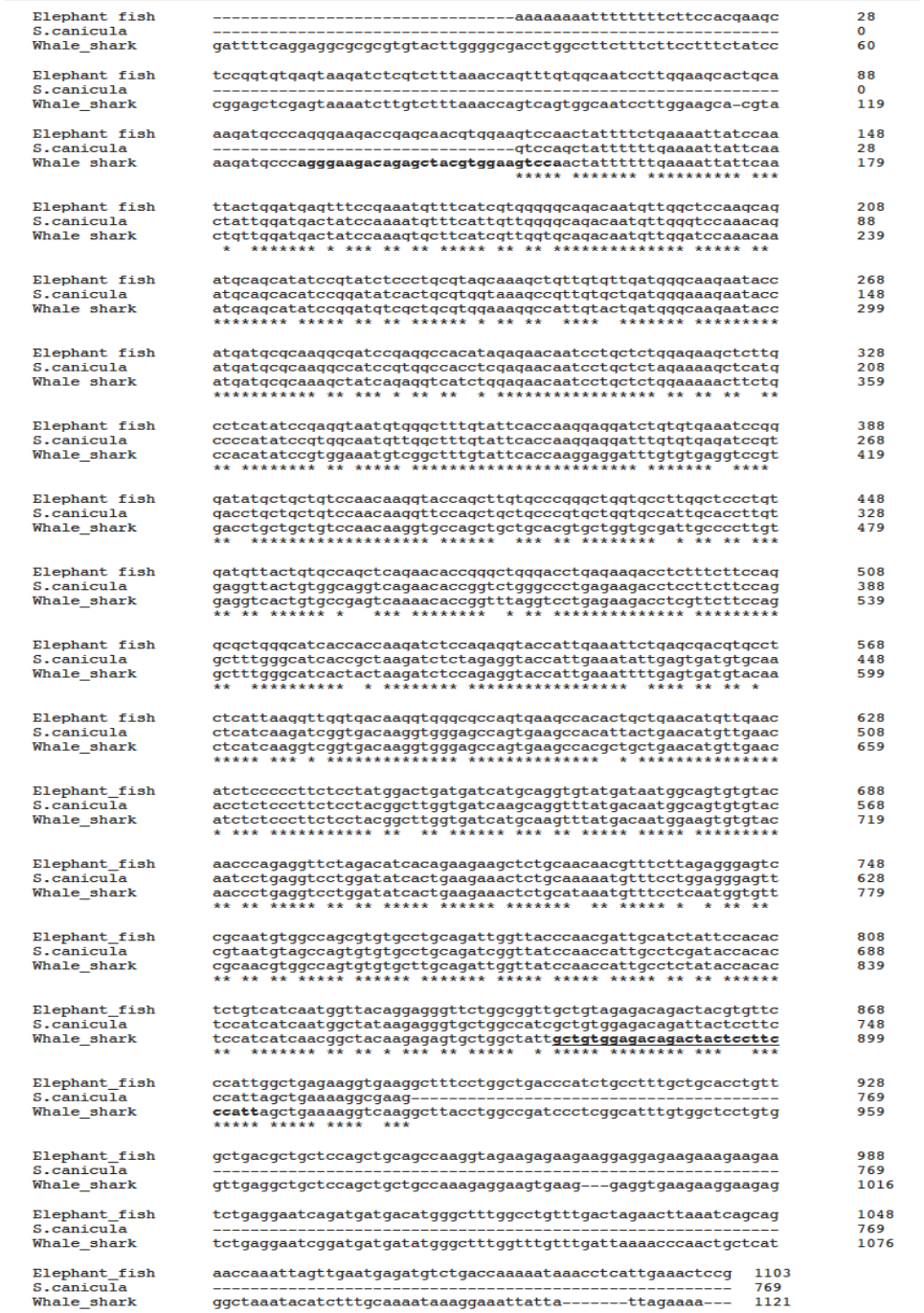


**A3:** Alignment (Clustal Omega) of the three RPL-P0 sequences from species that are the closest to *Squalus acanthias*. The sequences were from Elephant Fish (*Callorhinchus mili* ; Ac. No. JX207461), Cat shark (*Scyliorhinus canicula*; Ac. No. AY392168.1) and Whale shark (*Rhincodon typus*; Ac. No. XM_020527693). **Conserved primer regions** are bolded and underlined; * = same nucleotide in all three sequences.

Elasmobranch RPL-P0 cloning primers  Product = 775bp

Elas RPLP0 sense Phusion Tm = 69.8˚C

AGGGAAGACA GAGCTACGTG GAAGTCCA

Elas RPLP0 anti Phusion Tm = 68.6˚C

AATGGGAAGG AGTAGTCTGT CTCCACAGC

**A3.1**: Elasmobranch RPL-P0 primers used to produce *the Squalus acanthias* RPL-P0 DNA fragment using Phusion DNA polymerase in a PCR reaction. The sequence generated was then used to create primers for QPCR experiments. The RPL-P0 expected product size and Phusion DNA polymerase associated melting temperatures (Tm) are indicated.

```
  1                                                                  AC
    Tyr Phe Met Lys Ile Ile Gln Leu Leu Asp Asp Tyr Pro Lys Cys Phe Ile     17
  3 TAT TTT ATG AAA ATC ATC CAA CTA TTG GAT GAC TAT CCA AAA TGT TTC ATT
    Val Gly Ala Asp Asn Val Gly Ser Lys Gln Met Gln Gln Ile Arg Ile Ser     34
 54 GTT GGG GCG GAC AAT GTT GGG TCC AAG CAG ATG CAG CAG ATC CGT ATA TCG
    Leu Arg Gly Lys Ala Val Val Leu Met Gly Lys Asn Thr Met Met Arg Lys     51
105 CTG CGT GGT AAG GCT GTC GTG CTG ATG GGC AAG AAT ACC ATG ATG CGT AAG
    Ala Ile Arg Gly His Leu Glu Asn Asn Ser Ala Leu Glu Lys Leu Leu Pro     68
156 GCC ATC CGA GGC CAC TTG GAG AAC AAT TCT GCT TTG GAA AAG CTC CTG CCT
    His Ile Arg Gly Asn Val Gly Phe Val Phe Thr Lys Glu Asp Leu Cys Glu     85
207 CAT ATC CGT GGC AAT GTT GGC TTT GTA TTC ACC AAG GAG GAT TTG TGT GAA
    Val Arg Asp Met Leu Leu Ser Asn Lys Val Pro Ala Ala Ala Arg Ala Gly    102
258 GTC CGT GAC ATG CTG CTG TCC AAC AAG GTC CCA GCT GCT GCT CGT GCT GGT
    Ala Ile Ala Pro Cys Glu Val Thr Val Pro Gly Gln Asn Thr Gly Leu Gly    119
309 GCG ATT GCC CCT TGT GAG GTA ACT GTG CCA GGT CAA AAC ACA GGC TTG GGT
    Pro Glu Lys Thr Ser Phe Phe Gln Ala Leu Gly Ile Thr Thr Lys Ile Ser    136
360 CCT GAG AAG ACC TCC TTC TTC CAG GCT TTG GGC ATC ACC ACC AAG ATC TCC
    Arg Gly Thr Ile Glu Ile Leu Ser Asp Val Gln Leu Ile Lys Ile Gly Asp    153
411 AGA GGT ACC ATT GAA ATT CTG AGT GAC GTA CAA CTC ATC AAG ATC GGT GAC
    Lys Val Gly Ala Ser Glu Ala Thr Leu Leu Asn Met Leu Asn Ile Ser Pro    170
462 AAG GTG GGA GCC AGT GAA GCC ACT CTG CTG AAC ATG TTG AAC ATC TCT CCC
    Phe Ser Tyr Gly Leu Val Ile Arg Gln Val Tyr Asp Asn Gly Ser Val Tyr    187
513 TTC TCC TAT GGC TTG GTG ATC AGG CAG GTT TAT GAT AAT GGA AGT GTG TAC
    Asn Pro Glu Val Leu Asp Ile Thr Glu Glu Thr Leu Gln Lys Cys Phe Leu    204
564 AAC CCT GAG GTC CTG GAC ATC ACC GAA GAA ACT CTG CAA AAG TGT TTC CTG
    Glu Gly Val Arg Asn Val Ala Ser Val Cys Leu Gln Ile Gly Tyr Pro Thr    221
615 GAG GGA GTC CGC AAT GTG GCC AGT GTG TGT CTG CAG ATT GGT TAC CCA ACC
    Ile Ala Ser Ile Pro His Ser Ile Ile Asn Gly Tyr Lys Arg Val Leu Ala    238
666 ATT GCC TCT ATA CCA CAC TCC ATC ATC AAT GGC TAC AAG AGG GTG CTG GCT
    Val                                                                239
717 GTC
```

**A3.2:** Interleaved nucleotide and amino acid (3 letter codes) sequences of *Squlaus acanthias* RPL-P0 cDNA and RPL-P0 partial amino acid sequences. The qPCR primer sites are underlined.

| |
|---|
| Squal RPL-P0 QPCR2 sen Taq Tm = 63 ˚C Product = 128bp |
| GGAGAACAAT TCTGCTTTGG AAAAGCTCCT |
| Squal RPL-P0 QPCR2 anti Taq Tm = 64 ˚C |
| GCAGCAGCTG GGACCTTGTT |

**A3.3:** *Squalus acanthias* RPL-P0 qPCR primers designed for qPCR experiments. The Taq DNA polymerase melting temperature (Tm) and the expected product size are indicated.

```
Squalus RPL-P0          1 -----ACTATTTTATGAAAATCATCCAACTATTGGATGACTATCCAAAAT      45
                            -|||||||-|||||||-||-||||||||||||||||||||||||
ScyliorhinusRPL-P0      1 gtccagctatttttgaaaattattcaactattggatgactatccaaaat      50

Squalus RPL-P0         46 GTTTCATTGTTGGGGCGGACAATGTTGGGTCCAAGCAGATGCAGCAGATC      95
                           ||||||||||||||||-||||||||||||||||-||||||||||-|||
ScyliorhinusRPL-P0     51 gtttcattgttggggcagacaatgttgggtccaaacagatgcagcacatc     100

Squalus RPL-P0         96 CGTATATCGCTGCGTGGTAAGGCTGTCGTGCTGATGGGCAAGAATACCAT     145
                           ||-|||||-||||||||||-||-||-||||||||||-||||||||||
ScyliorhinusRPL-P0    101 cggatatcactgcgtggtaaagccgttgtgctgatgggaaagaataccat     150

Squalus RPL-P0        146 GATGCGTAAGGCCATCCGAGGCCACTTGGAGAACAATTCTGCTTTGGAAA     195
                           ||||||-||||||||||-|||||||-|-|||||||||-|||||-|-||||
ScyliorhinusRPL-P0    151 gatgcgcaaggccatccgtggccacctcgagaacaatcctgctctagaaa     200

Squalus RPL-P0        196 AGCTCCTGCCTCATATCCGTGGCAATGTTGGCTTTGTATTCACCAAGGAG     245
                           |||||-||||-||||||||||||||||||||||||||||||||||||||
ScyliorhinusRPL-P0    201 agctcatgccccatatccgtggcaatgttggctttgtattcaccaaggag     250

Squalus RPL-P0        246 GATTTGTGTGAAGTCCGTGACATGCTGCTGTCCAACAAGGTCCCAGCTGC     295
                           ||||||||||--||||||||-||||||||||||||||||-||||||||
ScyliorhinusRPL-P0    251 gatttgtgtgagatccgtgacctgctgctgtccaacaaggttccagctgc     300

Squalus RPL-P0        296 TGCTCGTGCTGGTGCGATTGCCCCTTGTGAGGTAACTGTGCCAGGTCAAA     345
                           |||-||||||||||-|||||-||||||||||-||||||-||||||||-|
ScyliorhinusRPL-P0    301 tgcccgtgctggtgccattgcaccttgtgaggttactgtggcaggtcaga     350

Squalus RPL-P0        346 ACACAGGCTTGGGTCCTGAGAAGACCTCCTTCTTCCAGGCTTTGGGCATC     395
                           ||||-||--||||-||||||||||||||||||||||||||||||||||
ScyliorhinusRPL-P0    351 acaccggtctgggccctgagaagacctccttcttccaggctttgggcatc     400

Squalus RPL-P0        396 ACCACCAAGATCTCCAGAGGTACCATTGAAATTCTGAGTGACGTACAACT     445
                           |||-|-||||||||-||||||||||||||||--|||||||-||-||||||
ScyliorhinusRPL-P0    401 accgctaagatctctagaggtaccattgaaatattgagtgatgtgcaact     450

Squalus RPL-P0        446 CATCAAGATCGGTGACAAGGTGGGAGCCAGTGAAGCCACTCTGCTGAACA     495
                           ||||||||||||||||||||||||||||||||||||||||--|-||||||||
ScyliorhinusRPL-P0    451 catcaagatcggtgacaaggtgggagccagtgaagccacattactgaaca     500

Squalus RPL-P0        496 TGTTGAACATCTCTCCCTTCTCCTATGGCTTGGTGATCAGGCAGGTTTAT     545
                           |||||||||-||||||||||||||-||||||||||||||-||||||||||
ScyliorhinusRPL-P0    501 tgttgaacacctctcccttctcctacggcttggtgatcaagcaggtttat     550

Squalus RPL-P0        546 GATAATGGAAGTGTGTACAACCCTGAGGTCCTGGACATCACCGAAGAAAC     595
                           ||-||||||-||||||||||-|||||||||||||||-||||||-||||||||
ScyliorhinusRPL-P0    551 gacaatggcagtgtgtacaatcctgaggtcctggatatcactgaagaaac     600

Squalus RPL-P0        596 TCTGCAAAAGTGTTTCCTGGAGGGAGTCCGCAATGTGGCCAGTGTGTGTC     645
                           |||||||||-|||||||||||||||||||-||-|||||-||||||||||||-|
ScyliorhinusRPL-P0    601 tctgcaaaaatgtttcctggagggagttcgtaatgtagccagtgtgtgcc     650

Squalus RPL-P0        646 TGCAGATTGGTTACCCAACCATTGCCTCTATACCACACTCCATCATCAAT     695
                           |||||||-|||||-||||||||||||||-|||||||||||||||||||||
ScyliorhinusRPL-P0    651 tgcagatcggttatccaaccattgcctcgataccacactccatcatcaat     700

Squalus RPL-P0        696 GGCTACAAGAGGGTGCTGGCTGTC--------------------------     719
                           |||||-|||||||||||||||--||
ScyliorhinusRPL-P0    701 ggctataagagggtgctggccatcgctgtggagacagattactccttccc     750

Squalus RPL-P0        720 --------------------     719

ScyliorhinusRPL-P0    751 attagctgaaaaggcgaag     769
```

**A3.4** An alignment of RPL-P0 Sequences from the sharks *Squalus acanthias* (this study) and *Scyliorhinus canicula* (Gene bank Ac. No. AY392168.1). Where | = same nucleotide, and . = different nucleotides. The sequences are 90.96% homologous. Which was higher than that for Whale shark, which was only 89.99% homologous to *Squalus acanthias*.

**UT-1 and NCC**

Cloning and sequencing experiments were not needed for *Squalus acanthias* UT-1 long and short splice variants or for NCC as the sequences for these were already available in the gene bank with ascension numbers: (see below). These sequences were used to design UT-1 and NCC primers for this study.

**NCC accession number**: MK256760

**Squalus UT1 long accession number**: HAGV01114645

**Squalus UT1 short accession number**: AF257331/ HAGV01114644

**Partial Brain UT sequence accession numbers**: HAGW01085140 and HAGW01085138

**AQP3-2 accession number**: HAGV01072450

**AQP3-2 Spliceoform accession number**: HAGV01050719